



# Aquifer-System Compaction: Analyses and Simulations-the Holly Site, Edwards Air Force Base, Antelope Valley, California

By Michelle Sneed and Devin L. Galloway

U.S. Geological Survey Water-Resources Investigations Report 00-4015

## CONTENTS

Abstract.....	1
 Introduction .....	2
Purpose and Scope .....	5
Location .....	5
Development of the Ground-Water Resource and Resulting Land Subsidence .....	6
Previous Studies.....	7
Hydrogeologic Setting.....	8
Geologic Framework .....	8
 Aquifer Systems .....	9
Ground-Water Levels.....	13
Aquifer-System Compaction .....	18
Analytical Approach .....	23
Principle of Effective Stress.....	24
Preconsolidation Stress .....	25
Elastic and Inelastic Compressibility (Specific Storage).....	27
Aquifer-System Storage Coefficients .....	28
Theory of Hydrodynamic Consolidation .....	29
Parameter Range Estimates .....	29
Vertical Hydraulic Conductivity .....	30
Preconsolidation Stress .....	30
Elastic and Inelastic Storage Coefficients (Specific Storage).....	31
Holly Model.....	36
Formulation of Numerical Model .....	36
 Spatial and Temporal Discretization.....	36
Boundary Conditions .....	39
Initial Conditions .....	41
Convergence Criteria and Mass Balance Criteria .....	41
Assumptions and Limitations .....	42
Simulations .....	43
History Matching.....	44
Sensitivity Analysis .....	46
Analyses.....	53
Simulated Compaction .....	53
Future Compaction Scenarios.....	53
Summary.....	61
References Cited.....	61

## FIGURES

1–4. Maps showing:	
1. Location of Antelope Valley and the Holly site (8N/10W-1Q).....	2
2. General surficial geology and location of ground-water subbasins and geologic section, Antelope Valley, California .....	3
3. Location of selected well fields, observation wells, and bench marks near the Holly site (8N/10W-1Q) in the south-central part of Edwards Air Force Base, Antelope Valley, California .....	4
4. Ground-water levels in the Lancaster subbasin, Antelope Valley, California, 1915 .....	6

5. Lithologic and geophysical logs of the Holly site (8N/10W-1Q), Edwards Air Force Base, Antelope Valley, California .....	10
6. Generalized geologic section showing relation of lacustrine deposits to younger and older alluvium and aquifers in the Lancaster and North Muroc subbasins, Edwards Air Force Base, Antelope Valley, California .....	11
7. Conceptual model of the aquifer systems at the Holly site (8N/10W-1Q) including the piezometers and the borehole extensometer, Edwards Air Force Base, Antelope Valley, California .....	12
8. Map showing change in ground-water levels in the Lancaster subbasin, Antelope Valley, California, 1915–91....	14
9. Map showing water-level surface of the confined aquifer system, spring 1992, location of selected wells, and hydrographs of wells 8N/10W-28B1 (1951-97) and 9N/10W-24C1 (1952–99), Edwards Air Force Base, Antelope Valley, California .....	15
10. Graphs showing water levels in piezometers HO-1, HO-2, HO-3, and HO-4 at the Holly site (8N/10W-1Q), Edwards Air Force Base, Antelope Valley, California, 1990–97 .....	16
11. Graphs showing water-level fluctuations in piezometers HO-1 and HO-3 at the Holly site (8N/10W-1Q), Edwards Air Force Base, Antelope Valley, California .....	17
12. Map showing area of flowing wells, land subsidence, and two fissures in Antelope Valley, California, for the period about 1930–92, and graphs showing ground-water levels in wells 7N/10W-05E1 and 7N/12W-15F1 and subsidence at bench marks 1171A and 474 .....	19
13. Schematic diagram showing the borehole extensometer at the Holly site (8N/10W-1Q), Edwards Air Force Base, Antelope Valley, California .....	21
14. Graph showing aquifer-system compaction and water levels measured at the Holly site (8N/10W-1Q), Edwards Air Force Base, Antelope Valley, California .....	22
15. Diagram showing principle of effective stress, as applied to land subsidence .....	25
16–19. Graphs showing:	
16. Compression of highly compressible clay and sand samples.....	26
17. Change in land-surface elevation for various time intervals for selected bench marks, and estimated water levels (1908–97) for the middle aquifer near the Holly site (8N/10W-1Q), Edwards Air Force Base, Antelope Valley, California.....	30
18. Combined water levels for piezometers HO-2 and HO-3 and cumulative vertical compaction at the Holly extensometer, and applied stress and compaction at the Holly site (8N/10W-1Q), Edwards Air Force Base, Antelope Valley, California, 1990-97.....	32
19. Sample time series used in stress/strain analyses of the Holly site (8N/10W-1Q), Edwards Air Force Base, Antelope Valley, California.....	34
20. Diagram showing relation of model domain to the conceptual model and short normal resistivity log of the Holly site (8N/10W-1Q), Edwards Air Force Base, Antelope Valley, California .....	37
21–31. Graphs showing:	
21. Measured or estimated depth to water for piezometers HO-1, HO-2 and HO-3 (combined), and HO-4 used in the 1990–97 model simulation of the Holly site (8N/10W-1Q), Edwards Air Force Base, Antelope Valley, California .....	39
22. Water levels used for input in the historical model for the upper, middle, and lower aquifers at the Holly site (8N/10W-1Q), Edwards Air Force Base, Antelope Valley, California.....	40
23. Simulated compaction and measured or estimated land subsidence at bench marks P1155 and LS42 near the Holly site (8N/10W-1Q), Edwards Air Force Base, Antelope Valley, California, 1908-97.....	44
24. History matches for 1990–97 for simulated and measured compaction and error and simulated and measured displacement-stress trajectories for the Holly site (8N/10W-1Q), Edwards Air Force Base, Antelope Valley, California.....	45
25. Distribution of error computed between measured and simulated compaction for 35 selected values of $K'_v$ and $S'_{skv}$ of the aquitards at the Holly site (8N/10W-1Q), Edwards Air Force Base, Antelope Valley, California .....	48
26. Simulated compaction by aquifer-system component, 1908–97, at the Holly site (8N/10W-1Q), Edwards Air Force Base, Antelope Valley, California.....	54
27. Simulated deformation by aquifer-system component, 1990–97, at the Holly site (8N/10W-1Q), Edwards Air Force Base, Antelope Valley, California.....	55
28. Hydraulic-head profiles of the Holly site (8N/10W-1Q), Edwards Air Force Base, Antelope Valley, California, for 1908–97 and 1990–97 .....	56

29. Future scenario—1996 pumping rates for 1997 to 2026 at the Holly site (8N/10W-1Q), Edwards Air Force Base, Antelope Valley, California .....	58
30. Future scenario—1997 aquifer water levels held constant through year 2096 at the Holly site (8N/10W-1Q), Edwards Air Force Base, Antelope Valley, California .....	59
31. Future scenario—no pumping for 1997 to 2096 at the Holly site (8N/10W-1Q), Edwards Air Force Base, Antelope Valley, California .....	60

## TABLES

1. Measured or estimated land-surface-elevation changes for selected bench marks at Edwards Air Force Base, Antelope Valley, California .....	30
2. Summary of skeletal storage coefficients and equivalent skeletal specific storages estimated from the results of the stress/strain analyses of the Holly site (8N/10W-1Q), Edwards Air Force Base, Antelope Valley, California.....	36
3. Values of hydraulic parameters derived from the best history matches between simulated aquifer-system compaction and measured or estimated compaction at the Holly site (8N/10W-1Q), Edwards Air Force Base, Antelope Valley, California .....	46

## CONVERSION FACTORS, VERTICAL DATUM, ABBREVIATIONS, SYMBOLS, AND WELL-NUMBERING SYSTEM

### CONVERSION FACTORS

	Multiply	By	To obtain
acre-foot (acre-ft)	1,223		cubic meter
acre-foot per year (acre-ft/yr)	1,223		cubic meter per year
foot (ft)	0.3048		meter
foot per day (ft/d)	0.3048		meter per day
foot per foot (ft/ft)	1.000		meter per meter
foot per year (ft/yr)	0.3048		meter per year
foot squared per day (ft <sup>2</sup> /d)	0.0929		meter squared per day
inch (in.)	25.4		millimeter
mile (mi)	1.609		kilometer
square mile (mi <sup>2</sup> )	2.590		square kilometer

Temperature is given in degrees Celsius (°C), which can be converted to degrees Fahrenheit (°F) by the following equation:

$$^{\circ}\text{F}=1.8(^{\circ}\text{C})+32.$$

### Vertical Datum

**Sea level:** In this report, "sea level" refers to the National Geodetic Vertical Datum of 1929 (NGVD of 1929)—a geodetic datum derived from a general adjustment of the first-order level nets of both the United States and Canada, formerly called Sea Level Datum of 1929.

### Abbreviations

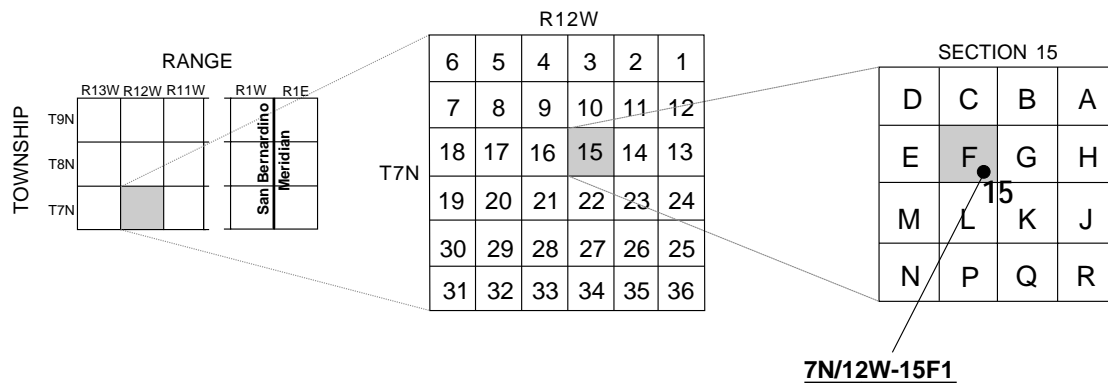
BAS5	Basic package, version 5 of MODFLOW-96
BCF5	Block-Centered Flow package, version 5 of MODFLOW-96
EAFB	Edwards Air Force Base
FHB1	Transient Specified-Flow and Specified-Head Boundaries package of MODFLOW-96
GPS	Global Positioning System
IBS1	Interbed Storage package of MODFLOW-96
InSAR	interferometric synthetic aperture radar
LVDT	linear voltage displacement transducer
NASA	National Aeronautics and Space Administration
SIP5	Strongly Implicit Procedure Solution package, version 5 of MODFLOW-96
SWP	State Water Project
ft/°C	foot per degree Celsius
ft <sup>-1</sup>	per foot

## Symbols, in order of appearance

$\sigma_e$	effective or intergranular stress
$\sigma_T$	total stress
$p$	pore-fluid pressure
$\mu_z$	vertical displacement
$\alpha_{ke}$	elastic skeletal compressibility
$\alpha_{kv}$	inelastic skeletal compressibility
$h$	hydraulic head
$\rho$	fluid density
$g$	gravitational acceleration
$\Delta$	change (for example, $\Delta\sigma_T$ means change in total stress)
$S_{sk}^*$	aquifer system skeletal specific storage
$\alpha_k^*$	aquifer system skeletal compressibility
$S'_{sk}$	aquitard skeletal specific storage
$S'_{ske}$	aquitard elastic skeletal specific storage
$\alpha'_{ke}$	aquitard elastic skeletal compressibility
$\sigma_{e(max)}$	past maximum effective or intergranular stress
$S'_{skv}$	aquitard inelastic skeletal specific storage
$\alpha'_{kv}$	aquitard inelastic skeletal compressibility
$S_{sk}$	aquifer skeletal specific storage
$S_{ske}$	aquifer elastic skeletal specific storage
$\alpha_{ke}$	aquifer elastic skeletal compressibility
$\alpha_{kv}$	aquifer inelastic skeletal compressibility
$\Sigma b'$	aggregate thickness of aquitards
$\Sigma b$	aggregate thickness of aquifers
$S'_k$	aquitard skeletal storage coefficient
$S_k$	aquifer skeletal storage coefficient
$S'_{ke}$	aquitard elastic skeletal storage coefficient
$S'_{kv}$	aquitard inelastic skeletal storage coefficient
$S_{ke}$	aquifer elastic skeletal storage coefficient
$\beta_f$	fluid compressibility of water
$S_w$	aquifer-system storage attributed to the pore water
$S'_{sw}$	specific storage of water of aquitards
$S_{sw}$	specific storage of water of aquifers
$n'$	porosity of the aquitards
$n$	porosity of the aquifers
$S^*$	aquifer-system storage coefficient
$\gg$	much greater than
$S_v^*$	aquifer system inelastic storage coefficient
$\approx$	approximately equal to
$\epsilon_{volume}$	volume strain
$\epsilon_z$	vertical strain
$\epsilon_x$	horizontal strain, $x$ direction
$\epsilon_y$	horizontal strain, $y$ direction
$\partial$	partial derivative
$z$	coordinate in $z$ direction (vertical)
$S'_s$	aquitard specific storage
$K'_v$	aquitard vertical hydraulic conductivity
$t$	time
$K'_v/S'_s$	aquitard vertical hydraulic diffusivity
$\tau$	time constant
$b'$	aquitard thickness
$Sce$	computed error
$\Sigma$	sum
$\mu_{zo}$	measured displacement (vertical)
$\mu_{zs}$	simulated displacement (vertical)
$n$	1,751

## Well-Numbering System

Wells are identified and numbered according to their location in the rectangular system for the subdivision of public lands. Identification consists of the township number, north or south; the range number, east or west; and the section number. Each section is divided into sixteen 40-acre tracts lettered consecutively (except I and O), beginning with "A" in the northeast corner of the section and progressing in a boustrophedonic manner to "R" in the southeast corner. Within the 40-acre tract, wells are sequentially numbered in the order they are inventoried. The final letter refers to the base line and meridian. In California, there are three base lines and meridians: Humboldt (H), Mount Diablo (M), and San Bernardino (S). All wells in the study area are referenced to the San Bernardino base line and meridian (S). Well numbers consist of 15 characters and follow the format 007N012W15F001S. In this report, well numbers are abbreviated and written 7N/12W-15F1. Wells in the same township and range are referred to only by their section designation, 15F1. The following diagram shows how the number for well 7N/12W-15F1 is derived.



# Aquifer-System Compaction and Land Subsidence: Measurements, Analyses, and Simulations—the Holly Site, Edwards Air Force Base, Antelope Valley, California

By Michelle Sneed and D.L. Galloway

## ABSTRACT

Land subsidence resulting from ground-water-level declines has long been recognized as a problem in Antelope Valley, California. At Edwards Air Force Base (EAFB), ground-water extractions have caused more than 150 feet of water-level decline, resulting in nearly 4 feet of subsidence. Differential land subsidence has caused sinklike depressions and earth fissures and has accelerated erosion of the playa lakebed surface of Rogers Lake at EAFB, adversely affecting the runways on the lakebed which are used for landing aircraft such as the space shuttles. Since 1990, about 0.4 foot of aquifer-system compaction has been measured at a deep (840 feet) borehole extensometer (Holly site) at EAFB. More than 7 years of paired ground-water-level and aquifer-system compaction measurements made at the Holly site were analyzed for this study. Annually, seasonal water-level fluctuations correspond to steplike variations in aquifer-system compaction; summer water-level drawdowns are associated with larger rates of compaction, and winter water-level recoveries are associated with smaller rates of compaction. The absence of aquifer-system expansion during recovery is consistent with the delayed drainage and resultant delayed, or residual, compaction of thick aquitards.

A numerical one-dimensional MODFLOW model of aquitard drainage was used to refine estimates of aquifer-system hydraulic parameters that control compaction and to predict potential future compaction at the Holly site. The analyses and simulations of aquifer-system compaction are

based on established theories of aquitard drainage. Historical ground-water-level and land-subsidence data collected near the Holly site were used to constrain simulations of aquifer-system compaction and land subsidence at the site for the period 1908–90, and ground-water-level and aquifer-system compaction measurements collected at the Holly site were used to constrain the model for the period 1990–97.

Model results indicate that two thick aquitards, which total 129 feet or about half the aggregate thickness of all the aquitards penetrated by the Holly boreholes, account for most (greater than 99 percent) of the compaction measured at the Holly site during the period 1990–97. The results of three scenarios of future water-level changes indicate that these two thick aquitards account for most of the future compaction. The results also indicate that if water levels decline to about 30 feet below the 1997 water levels an additional 1.7 feet of compaction may occur during the next 30 years. If water levels remain at 1997 levels, the model predicts that only 0.8 foot of compaction may occur during the same period, and even if water levels recover to about 30 feet above 1997 water levels, another 0.5 foot of compaction may occur in the next 30 years. In addition, only a portion of the compaction that ultimately will occur likely will occur within the next 30 years; therefore, the residual compaction and associated land subsidence attributed to slowly equilibrating aquitards is important to consider in the long-term management of land and water resources at EAFB.

## INTRODUCTION

Land subsidence, a sinking of the land surface, which results from ground-water-level declines, has long been recognized as a problem in Antelope Valley, California (fig. 1), and in other alluvial basins in the arid and semi-arid southwestern United States. The

earliest irrigation systems in the valley were dependent on surface streams, but because the streams were not a stable and reliable water source for crop production, these streams soon were augmented by ground-water systems (Thompson, 1929). Between about 1945 and 1968, ground water was pumped extensively in the Lancaster ground-water subbasin (fig. 2) to irrigate

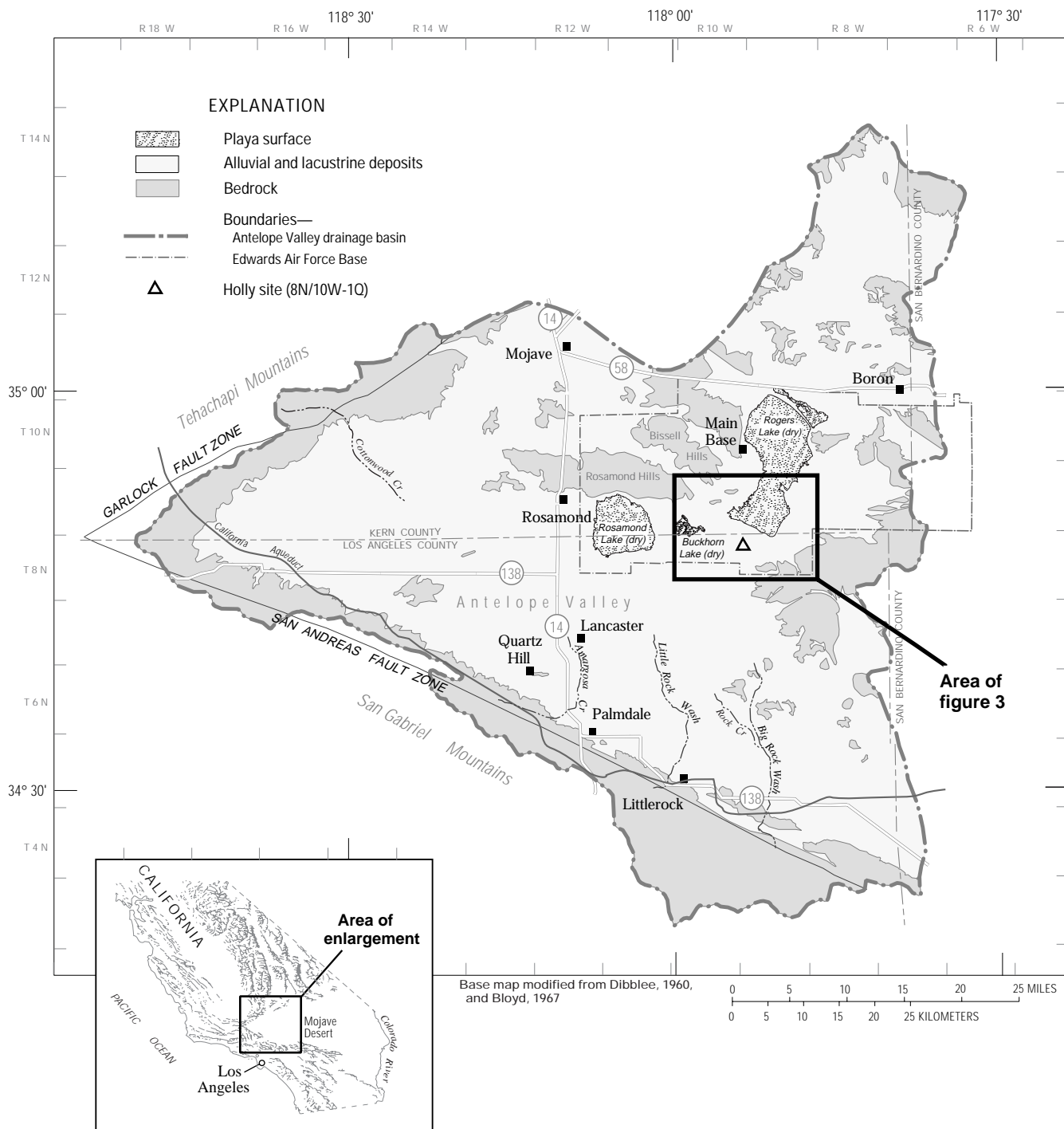
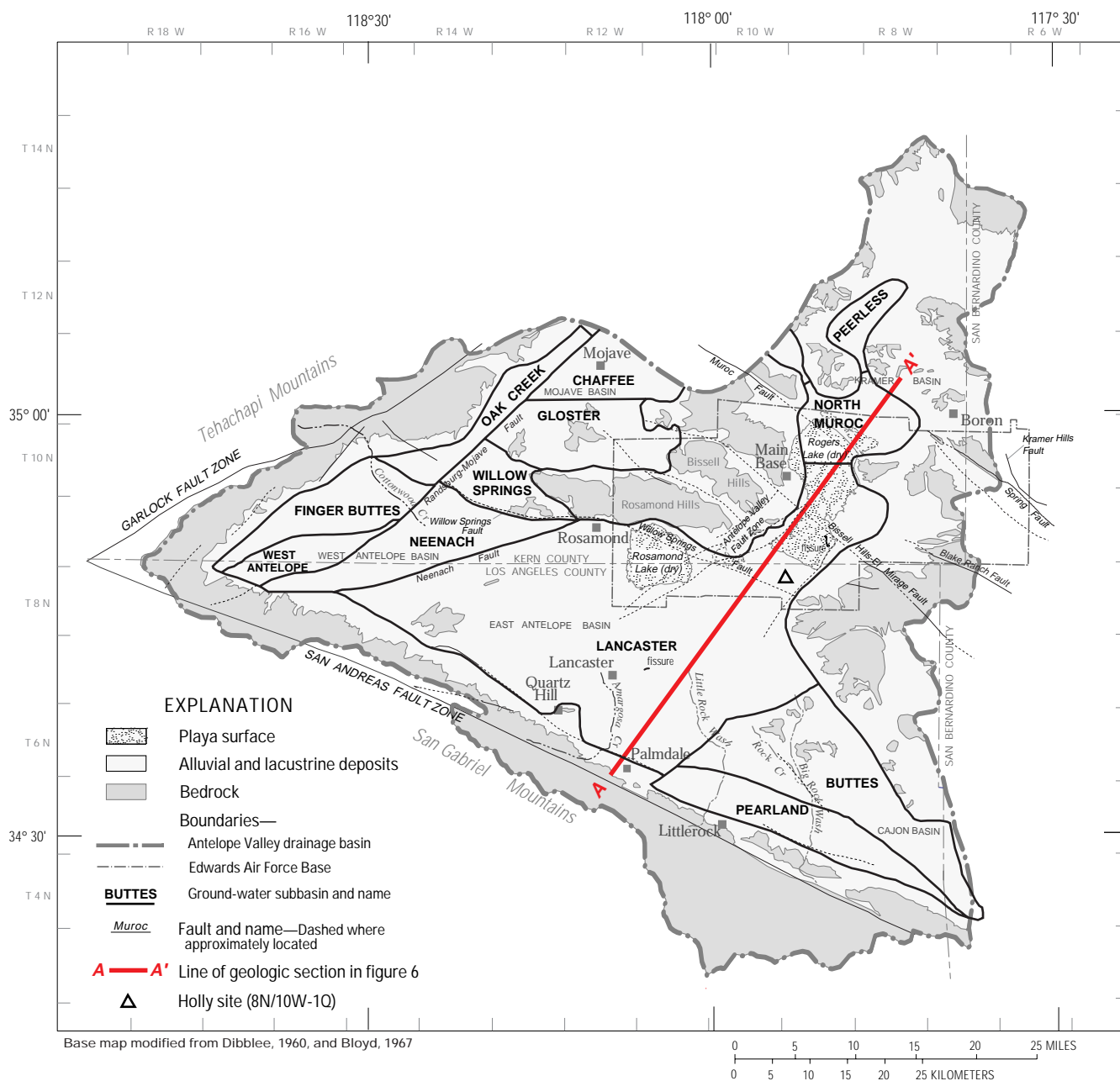


Figure 1. Location of Antelope Valley and the Holly site (8N/10W-1Q).

crops and to satisfy water demands at Edwards Air Force Base (EAFB). This extensive pumping contributed significantly to the more than 6 ft of subsidence that occurred at Lancaster and the 4 ft of subsidence that occurred at EAFB between 1926 and 1992 (Ikehara and Phillips, 1994). Since 1990, nearly 0.4 ft of aquifer-system compaction, a reduction in aquifer-system thickness, has been measured at the Holly site, EAFB (fig. 1).

In 1988, ground failures of the dry lakebed surface, or playa, of Rogers Lake at EAFB (figs. 2 and 3) prompted an investigation by the U.S. Geological Survey and the U.S. Department of the Air Force to determine the causes of sinklike depressions, earth fissures, and accelerated erosion of the lakebed, which were adversely affecting runways used by the Air Force Flight Test Center for landing aircraft such as the space shuttles. Early in the investigation, differential land



**Figure 2.** General surficial geology and location of ground-water subbasins and geologic section, Antelope Valley, California.



subsidence caused by compaction of the aquifer system was determined to be the likely cause of the lakebed deformation (Blodgett and Williams, 1992). In 1990, a borehole extensometer (nearly 840 ft in depth) and four piezometers were constructed near HOLLY (fig. 3), a horizontal and vertical control geodetic monument, to measure compaction and water levels of the aquifer system. The extensometer and the four piezometers have been monitored since their construction, providing a 7-year time series of ground-water levels and aquifer-system compaction.

Continued depletion of the aquifers in Antelope Valley is likely because of a growing demand for water and uncertain alternate sources of water supply. The population of the valley is projected to grow from about 260,400 in 1990 to about 650,000 by 2010 (California Department of Finance, 1992; Los Angeles County Department of Regional Planning, 1994), and water demand is expected to exceed projected "safe" supplies by the year 2004 (L.M. Takaichi, Kennedy/Jenks Consultants, unpub. data, 1995). The safe supply is based on the projected deliveries of imported water and the

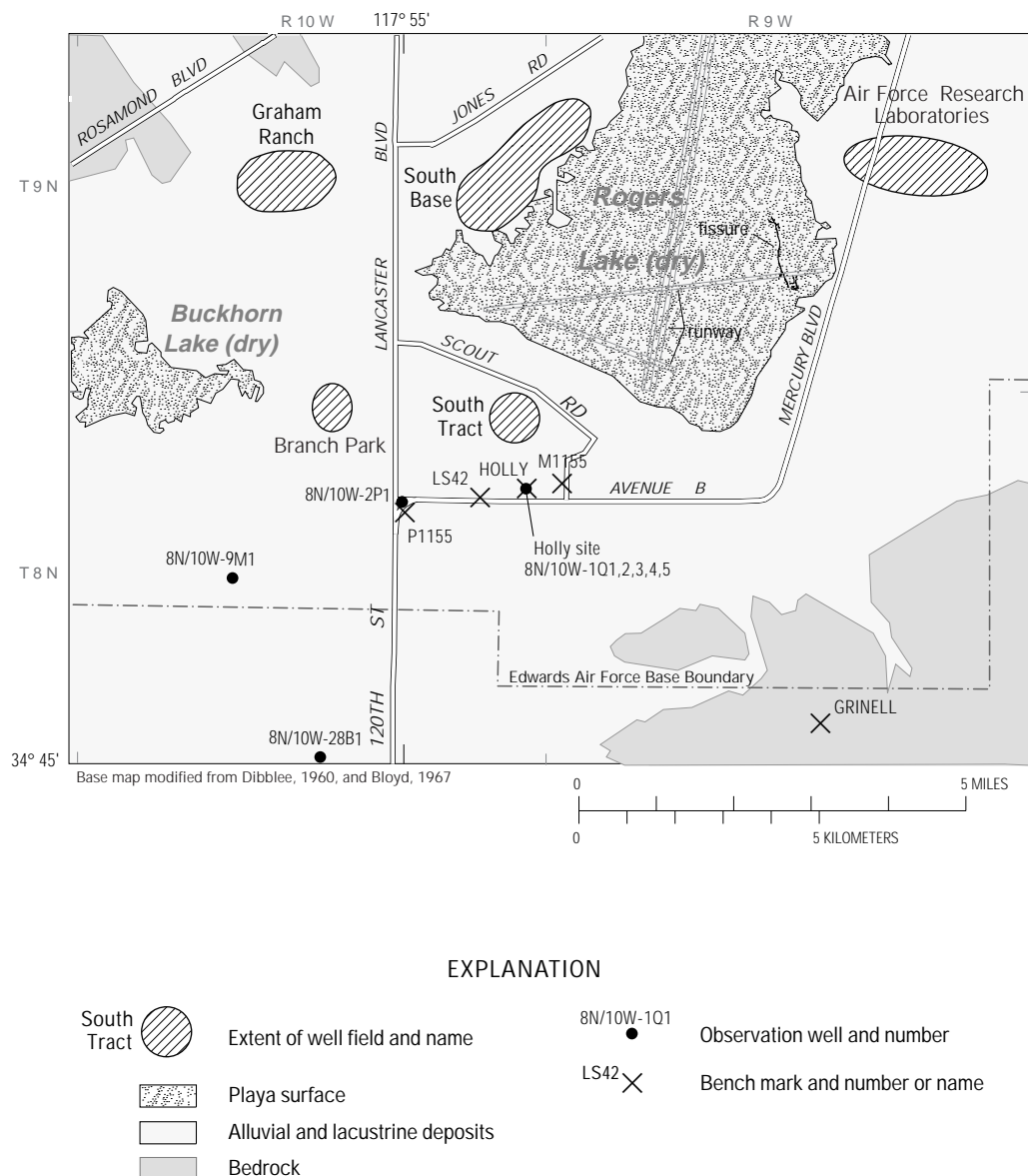


**Figure 3.** Location of selected well fields, observation wells, and bench marks near the Holly site (8N/10W-1Q) in the south-central part of Edwards Air Force Base, Antelope Valley, California. Areal extent of map is shown on figure 1.

assumption that the annual ground-water supply is equal to the estimated natural recharge (L.M. Takaichi, Kennedy/Jenks Consultants, unpub. data, 1995). Ground-water supplies throughout Antelope Valley and at EAFB are augmented by surface water imported from northern California by the State Water Project (SWP) by way of the California Aqueduct. The limited storage and delivery capacity of the SWP and the high degree of annual variability in water supplies owing to climatological and environmental factors make reliance on the ground-water supply necessary to sustain present and future levels of demand. Information about the physical processes of aquifer-system compaction at the Holly site may be useful not only to EAFB but also to those in the Antelope Valley who seek a balanced use of the ground-water resource with minimum additional risk from land subsidence.

## Purpose and Scope

The purpose of this report is to present ground-water level, aquifer-system compaction, and land subsidence data collected in the field and to present the results of simulations and analyses of aquifer-system compaction and land subsidence and the implications regarding future compaction and subsidence at the Holly site. Field measurements and simulations of aquifer-system compaction at the Holly site were used to constrain estimates of the critical properties that govern compaction of the aquitards. Formulations of vertical compression and expansion of the aquifer system to the applied stresses of ground-water-level changes were used to simulate historical subsidence and to predict possible future subsidence for selected scenarios of future ground-water-level changes at the Holly site. This study necessarily includes areas of Antelope Valley because the processes and properties explored at the Holly site are influenced by physical, hydrologic, and geologic boundaries that occur at the scale of the valley and because the processes and properties at the Holly site are being incorporated into regional models of ground-water flow and aquifer-system compaction of the Lancaster subbasin (fig. 2) (Tracy Nishikawa, U.S. Geological Survey, written commun., 1998; David Leighton, U.S. Geological Survey, written commun., 1998). Together, the site-specific (Holly site) and the regional models of EAFB may be useful to ground-water and land-subsidence management at EAFB.

More than 7 years of paired ground-water-level and aquifer-system compaction measurements made in the upper 1,100 ft at the Holly site were analyzed for this study. The focus of the analyses was the role of the clay deposits, both the thick aquitards and the thinner interbedded aquitards, in aquifer-system compaction. The analyses and simulations of aquifer-system compaction were based on established theories of aquitard drainage (Helm, 1975) and were done using one-dimensional models of coupled ground-water flow and skeletal deformation based on the elastic and inelastic compressibilities of the aquifers and the aquitards (Leake, 1990). Historical ground-water-level and land-subsidence data were used to constrain simulations of historical aquifer-system compaction and of land subsidence at the Holly site during the period 1908–97. Compaction and land subsidence were simulated to the year 2026 for one scenario in which water-level declines continued at the 1990's rates. Two scenarios were simulated to the year 2096 for possible future ground-water-level changes—static water levels and recovery.

## Location

Antelope Valley is an arid valley in the western corner of the Mojave Desert, about 50 mi northeast of Los Angeles (fig. 1). The triangular-shaped valley is bounded on the southwest by the San Gabriel Mountains, on the northwest by the Tehachapi Mountains, and on the north and the east by lower hills, ridges, and buttes. It is a topographically closed basin with surface-water runoff terminating in several playas. Average annual precipitation varies from more than 36 inches near the crests of the San Gabriel Mountains to less than 3 inches on the valley floor (Rantz, 1969). Antelope Valley covers nearly 2,400 mi<sup>2</sup> and includes the cities of Lancaster and Palmdale and EAFB.

EAFB encompasses nearly 470 mi<sup>2</sup> and includes the two prominent playas, Rogers and Rosamond Lakes. Both playas are used as emergency landing surfaces. Rogers Lake was once routinely used to land space shuttles, but presently is used only as an alternate landing site for the space shuttles and other aircraft. The Holly site is about 2 mi south of the southern shoreline of Rogers Lake and less than 0.75 mi south of the southernmost water-supply well in the South Tract well field (fig. 3).

## Development of the Ground-Water Resource and Resulting Land Subsidence

Prior to 1908, the early settlers in Antelope Valley drilled more than 300 wells in the central and lower parts of the valley; many of the wells tapped shallow artesian aquifers and flowed without pumping. The area of these flowing wells (fig. 4) covered more than 240 mi<sup>2</sup> (Johnson, 1911) and included what is presently the southern part of EAFB. Many of the wells

were drilled for domestic supply to obtain patents for government land during a period of homesteading and some were drilled to water livestock and crops (Johnson, 1911). Because the soil in the region of flowing wells was alkaline, attempts to farm the land were limited and, therefore, the quantity of water from the flowing wells used for irrigation probably was small (Thompson, 1929). Near the heads of the alluvial fans along the south side of the valley, the settlers diverted surface water from mountain streams primarily to

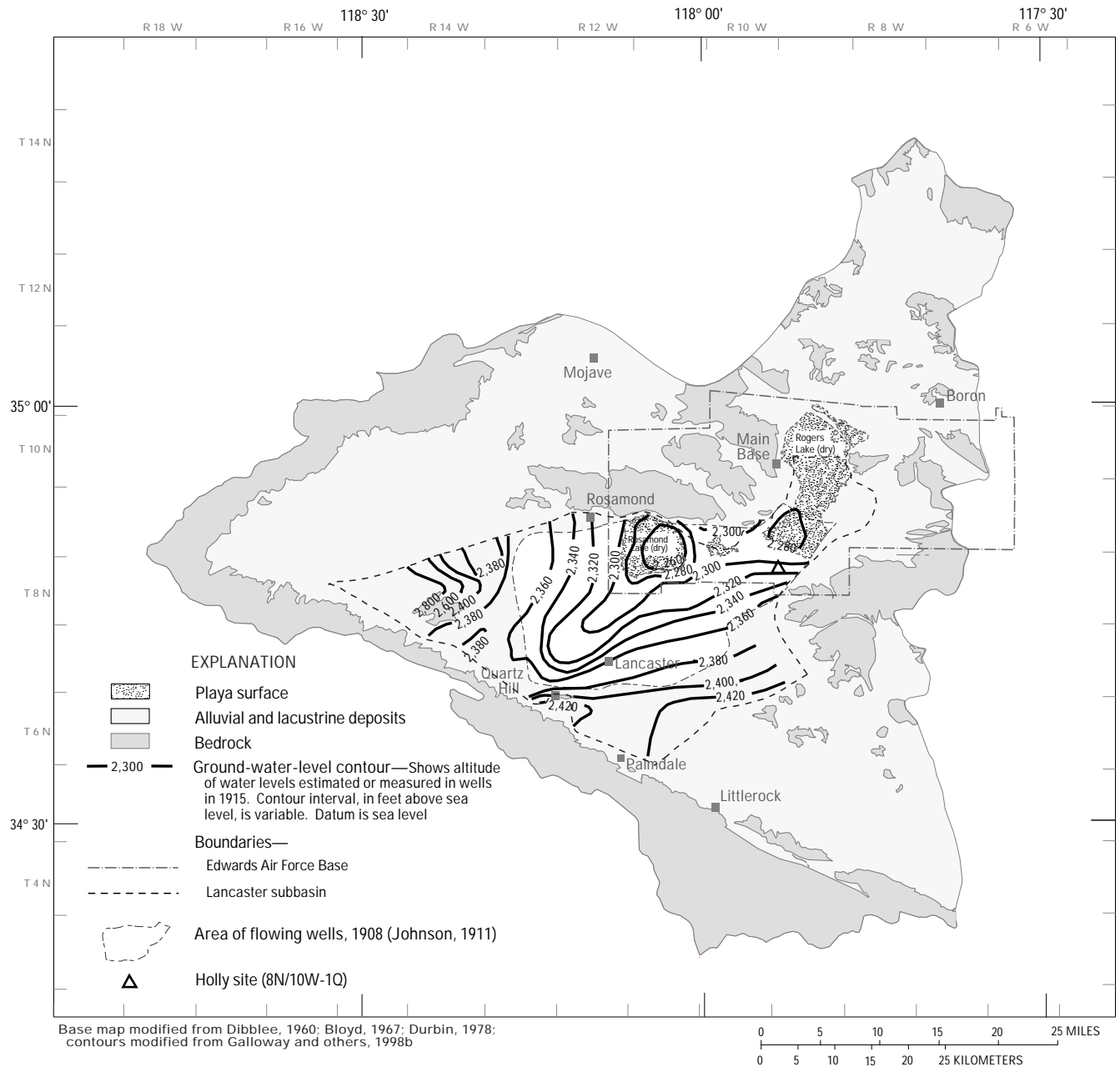


Figure 4. Ground-water levels in the Lancaster subbasin, Antelope Valley, California, 1915.

irrigate orchards. These early irrigation systems, which were dependent on the surface streams, failed to provide a stable and reliable water source for crop production and soon were augmented by ground-water systems.

By 1952, the areal extent of the flowing wells had decreased from 240 mi<sup>2</sup> to only 3 mi<sup>2</sup> (Dutcher and Worts, 1963). During the early 1950s, annual ground-water pumpage for crop production reached peak levels of about 350,000 to 400,000 acre-ft (Snyder, 1955; David Leighton, U.S. Geological Survey, written commun., 1999). Ground water remained the principal source of water supply but in the mid-1970s was augmented by imported water delivered from the newly constructed California Aqueduct as part of the State Water Project. By this time, irrigated acreage and ground-water use for crop production were steadily declining owing to, in part, the increasing depths to ground water and the associated costs of pumping. During the 1980s, the population of Antelope Valley nearly doubled and the predominant land use shifted from irrigated agriculture to urban; ground-water use again increased. By 1991, agricultural water use was only 20 percent of the peak levels of the late 1950s, and the predominant water demand was for municipal–industrial water use (Galloway and others, 1998b). Irrigated acreage had decreased by 80 percent, while urban land use had increased by more than 200 percent.

Historically, ground-water supplies have met 50 to 90 percent of the annual water demand in Antelope Valley and, until recently, nearly all the water demand at EAFB. For example, ground water provided about 60 percent of the total water supply in Antelope Valley (Templin and others, 1995; David Leighton, U.S. Geological Survey, written commun., 1999) during the nondrought year of 1992, a year that followed a prolonged (1987–91) drought in California. Variability in precipitation and in the amount of surface water delivered from the California Aqueduct emphasizes the importance of managing the local ground-water resources to meet present and future water demands and to mitigate land subsidence problems (Galloway and others, 1998b). Although recent pumpage is less than at any time since the 1930s, the 75,000 acre-ft (estimate for 1995; David Leighton, U.S. Geological Survey, written commun., 1999) of ground water pumped annually to meet water demand continues to exceed the estimated mean natural recharge to the valley (about 41,000 acre-ft; Durbin, 1978). Although the spatial distribution of recent (1990s) pumpage and

ground-water-level changes is substantially different than during the agricultural era, ground-water levels continue to decline in urban areas, near EAFB, and in some isolated agricultural areas (Carlson and Phillips, 1998; Galloway and others, 1998b).

Problems related to land subsidence thus far have been subordinate to problems of ground-water supply. The costs of pumping ground water played a major role in the reduction of agricultural ground-water use but is not yet a limiting factor for the development of municipal–industrial ground-water supplies. Beginning in 1972, the importation of surface water from northern California to Antelope Valley by way of the State Water Project California Aqueduct (fig. 1) has provided an alternate water resource, sustaining the growth of municipal–industrial water demand that, for the most part, is dependent on ground-water supplies. The limited storage and delivery capacity of the State Water Project and the high degree of annual variability in water supplies owing to climatological and environmental factors make reliance on the ground-water supply necessary to sustain present and future levels of demand. The economic and environmental consequences of continued ground-water mining (withdrawals in excess of recharge)—aquifer-system compaction and land subsidence—pose challenges to users of the depleted resource and may eventually play a role in limiting the development of municipal–industrial supplies.

## Previous Studies

Several studies of land subsidence have been done in the Antelope Valley. The earliest recognition of land subsidence in the valley may have been by the Office of the County Engineer of Los Angeles County as a result of surveys made between 1928 and 1960 (Mankey, 1963). More recently, Blodgett and Williams (1992) reported land subsidence and related land-surface deformation affecting the playas at EAFB; their report also describes the construction of the Holly extensometer. Londquist and others (1993) reported compaction and ground-water levels measured at the Holly site between May 1990 and November 1991, presented preliminary maps of land subsidence in the vicinity of EAFB, and described geologic and hydrogeologic information collected between 1989 and 1991 as part of hydrogeologic investigations to characterize the aquifer system at EAFB. Ikehara and Phillips

(1994) compared the results of repeat geodetic measurements made using spirit leveling and global positioning system surveys and calculated that more than 6.6 ft of subsidence attributable to aquifer-system compaction had occurred in Antelope Valley between 1926 and 1992. Ikehara and Phillips (1994) provided a summary of land-surface-elevation measurements made in Antelope Valley prior to 1992. Freeman (1996) described equipment and methods used to collect, record, process, and electronically store time-series data from EAFB monitoring sites, including the Holly site. Galloway and others (1998a) used interferometric synthetic aperture radar (InSAR) to detect and map land-surface displacements in Antelope Valley attributable to aquifer-system compaction that occurred between October 1993 and December 1995.

## HYDROGEOLOGIC SETTING

The Mojave Desert in California is a wedge-shaped block bounded by the San Andreas Fault Zone on the southwest, the Garlock Fault Zone on the northwest, and the Colorado River on the east (fig. 1). Uplifts of the San Gabriel and Tehachapi Mountains isolated the Mojave Desert from the Pacific Coast and created the interior drainage basins of the western Mojave Desert, such as the Antelope Valley (Hewett, 1954). Londquist and others (1993) provide a more complete and detailed description of the regional hydrogeologic setting of the Antelope Valley and its evolution.

The Holly site at EAFB is just south of the South Tract well field and Rogers Lake (fig. 3). Much of the site-specific, subsurface geologic and geophysical information was derived from boreholes drilled previously at or near the Holly site (Londquist and others, 1993; Rewis, 1993) and from several earlier studies (Johnson, 1911; Thompson, 1929; Dutcher and Worts, 1963; Durbin, 1978).

## Geologic Framework

Antelope Valley overlies five large sediment-filled structural basins—the Cajon Basin, the East Antelope Basin, the Kramer Basin, the Mojave Basin, and the West Antelope Basin (fig. 2)—separated by areas of extensively faulted, elevated bedrock (Bloyd, 1967). EAFB overlies two of these basins, the East

Antelope Basin and the Kramer Basin. These basins consist of Tertiary and Quaternary sediments eroded from the adjacent bedrock highlands; these sediments are more than 5,000 and 2,000 ft thick, respectively (Benda and others, 1960; Mabey, 1960). However, gravity measurements made in 1989 indicate thicknesses may be as much as 10,000 ft in the East Antelope Basin (Mabey, 1960). These measurements also indicate that this basin is an elongated northeast to southwest oriented trough; the northeast part is beneath the southwestern region of Rogers Lake and the southwest part is near Lancaster. The Kramer structural basin is more irregularly shaped and centered northeast of Rogers Lake (Mabey, 1960).

Strike-slip and normal faults are the major geologic structures in the western part of the Mojave block with some minor, localized folding. The San Andreas and Garlock Fault Zones are active strike-slip fault zones. Major faults in the Mojave Desert that intersect EAFB include Willow Springs, Bissell Hills-El Mirage, Blake Ranch, Spring, Kramer Hills, and Muroc Faults, and several unnamed faults that are collectively referred to as the Antelope Valley Fault Zone (fig. 2).

On and near EAFB, the bedrock complex consists of pre-Cenozoic igneous rocks and consolidated Tertiary sedimentary rocks (Hewett, 1954; Dibblee, 1963). Quartz monzonite is the predominant igneous rock type exposed in the hills at EAFB. Continental deposits of late Tertiary and early Quaternary age unconformably overlie the basement complex in the hills near EAFB (Dutcher and Worts, 1963). Lithologic logs for deep wells at EAFB suggest that these deposits overlie the basement complex within the Lancaster subbasin. The continental deposits consist of poorly sorted, well indurated conglomerate, sandstone, siltstone, shale, limestone, dolomite, volcanic tuff, and breccia (Dibblee, 1960; Dutcher and Worts, 1963).

A succession of alluvial deposits of Quaternary age overlies the continental deposits. These deposits are the result of erosion of the San Gabriel and the Tehachapi Mountains. The alluvium consists of unconsolidated to moderately indurated, poorly sorted gravel, sand, silt, and clay deposited as alluvial fans or deposited along stream channels and floodplains, and of interbedded lacustrine sediments deposited in pluvial times. Older units within the alluvium typically are more consolidated and indurated than the younger units (Dutcher and Worts, 1963; Durbin, 1978). Lacustrine deposits interbedded within the alluvium consist

of fine-grained sand, silt, and clay that accumulated in a relatively large lake, or marsh, that at times covered large parts of the Antelope Valley (Dibblee, 1967). These lacustrine deposits consist primarily of thick layers of blue-green silty clay and a brown clay with interbedded sand and silty-sand layers. Near the southern limit of the valley, the lacustrine deposits are beneath as much as 800-900 ft of alluvium, but near the northern limit the lacustrine deposits are exposed at land surface. Rosamond Lake and Rogers Lake playas are underlain by about 100 ft of fine-grained lacustrine deposits from ancient Lake Thompson, which covered most of Antelope Valley in Pleistocene time (Motts and Carpenter, 1970).

Surface geophysical studies including gravity surveys, seismic-refraction surveys, and vertical electric soundings were done at EAFB in 1989. These were done to define the basement surface, to map the subsurface distribution of fine-grained and coarse-grained sediments, and to identify potential aquifers and areas where ground-water withdrawals might further intensify land-subsidence problems (Londquist and others, 1993). In addition to these surveys, numerous borehole-geophysical surveys were made at the completion of the deepest borehole at each of several monitoring cluster wells constructed at EAFB during 1989–92; the surveys are described in Londquist and others (1993) and Rewis (1993). Surface geophysical information on parts of EAFB and site-specific borehole geophysical information on EAFB, including the Holly site, aid in delineation of the areal and vertical extent of aquifer-system compaction and land subsidence.

At the Holly site, the subsurface geology consists of alluvial and lacustrine deposits from land surface to about 840 ft below land surface, continental deposits from about 840 to 1,075 ft below land surface, and decomposed basement complex at 1,075 ft below land surface. The Holly site is contained within the East Antelope structural basin and the Lancaster ground-water subbasin (fig. 2). The alluvium consists of arkosic interbedded gravel, sand, and clay (fig. 5A) and the lacustrine deposits consist of massive clay. Lithologic and geophysical logs of the Holly site reveal the general heterogeneity, and the resistivity logs show two relatively thick fine-grained units 120 to 186 ft (principally clay) and 302 to 365 ft below land surface (fig. 5B). The upper fine-grained unit is interpreted as a regionally extensive lacustrine blue-clay unit, as defined by Dutcher and Worts (1963); it confines the

middle and lower aquifers at the Holly site. The deeper fine-grained unit, which is entirely within the middle aquifer, is electrically more resistive and more heterogeneous than the upper fine-grained unit. Thinner aquitards, ranging from 1- to 18-ft thick, also are evident in the resistivity logs. The contact between the alluvium and underlying continental deposits is defined by an anomaly which occurs in the spontaneous potential and resistivity logs at 837.5 ft below land surface, below which the baseline of the resistivity logs shift to a lower resistivity by about 10 ohm-m. This resistivity shift is interpreted as a chemical transition to more highly conductive fluid; the specific conductance of water sampled from piezometers screened below this shift is about 3 to 4 times higher than the water sampled from piezometers screened above the shift (Londquist and others, 1993). Coarse-grained quartz monzonite, interpreted as decomposed basement bedrock, was encountered at 1,075 ft below land surface and cored in the interval 1,097 to 1,107 ft (fig. 5A) (Londquist and others, 1993).

## Aquifer Systems

Before the development of agriculture in the Antelope Valley in the early 1900s, ground water flowed from recharge areas near the San Gabriel and the Tehachapi Mountains toward meadows, marshes, and springs (now dry) near the center of the valley. Most of this ground water discharged by evapotranspiration. The primary source of natural recharge to the Antelope Valley is stream runoff that infiltrates the thick alluvial fans emanating from mountain fronts along Big Rock Wash, Little Rock Wash, and Amargosa Creek among others (fig. 1). Estimates of the mean annual natural ground-water recharge to the valley range from 40,700 to 58,000 acre-ft (California Department of Water Resources, 1947; Snyder, 1955; Weir and others, 1965; Durbin, 1978). Ground water no longer discharges into the meadows that once thrived near the center of the valley because ground-water levels have been lowered extensively by nearly a century of ground-water resource development. Presently (1990s), nearly all aquifer-system discharge occurs through pumping wells.

In Antelope Valley, basin-fill sediments constitute a vast ground-water basin. Conceptually, the ground-water basin has been subdivided into 12 subbasins (Thayer, 1946) of which the Lancaster subbasin





(fig. 2), located in the central part of the valley and underlying a part of EAFB, is the largest and most developed. The aquifer systems in the Lancaster subbasin consist of transmissive aquifers interbedded with relatively nontransmissive aquitards (Dutcher and Worts, 1963; Durbin, 1978; Londquist and others, 1993).

Conceptually, the ground-water flow system in the Antelope Valley was divided into three aquifers—a shallow unconfined aquifer (the upper aquifer), which is thin and generally unproductive; a deeper and thicker confined aquifer (the middle aquifer), which is where most of the ground water is produced; and the deepest confined aquifer (the lower aquifer), which is thinner and produces less water than the middle aquifer (fig. 6) (David Leighton, U.S. Geological Survey, written commun., 1998). In previous reports (Dutcher and

Worts, 1963; Bloyd, 1967; Durbin, 1978; Londquist and others, 1993; Ikehara and Phillips, 1994; Rewis, 1995; Carlson and others, 1998; Galloway and others, 1998b), the upper aquifer is termed the “principal aquifer” and the middle and lower aquifers are collectively termed the “deep aquifer.” More recent data indicate that the system can be divided into three aquifers in the Lancaster subbasin. These aquifers consist of poorly consolidated, variably sorted beds of clay, silt, sand, and gravel. At moderate depths, the upper aquifer is partly confined by fine-grained interbedded aquitards, which, in places, is separated from the middle aquifer by laterally extensive, thick lacustrine deposits (fig. 6). These lacustrine deposits, commonly referred to as the blue clay, confine parts of the middle aquifer, except near the northern part of Rogers Lake where the deposits thin to extinction. At Lancaster, which is near the center of the Lancaster subbasin, the confining clay bed is about 150 ft thick with the upper boundary of the bed about 750 ft below land surface (from lithologic log data of cluster well 7N/12W-27F5-8 from U.S. Geological Survey well file).

The ground-water system at the Holly site is part of the Lancaster subbasin and consists of two aquifer systems—an unconfined system and a confined system, which are separated by lacustrine deposits that form a confining unit (fig. 7) (Londquist and others, 1993). The Holly site is near the northern extent of the unconfined aquifer system. At this site, the upper aquifer is unconfined and has a water table about 55 ft below land surface and a saturated thickness of about 65 ft. The confined-aquifer system at the site extends about 900 ft below the confining unit, or nearly 1,100 ft below land surface, where it is underlain by weathered bedrock (figs. 5A and 7). Within the confined-aquifer system, the middle and lower aquifers were defined on the basis of water chemistry, ground-water levels, and geophysical measurements (Londquist and others, 1993). Presently, ground water in the confined-aquifer system at the Holly site flows northwestward toward a pumping depression within and surrounding the South Tract well field; most of the ground water pumped in this well field is produced from the middle aquifer.

Hydraulic properties determined from pumping tests of the middle aquifer in the vicinity of the Holly site (summarized by Londquist and others, 1993), ranged from 4,600 to 25,900 ft<sup>2</sup>/d for transmissivity,  $3.6 \times 10^{-4}$  to  $2.3 \times 10^{-3}$  for storage coefficient, and  $9.2 \times 10^{-2}$  to  $1.7 \times 10^{-2}$  ft/d for the vertical hydraulic conductivity of the confining unit. An estimate of the

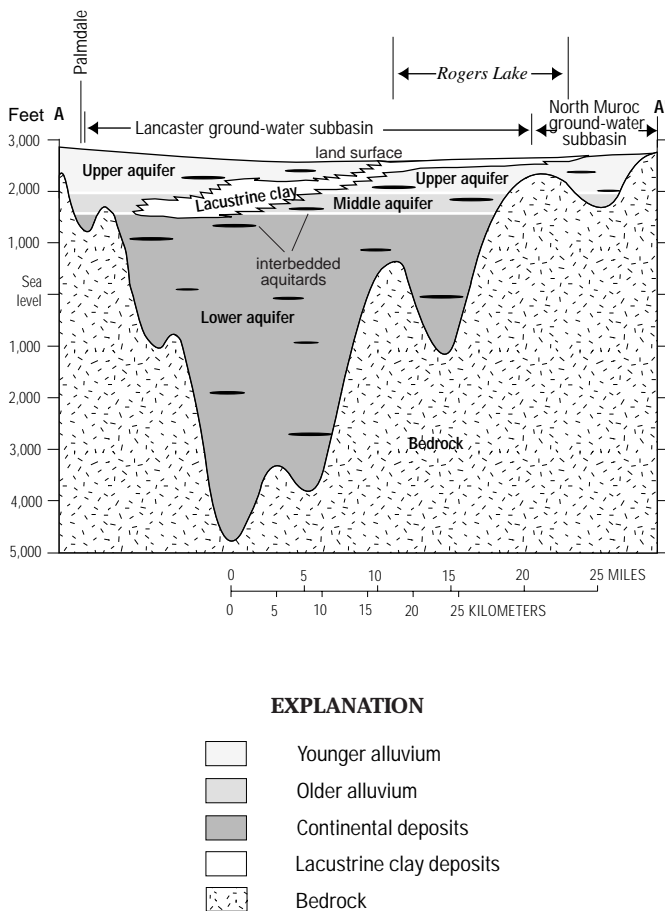


**Figure 6.** Generalized geologic section showing relation of lacustrine deposits to younger and older alluvium and aquifers in the Lancaster and North Muroc subbasins, Edwards Air Force Base, Antelope Valley, California. Line of section shown in figure 2.



specific storage,  $7.38 \times 10^{-6} \text{ ft}^{-1}$ , and an upper limiting estimate for aquifer vertical hydraulic conductivity,  $2.0 \times 10^{-2} \text{ ft/d}$ , for the lower aquifer were made from water-level responses to theoretical earth tides and atmospheric loading measured in piezometer HO-1 at the Holly site (Rummler, 1996). The responses of a well in the Graham Ranch area of EAFB (fig. 3) to theoretical earth tides, atmospheric loading, and the 1992 earthquake at Landers, California, were used to estimate aquifer specific storage,  $4.57 \times 10^{-7} \text{ ft}^{-1}$ , and aquifer vertical hydraulic conductivity,  $1.9 \times 10^{-2} \text{ ft/d}$  (Galloway, 1993). The hydraulic tests and methods used to compute these estimates are limited by design

and theoretical assumptions to the elastic range of the aquifer system's response. As such, these storage estimates are more representative of storage attributable to the aquifers rather than the aquitards.

Durbin (1978) estimated hydraulic properties for the deep aquifer (middle and lower aquifers combined) within the area of EAFB, including the area of the Holly site, for purposes of modeling ground-water flow in Antelope Valley. These estimates are  $1.0 \times 10^{-3}$  for storage coefficient and range from 1,700 to 14,000  $\text{ft}^2/\text{d}$  for transmissivity. The Durbin (1978) model uses  $1.0 \times 10^{-2} \text{ ft/d}$  for the vertical hydraulic conductivity of

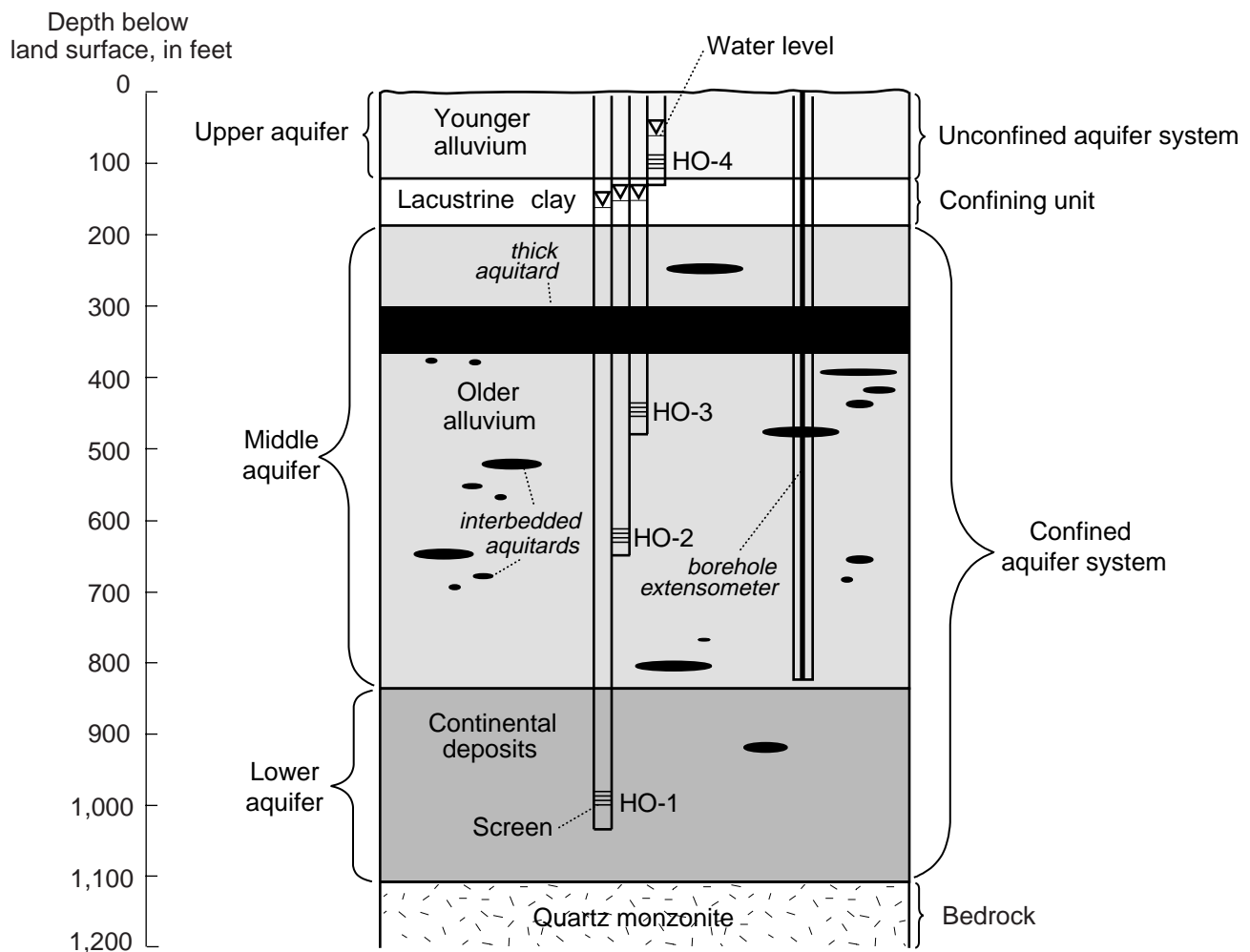


**Figure 7.** Conceptual model of the aquifer systems at the Holly site (8N/10W-1Q) including the piezometers (HO-1, HO-2, HO-3, and HO-4) and the borehole extensometer, Edwards Air Force Base, Antelope Valley, California. (Modified from Londquist and others, 1993)

the confining unit and does not explicitly simulate aquifer-system compaction.

### Ground-Water Levels

In 1915, prior to significant ground-water development in the upper aquifer of the Lancaster subbasin, the potentiometric surface was near or above land surface in many areas (fig. 4) (Durbin, 1978). Between 1915 and 1991, ground-water levels declined more than 100 ft throughout most of the Lancaster subbasin and as much as 300 ft near the southern and western margins of the subbasin (fig. 8). The hydrograph for well 7N/12W-15F1, which is in Lancaster, shows seasonal water-level fluctuations and a longer-period, monotonic water-level decline of more than 150 ft since the early 1940s (fig. 8).

East of Lancaster, water levels at well 7N/10W-05E1 recovered nearly 50 ft between 1970 and 1991 (fig. 8) owing to a reduction in irrigated acreage and ground-water pumping in this region. Ground-water levels presently are recovering in the eastern and western rural areas of the subbasin, areas that previously were intensely pumped to irrigate crops. Water levels continue to decline in the urban areas around Lancaster and Palmdale, in isolated agricultural areas where ground-water pumpage is high, and at EAFB. Recent estimates of annual ground-water pumpage in Antelope Valley [about 75,000 acre-ft in 1995 (David Leighton, U.S. Geological Survey, written commun., 1999)] are about one-fourth of the annual peak volumes pumped during the 1950s (more than 300,000 acre-ft), but the present quantity continues to exceed (overdraft) the estimated annual natural ground-water recharge.

Prior to the development of ground-water resources in Antelope Valley and until about 1914 to 1919, the confined aquifer system in the southern area of Rogers Lake playa and in adjacent areas south and west of the playa likely was under artesian conditions (Johnson, 1911; Thompson, 1929). Thompson (1929) described the playa surface as “puffy, ‘self-rising’ ground... covered with more or less alkali.” Prior to 1940, hydraulic heads throughout the Lancaster subbasin generally were higher in the confined aquifer system than in the unconfined aquifer system, and it is likely that ground water discharged through the playa surface by evaporation. The Buckhorn Springs (Waring, 1915), now dry, and other springs nearer to Rogers Lake, also now dry (Dutcher and Worts, 1963), supported marsh vegetation. As a result of increased pumpage in both the unconfined and confined aquifer

systems after 1940, heads in the middle and lower aquifers became lower than heads in the upper aquifer and the shallow water-bearing zones. Ground water in the water-bearing zones in the shallow subsurface of the unconfined aquifer system began to flow downward to the confined aquifer system rather than flowing upward and discharging from springs (Motts and Carpenter, 1970).

Since 1951, ground water has been the principal source of water supply for EAFB, where more than 150 ft of ground-water-level decline has affected much of the southern Rogers Lake area. Presently (1990s), ground-water levels in these areas continue to fluctuate tens of feet in response to seasonal pumping, with water levels in many wells showing long-term declines averaging more than 1 ft/yr. The long-term decline in ground-water levels is shown by the hydrographs of wells 8N/10W-28B1 and 9N/10W-24C1, which are about 5 mi southwest and 5 mi north of the Holly site, respectively (fig. 9). In 1999, ground water in the unconfined, upper aquifer at the Holly site was about 57 ft below land surface, whereas ground water in the middle and lower aquifers at the Holly site was confined and generally 100 to 110 ft lower than the ground-water levels in the upper aquifer (fig. 7). Seasonal variation in pumping at the South Tract wells controls the seasonal fluctuations in the ground-water levels in the middle and lower aquifers, which constitute the more transmissive parts of the confined aquifer system at the Holly site.

Since 1990, the U.S. Geological Survey routinely has measured the ground-water levels in four piezometers (fig. 7) constructed in two boreholes at the Holly site. The time-series measurements consist of periodic (about monthly) measurements made using graduated tapes and continuous (about hourly) measurements made using pressure transducers and recorded with dataloggers. The methods of measurement and data processing are discussed in detail in Freeman (1996). Hydrographs for each of the Holly piezometers (HO-1, HO-2, HO-3, and HO-4) for May 1990 through December 1997 are shown in figure 10. For this period, piezometer HO-4, completed in the upper aquifer (unconfined), shows a steady water-level decline (nearly 5 ft) without a significant seasonal variation, whereas water levels in piezometers HO-2 and HO-3, completed in the middle aquifer, nearly track each other and show marked seasonal changes ranging from 10 to 17 ft (fig. 10). Seasonal variations were smaller for the period 1990–93 compared with

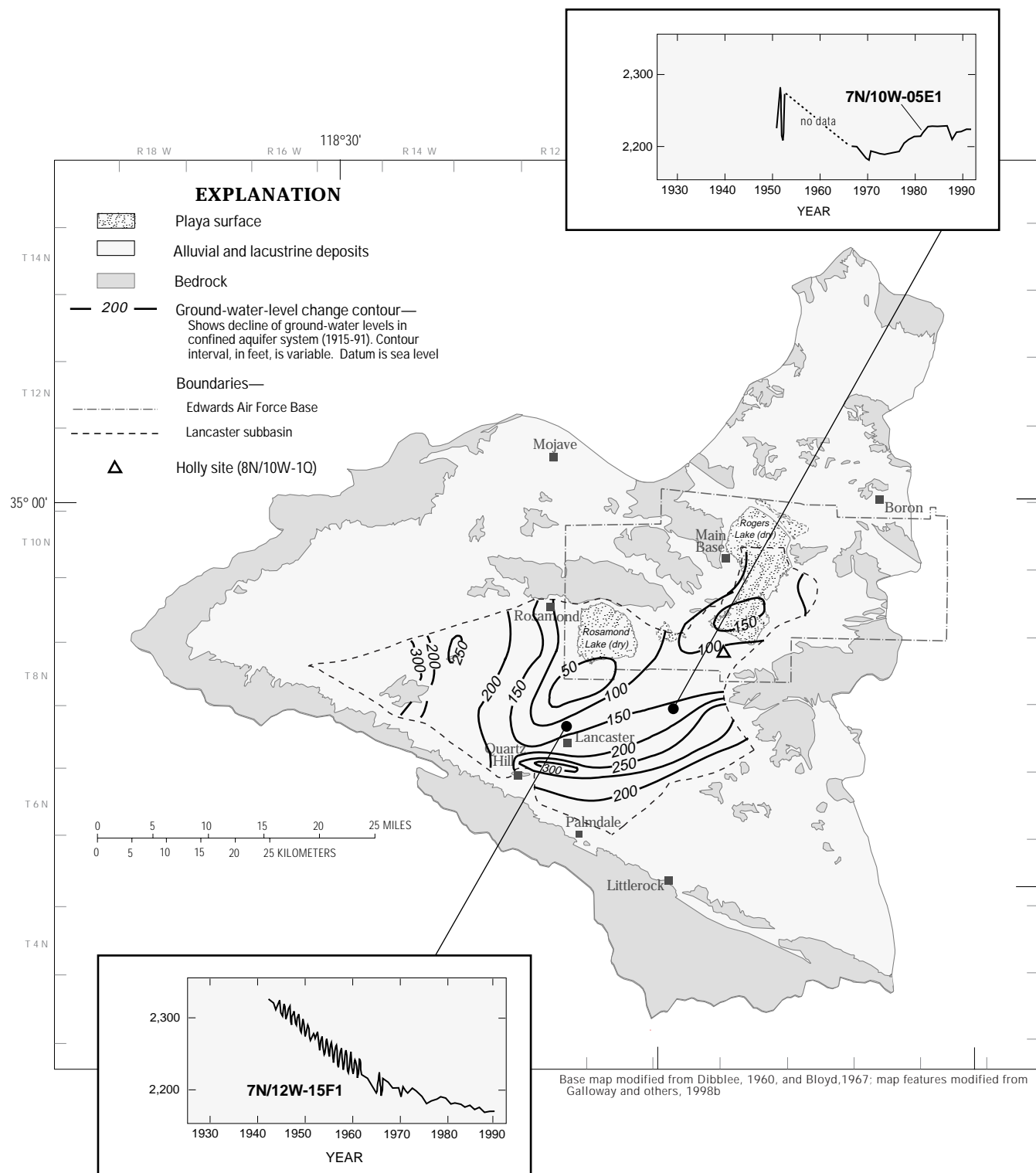


**Figure 8.** Change in ground-water levels in the Lancaster subbasin, Antelope Valley, California, 1915–91.

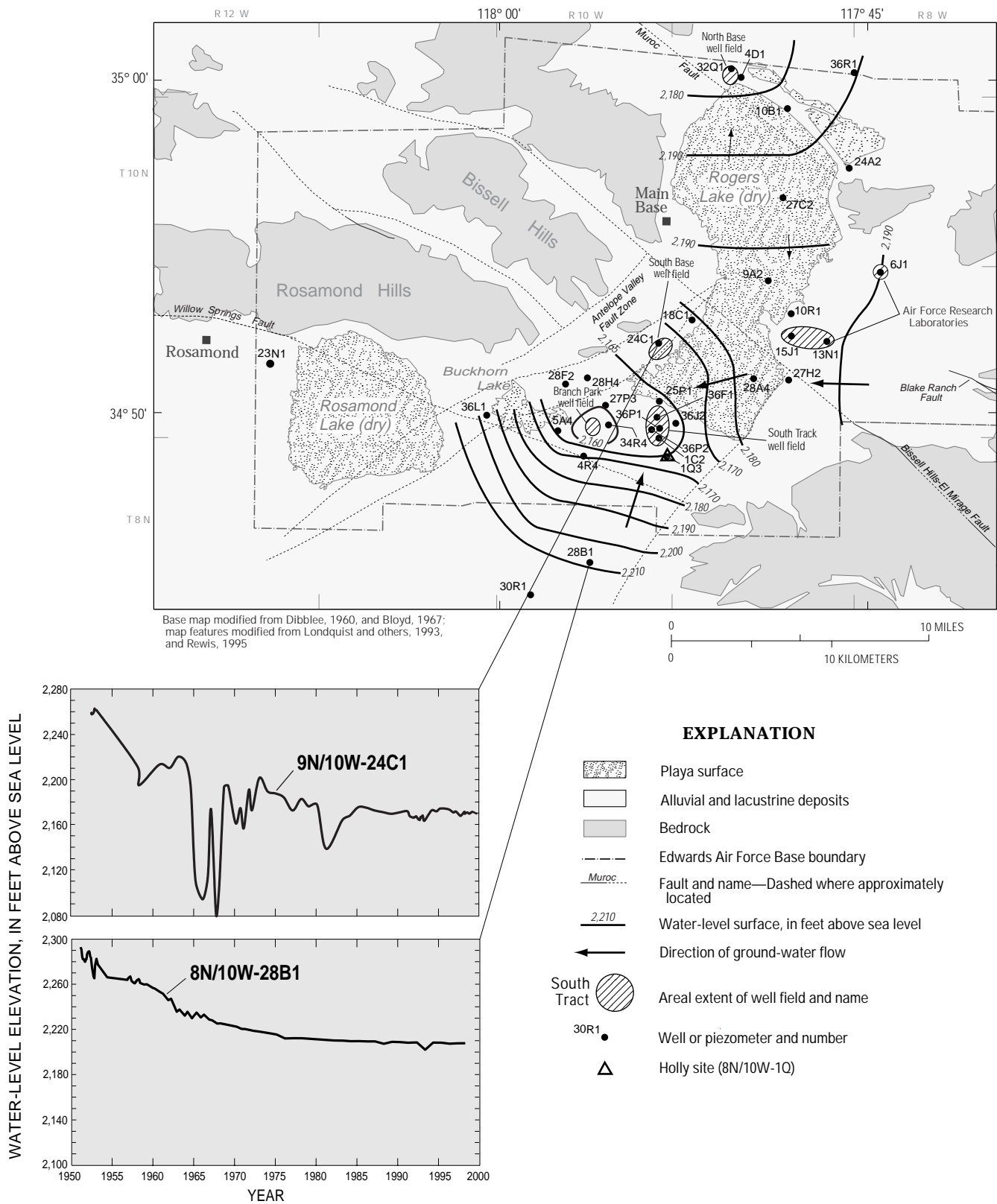


**Figure 9.** Water-level surface of the confined aquifer system, spring 1992, location of selected wells, and hydrographs of wells 8N/10W-28B1 (1951–97) and 9N/10W-24C1 (1952–99), Edwards Air Force Base, Antelope Valley, California.

variations for the period 1993–97. The largest seasonal variation occurred from winter to summer 1996.

Similar longer-term trends in the variation of the seasonal peaks and troughs are evident by the gradual increase in seasonal maximum and minimum water levels between 1990 and 1993 and by the general reversal in that trend between 1993 and 1997 (fig. 10). Both trends, seasonal and longer-term variation of the seasonal fluctuations in piezometers HO-2 and HO-3, which are completed in the middle aquifer within the production zone, are evident in the hydrograph for piezometer HO-1, completed in the lower aquifer below the production zone. However, the water-level response in piezometer HO-1 is attenuated and time lagged compared with the water-level responses in piezometers HO-2 and HO-3. The seasonal variation in piezometer HO-1 is only 4.5 to 8 ft (fig. 10), and the onsets of the winter recovery and summer drawdown lag the onsets of these periods in the piezometers (HO-2 and HO-3) screened in middle aquifer by about 1 month.

Water-level fluctuations at higher frequencies (hours to days) also are evident in the middle and lower aquifers at the Holly site. These fluctuations include responses to daily pumping cycles at the South Tract well field, barometric pressure variations, earth tides,

and earthquakes (fig. 11). The water-level response (HO-3) to daily pumping in the upper zone of the confined aquifer varies about 0.1 to 0.5 ft (fig. 11A) and is larger for piezometer HO-2 (not shown) and HO-3 than for HO-1.

Some of these data on water-level responses to daily pumping were used with compaction data to calculate aquifer elastic storage coefficients from the measured stress/strain response. Some of the longer-term seasonal water-level responses and the measured and estimated strain responses were used to compute aquitard inelastic storage coefficients. These methods and results are discussed in a later section of this report.

Variations in atmospheric pressure at land surface typically cause water-level changes in wells completed in confined and deep unconfined aquifers (Jacob, 1940; Weeks, 1979). For wells open to the atmosphere, such as the Holly piezometers, the water-level response is opposite in sense and generally only a fraction of the barometric pressure change (barometric efficiency of the well). Water levels in piezometers screened in the middle and lower aquifers typically fluctuate about 0.08 ft in response to daily changes in atmospheric pressure and fluctuate as much as 0.5 ft during some severe storms (fig. 11B). The three

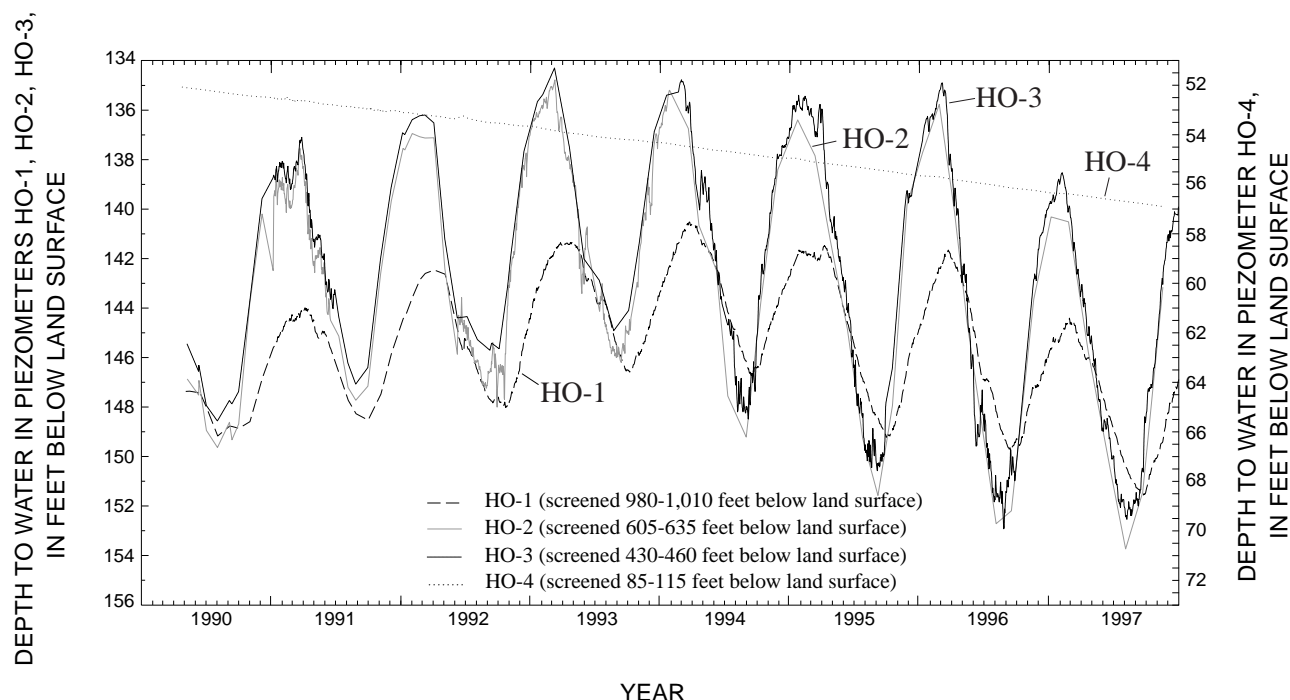


**Figure 10.** Water levels in piezometers HO-1, HO-2, HO-3, and HO-4 at the Holly site (8N/10W-1Q), Edwards Air Force Base, Antelope Valley, California, 1990–97.

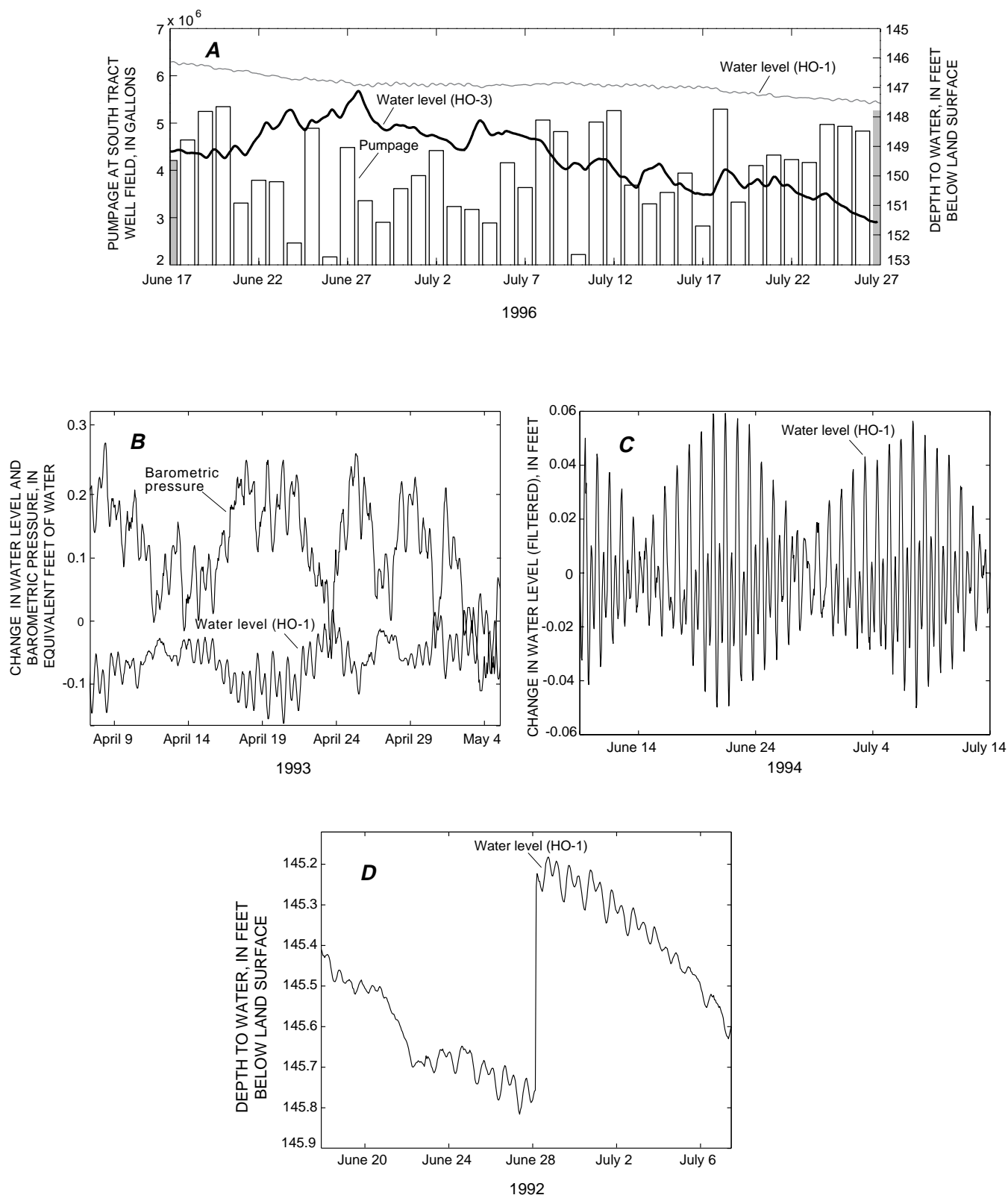


**Figure 11.** Water-level fluctuations in piezometers HO-1 and HO-3 at the Holly site (8N/10W-1Q), Edwards Air Force Base, Antelope Valley, California. **A**, Responses in piezometers HO-1 and HO-3 to daily ground-water pumping at the South Tract well field. **B**, Response in piezometer HO-1 to barometric pressure. **C**, Response in piezometer HO-1 to earth tides. **D**, Response in piezometer HO-1 to the June 28, 1992, earthquake at Landers, California.

piezometers screened in the middle and lower aquifers (HO-1, HO-2, and HO-3) also showed some sensitivity to earth tides, but HO-1 showed the most sensitivity (fig. 11C). Daily tidal fluctuations in HO-1 range from less than 0.02 to more than 0.05 ft during the tidal cycle. HO-1 was continuously monitored during the June 28, 1992, earthquake at Landers, California ( $M_L = 7.3$ ); the earthquake caused a 0.53 ft step increase in water level followed by an exponential decay (fig. 11D). Analyses indicate that the aquifer systems tapped by wells in the EAFB area were subjected to a coseismic volume strain step of about  $0.8 \times 10^{-6}$  compressive strain (Roeloffs and others, 1995).

### Aquifer-System Compaction

Long-term ground-water-level declines in Antelope Valley have resulted in the compaction of aquitards interspersed throughout the alluvial aquifer systems causing a vast, one-time release of “water of compaction” and land subsidence. Accompanying this release of water is a largely nonrecoverable reduction in the pore volume of the compacted aquitards and an overall reduction in the storage capacity of the aquifer system. This water of compaction is, in effect, a nonrenewable resource that can be mined only at the expense of incurring land subsidence and reducing ground-water storage capacity.

Aquifer-system compaction and resultant land subsidence in Antelope Valley, which includes EAFB, is attributed to ground-water-level declines (Blodgett and Williams, 1992; Londquist and others, 1993; Ikehara and Phillips, 1994; Galloway and others, 1998a). A historical relation (1926–92) between ground-water-level declines and regional land subsidence in the valley was established using water-level measurements and elevation data from spirit leveling and Global Positioning System (GPS) surveys (Ikehara and Phillips, 1994). By 1992, more than 6.6 ft of subsidence attributable to ground-water withdrawals had occurred in parts of Antelope Valley (fig. 12), with 290 mi<sup>2</sup> affected by more than 1 ft of land subsidence. Subsidence in the valley has permanently reduced aquifer-system storage by about 50,000 acre-ft (a conservative estimate by Ikehara and Phillips, 1994), an amount approximately equivalent to the estimated mean annual natural recharge of the valley. A radiometric-remote sensing technique, interferometric synthetic aperture radar (InSAR), was used to develop spatially detailed maps of land subsidence that occurred in Antelope Valley

between October 20, 1993, and December 22, 1995, (Galloway and others, 1998a). In Galloway and others (1998a), these maps show two localized areas of maximum subsidence (approximately 0.16 ft), one area near Lancaster (coincident with the area of historical maximum subsidence shown in fig. 12) and another area near southern Rogers Lake (approximately 8 mi south-southwest of the Holly site in fig. 12).

The distribution and the magnitude of subsidence (fig. 12) reflect, in part, the changing shape and position of the water-level surfaces of the aquifer (fig. 8) and the areal distribution and aggregate thickness of compressible sediments but also may be affected by uneven bedrock subcrops. Historically, the largest amounts of subsidence have occurred in two areas—one area centered in Lancaster and the other area about 10 mi east of Lancaster (fig. 12), where large quantities of ground water were once pumped for irrigation and where the aggregate thickness of fine-grained, compressible sediments is substantial. In general, there is good correlation between the area of flowing wells in 1908 reported by Johnson (1911) and the mapped area of historical land subsidence (fig. 12). Despite the large water-level declines along the western and southern margins of the Antelope Valley (fig. 8), no significant land subsidence has been measured in these areas (fig. 12). This lack of significant subsidence may be explained by the relative absence of fine-grained, compressible sediments in recent and older buried alluvial fans occurring in these areas. The thick, laterally extensive lacustrine deposits present in the central part of the subbasin are absent in the western part of the subbasin and in the extreme southern part of the subbasin near Palmdale (figs. 2 and 6). No appreciable thickness of interbedded aquitards has been mapped in the upper aquifer in these regions (Durbin, 1978; Londquist and others, 1993).

Differential land subsidence in Antelope Valley has caused the formation of earth fissures (figs. 2 and 12) and has altered surface drainage gradients, contributing to erosion and flooding problems; these problems are particularly evident on Rogers Lake playa at EAFB (Dinehart and McPherson, 1998). In January 1991, an earth fissure ruptured the surface of Rogers Lake (fig. 3) prompting the closure of the southern part of the lakebed to aircraft operations, including landings of the National Aeronautics and Space Administration (NASA) space shuttles (Blodgett and Williams, 1992). The fissure was as much as 6-ft wide and at least 12-ft

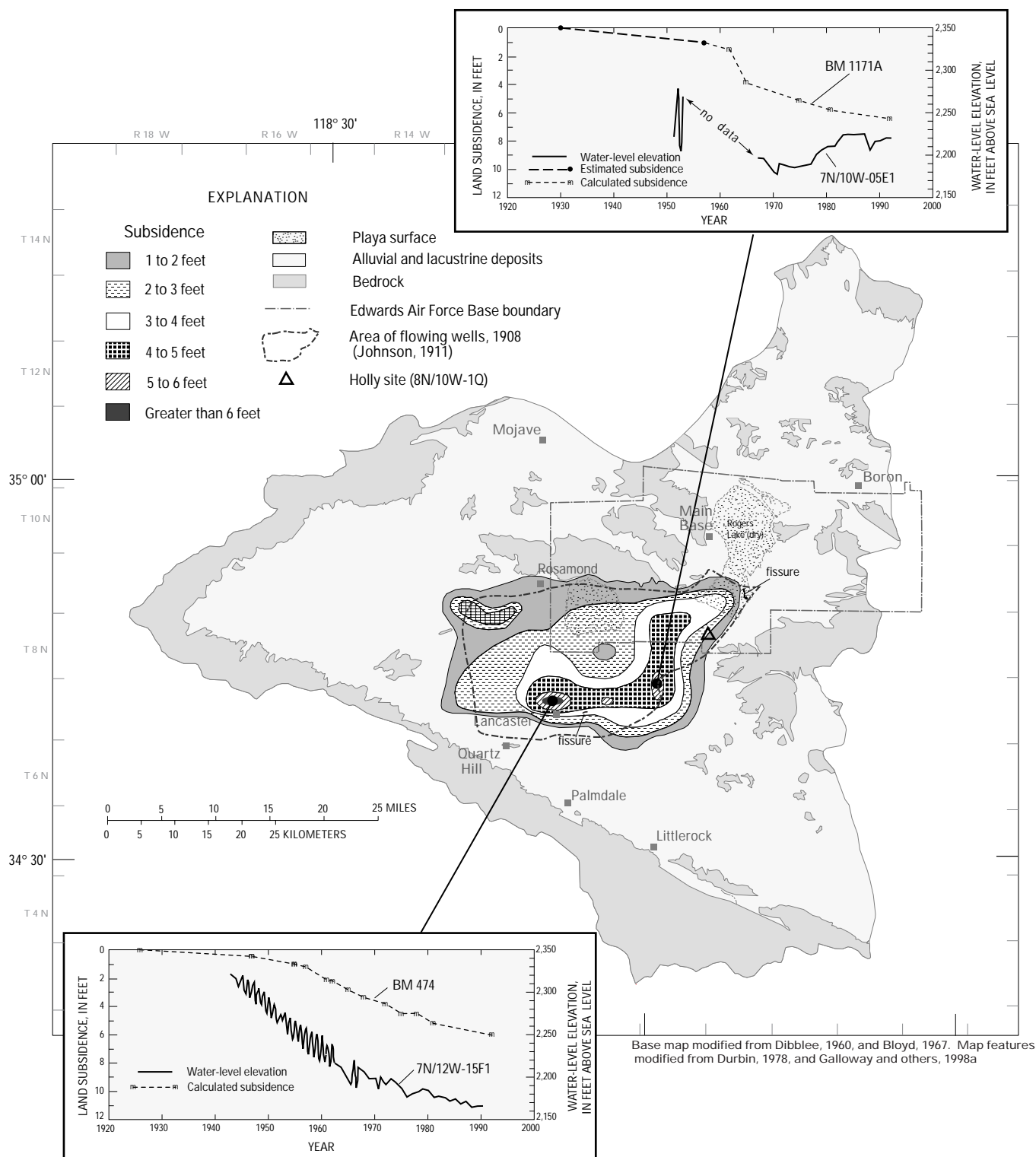


**Figure 12.** Area of flowing wells, land subsidence, and two fissures in Antelope Valley, California, for the period about 1930–92, and graphs showing ground-water levels in wells 7N/10W-05E1 and 7N/12W-15F1 and subsidence at bench marks 1171A and 474.



deep and extended more than 1,200 ft; it formed near the margin of the ground-water subbasin in an area where inspection showed recent (10 to 20 years) *en echelon* (staggered) traces of healed fissures. T.L. Holzer and M.M. Clark (U.S. Geological Survey, unpub. data, 1981) described a similar 2,000-ft long and 7-ft deep arcuate earth fissure (figs. 3 and 12); this fissure was first noticed in 1978 by residents about 7 mi east-northeast of the city of Lancaster. Large earth fissures forming at the margins of alluvial basins or where there is a sharp change in thickness related to a change in the depth to bedrock have been associated with differential aquifer-system compaction throughout the western United States (Holzer, 1984). Many other, generally smaller, earth fissures have been mapped in a 15-mi<sup>2</sup> area in the northwest part of Lancaster; these fissures were attributed to tensional forces created by regional land subsidence (Charles Swift, Geolabs-Westlake Village, written commun., 1991).

Since 1990, the U.S. Geological Survey has measured ground-water levels in four piezometers (HO-1, HO-2, HO-3, and HO-4) and has measured aquifer-system compaction at the borehole extensometer at the Holly site (8N/10W-1Q, fig. 3). The extensometer provides a measure of compaction from 15 to about 840 ft below land surface at a minimum resolution of  $1.0 \times 10^{-3}$  ft. Drilling logs representative of the extensometer borehole are described in Londquist and others (1993) and construction of the extensometer is described in Blodgett and Williams (1992). The extensometer was retuned and reinstrumented in August 1992 to minimize frictional contact between the 2- and 6-inch casings (fig. 13). The most recent configuration is described in Freeman (1996).

The extensometer at the Holly site (fig. 13) is a counterweighted pipe extensometer (for a description of borehole extensometric methods commonly used by the U.S. Geological Survey, see Riley, 1984). A 2-inch diameter steel pipe was placed atop a concrete anchor at a depth of 840 ft and suspended inside a 6-inch diameter steel casing cemented in the formation to a depth of 810 ft; the bottom 30 ft of the extensometer was left uncased. The 6-inch casing string includes two telescoping slip joints that can accommodate as much as 20 ft of compressive displacement before the casing resists further compressive stresses. The 2-inch diameter extensometer pipe is supported using the

mechanical advantage of an asymmetric counterweighted lever (balance beam) to place the upper half of the pipe in tension to minimize frictional contact with the 6-inch well casing. The vertical displacement of this 2-inch pipe relative to the reference platform provides a measure of compaction between the base of the reference platform (15 ft below land surface) and the base of the extensometer (840 ft below land surface). The reference platform at the Holly site is a leveled steel instrument table that spans and is supported by two steel-pipe piers cemented at 15 ft below land surface in oversized boreholes. The instrument table provides a stable reference with a minimum of temperature and moisture effects related to the deformation of surface soils.

The extensometer assembly is housed in an insulated shelter that sits atop a concrete pad foundation that is mechanically decoupled from the piers and the extensometer casings. Two analog devices, a machinist's dial gage and a drum recorder, and one digital device, a linear voltage displacement transducer (LVDT), are positioned to measure displacement between the pipe extensometer and the reference platform. The change in the distance between the pipe extensometer and the reference platform is the measure of displacement in the depth interval of 15 to 840 ft below land surface.

Measurements of aquifer-system compaction were made at the Holly extensometer from May 1990 through December 1997 (fig. 14A). Throughout this period, compaction was measured by comparing successive, near-monthly readings of the dial gage analog device. Since August 1992, hourly measurements also were made; these measurements were made using the LVDT and recorded with a datalogger. Some missing data exist because of instrument failure or operator error. The principal mode of the compaction signal is a seasonally dependent step response. Larger rates of compaction are associated with summer water-level drawdowns, and despite ground-water-level recoveries of more than 10 ft during the winter, compaction continues, albeit at a smaller rate.

Aquifer-system deformation occurs in response to short-term (daily) pumping cycles during the summer and winter. The compaction responses to daily pumping are superimposed upon the seasonal response and are related to the concurrent water-level change

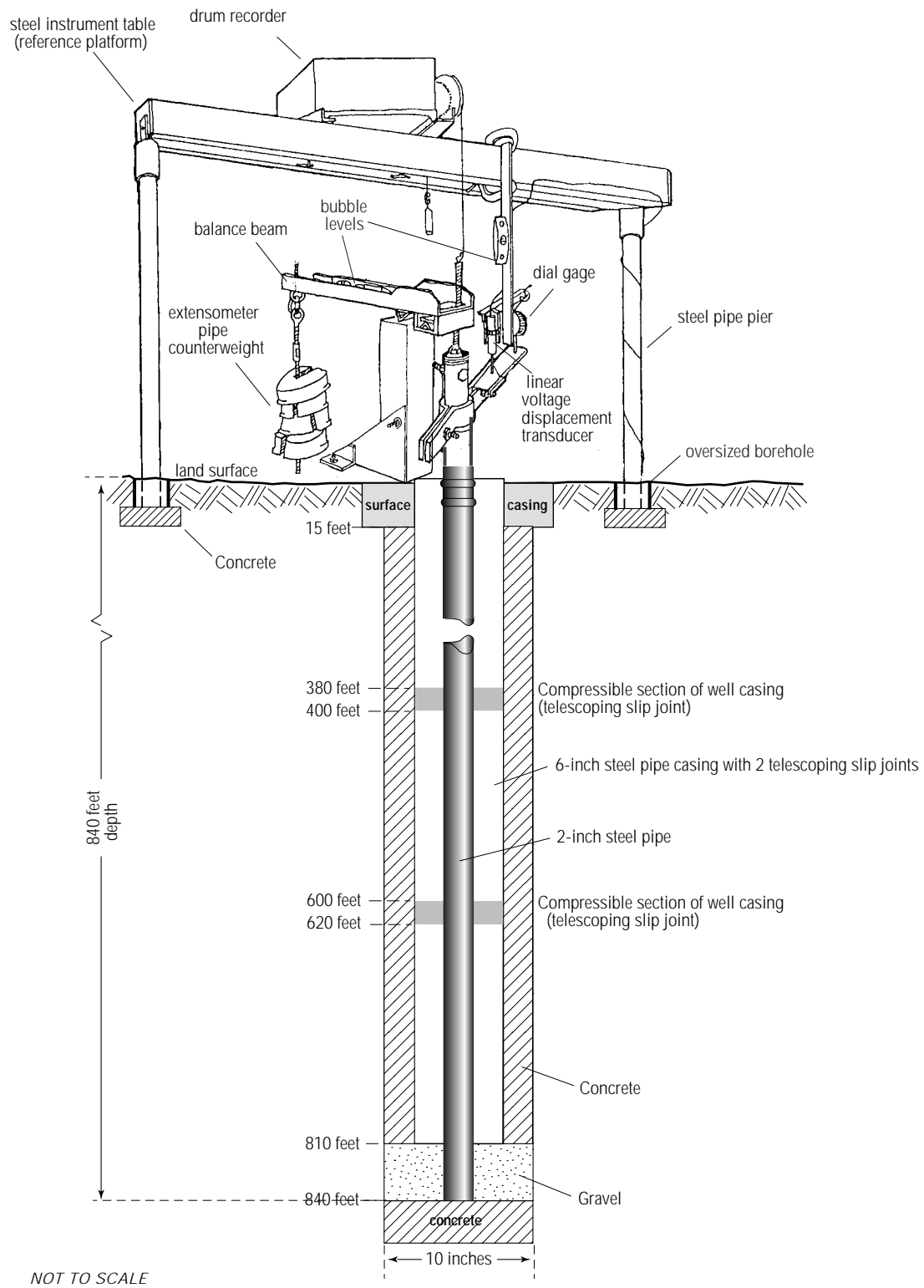


**Figure 13.** Borehole extensometer at the Holly site (8N/10W-1Q), Edwards Air Force Base, Antelope, Valley, California.

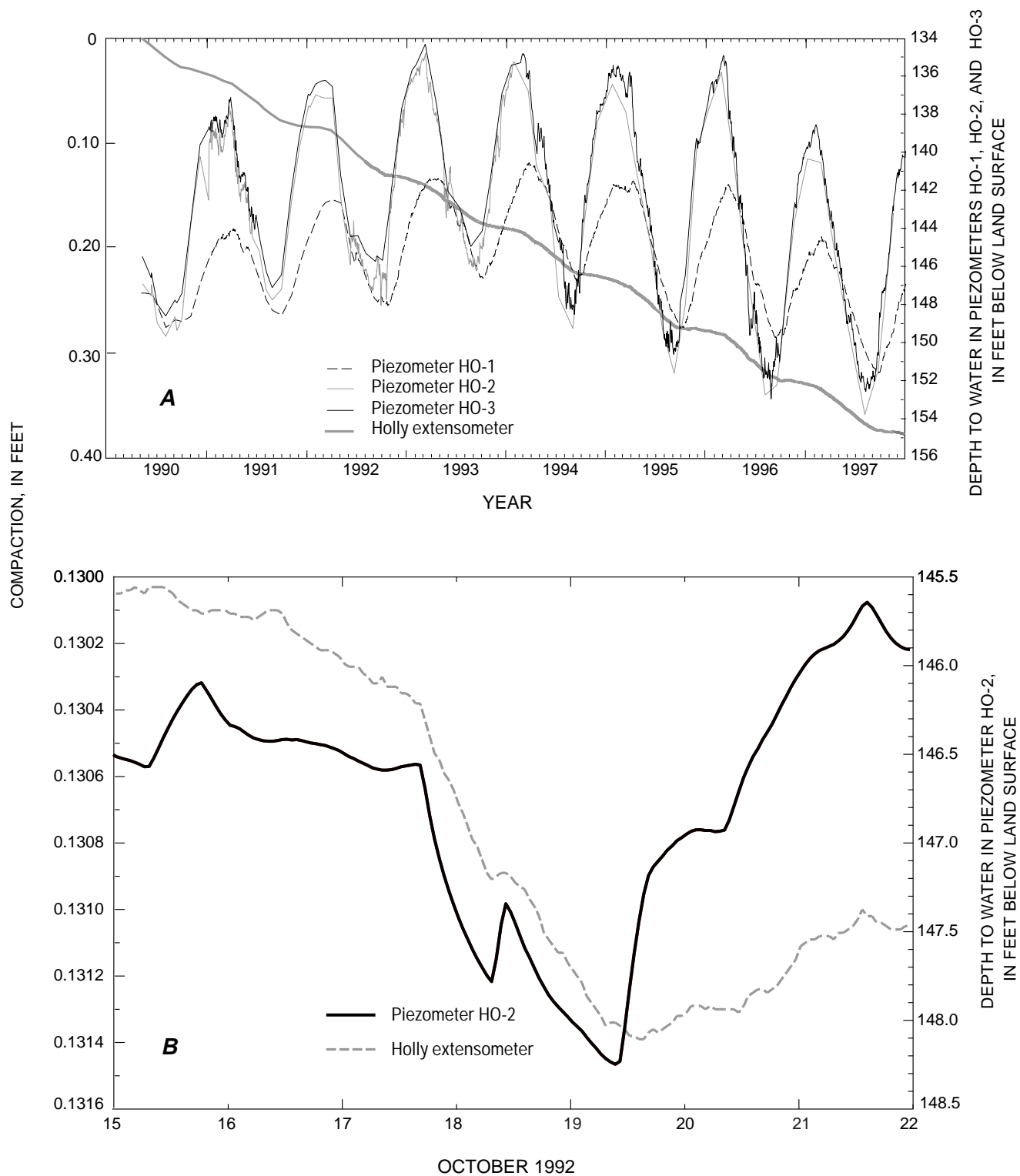


**Figure 14.** Aquifer-system compaction and water levels measured at the Holly site (8N/10W-1Q), Edwards Air Force Base, Antelope Valley, California. **A**, Period of record, 1990–97. **B**, 1 week, October 16, 1992, through October 22, 1992.

(fig. 14). Compaction is related to water-level draw-down in the middle aquifer, and rebound from compaction is related to water-level recovery (fig. 14B). Other factors that potentially can affect the compaction of the aquifer system and compaction measurements include atmospheric loading caused by changes in barometric pressure at land surface and diurnal fluctuations of shelter and equipment temperatures. Attempts were made to clarify the response of the aquifer system to atmospheric loading, but the compaction response to barometric pressure changes measured in the compaction signal was too weak to adequately define this relation. The extensometer and its shelter were specifically designed to compensate for, and thereby minimize, the effects of temperature variation on compaction measurements. The measured displacement response to diurnal temperature variation was small ( $5.0 \times 10^{-6}$  ft/°C) compared with the responses to daily and seasonal ground-water-level changes. The effects of atmospheric pressure and temperature variations on compaction measurements were relatively insignificant and, therefore, no attempt was made to filter these responses from the compaction signal.

To determine whether any land subsidence could be attributed to aquifer-system compaction occurring below the anchor depth of the extensometer, 840 ft, repeat geodetic measurements of the HOLLY geodetic monument (fig. 3) were made. Differential GPS surveys established horizontal and vertical control between geodetic monuments GRINELL and M1155 (about 4.6 mi distant). GRINELL is on EAFB in a granitic outcrop. M1155 is located in alluvium about 0.5 mi from HOLLY. GRINELL is the control geodetic monument, which is assumed to be fixed horizontally and vertically. The position of M1155 was determined relative to this assumed fixed position. Differential elevations for the two monuments were established using spirit leveling surveys between M1155 and HOLLY. The differential GPS surveys indicate that, relative to GRINELL, land subsidence was 0.45 and 0.58 ft at M1155 for the intervals August 6, 1992, to January 5, 1998, and August 6, 1992, to August 6, 1998, respectively. Results of the differential leveling surveys indicate that subsidence at HOLLY was 0.38 and 0.51 ft for the intervals August 6, 1992, to January 5, 1998, and August 6, 1992, and August 6, 1998, respectively. The expected measurement error for the vertical component

of the GPS surveys is plus or minus 0.19 ft (Marti Ikehara, U.S. Geological Survey, written commun., 1998); however, actual error may be higher. Data on these elevation changes indicate a moderately steep gradient ( $2.65 \times 10^{-5}$  ft/ft) of subsidence between M1155 and HOLLY.

Aquifer-system compaction measured by the Holly extensometer was 0.259 between August 6, 1992, and January 5, 1998, ft and 0.292 ft between August 6, 1992, and August 6, 1998. InSAR data for the interval between October 20, 1993, and December 22, 1995, show that 0.131 ft ( $\pm 0.03$ – $0.07$  ft) of land subsidence occurred in the vicinity of the Holly site (Galloway and others, 1998a). Compaction measured by the Holly extensometer for this same period was 0.101 ft, which is comparable to the InSAR-measured amount (Galloway and others, 1998a).

These discrepancies in magnitude between aquifer-system compaction and land subsidence measured by the different techniques suggest that a significant part of total aquifer-system compaction, perhaps as much as one-third, is not being measured. Some compaction may not have been measured because the extensometer may not have measured all deformation either because the extensometer was faulty or because a significant amount of compaction was occurring below the extensometer anchor. The discrepancies in compaction also may have resulted because the assumption that GRINELL was stable during the period August 6, 1992, to August 6, 1998, was invalid or because the error for at least one of the GPS surveys was larger than expected. Future differential surveys should help resolve the cause of this discrepancy.

## ANALYTICAL APPROACH

Land subsidence caused by the withdrawal of fluids from porous media is attributed to the nonrecoverable compaction of aquitards during the time-dependent and typically slow process of aquitard drainage that commonly accompanies the decline in hydraulic head in adjacent aquifers. This concept, known as the aquitard-drainage model, provides the theoretical basis of many successful subsidence studies related to the production of ground water, oil, and gas. [For a review of the history of the aquitard-drainage model,

see Holzer (1998)]. The results of early field (Meinzer and Hard, 1925; Meinzer, 1928) and laboratory (Terzaghi, 1925, 1943) studies indicated that the prevailing concept of a rigid aquifer or aquitard skeleton was incompatible with field observations indicating that the expansion of pore water alone could not account for the water produced from the Dakota Sandstone artesian aquifer. The recognition of this incompatibility led to the development of two fundamental principles underlying aquifer-system mechanics—the principle of effective stress and the theory of one-dimensional hydrodynamic soil consolidation (Terzaghi, 1925, 1943). Studies of land subsidence and aquifer-system compaction in the Santa Clara Valley (Tolman and Poland, 1940; Poland and Green, 1962; Green, 1964; Poland and Ireland, 1988) and the San Joaquin Valley (Poland, 1960; Miller, 1961; Riley, 1969; Helm, 1975; Poland and others, 1975; Ireland and others, 1984) in California have resulted in the development of theoretical and field applications of Terzaghi's (1925, 1943) laboratory-derived principle of effective stress and theory of hydrodynamic consolidation to the compaction of aquifer systems. [For a review of the evolution of the concepts and methodologies of aquifer mechanics, with a focus on the role of early studies of land subsidence and aquifer-system compaction, see Riley (1998)].

For purposes of this report, compaction describes the inelastic and largely irreversible aquitard or aquifer-system compression, reflecting rearrangement of the pore structure under effective stresses greater than the maximum past stress, and is synonymous with the term “virgin consolidation” used in the field of soil mechanics. We use the term compaction to refer to both the process and the final result within the context that compaction may include a very small recoverable component (1 to 5 percent) (Riley, 1998) of deformation that may be realized when stresses are reduced. The soil-mechanics term “consolidation” is used in this report when referring to original work from soil mechanics research on compaction resulting from drainage of a clay layer. In other contexts, we refer to the geologic meaning of the term which refers to any process by which loose earth materials become compacted, including cementation, diagenesis, recrystallization, dehydration, and metamorphism.

In the report, we review the concepts relating the compressibility of the aquifer system and its storage properties. In later sections, we use these relations to derive estimates of specific storage of the aquifers and

aquitards. We also review the concepts relating the theory of hydrodynamic consolidation to the aquitard drainage model. These relations are used in later sections to simulate the compaction of the aquifer system.

## Principle of Effective Stress

The relation between changes in pore-fluid pressure and compression of the aquifer system is based on the principle of effective stress (Terzaghi, 1925),

$$\sigma_e = \sigma_T - p, \quad (1)$$

where effective or intergranular stress ( $\sigma_e$ ) is the difference between total stress ( $\sigma_T$ ) and the pore-fluid pressure ( $p$ ) (fig. 15). The total stress represents the geostatic load—the weight per unit area of rock and fluid. Using this principle, if total stress remains constant, a change in pore-fluid pressure causes an equivalent change in effective stress within the aquifer system. This results in a small change in volume in an aquifer system that is governed by the compressibility of the aquifer-system skeleton,  $\alpha_k^*$ . When effective stress is reduced by an increase in pore-fluid pressure, the aquifer system expands elastically. When effective stress is increased by a reduction in pore-fluid pressure and the effective stress does not exceed the past maximum effective stress (preconsolidation stress), the aquifer system compresses elastically. The change in pore-fluid pressure and associated expansion or compression of the aquifer system is also expressed as a fully recoverable (elastic) vertical displacement ( $\mu_z$ ) of land surface. When a reduction in pore-fluid pressure causes an increase in effective stress to values greater than the preconsolidation stress, the pore structure of susceptible fine-grained aquitards in the system may undergo significant rearrangement. This rearrangement results in a permanent (inelastic) reduction of pore volume which results in vertical compaction of the aquitards within the aquifer system, also expressed as vertical displacement of land surface (fig. 15). This process can be quantified in terms of two skeletal compressibilities, one elastic,  $\alpha_{ke}$ , and one inelastic,  $\alpha_{kv}$ , each of which can be applied to the aquifer system as a whole or, if the stratigraphy is well defined, to the aquifers and the aquitards separately. The subscripts  $e$  and  $v$  refer to the elastic and virgin (inelastic) ranges of stress, respectively.

For purposes of this report, pore-fluid pressure,  $p$ , is expressed in terms of an equivalent hydraulic head,  $h$ ,

$$h = p/(\rho g), \quad (2)$$

where  $\rho$  is the fluid density of water and  $g$  is gravitational acceleration. Because we assume that gravity is constant, that fluid is uniform, and that changes in fluid density related to the compressibility of water are negligible, changes in hydraulic head are directly proportional to changes in fluid pressure. Although pressure has units of stress ( $ML^{-1}T^{-2}$ ) and head has units of

length ( $L$ ), we use these terms interchangeably throughout this report within the context of constant fluid density and gravity assumptions.

### Preconsolidation Stress

The past maximum effective stress of a material element in an aquifer system is termed the “preconsolidation stress” for that element. Figure 16 shows an idealized stress/strain plot from a one-dimensional (vertical), “drained” laboratory consolidation test on samples of aquifer-system material that have been cyclically loaded (stressed) and unloaded; the cyclic progression of the applied stress history is shown by

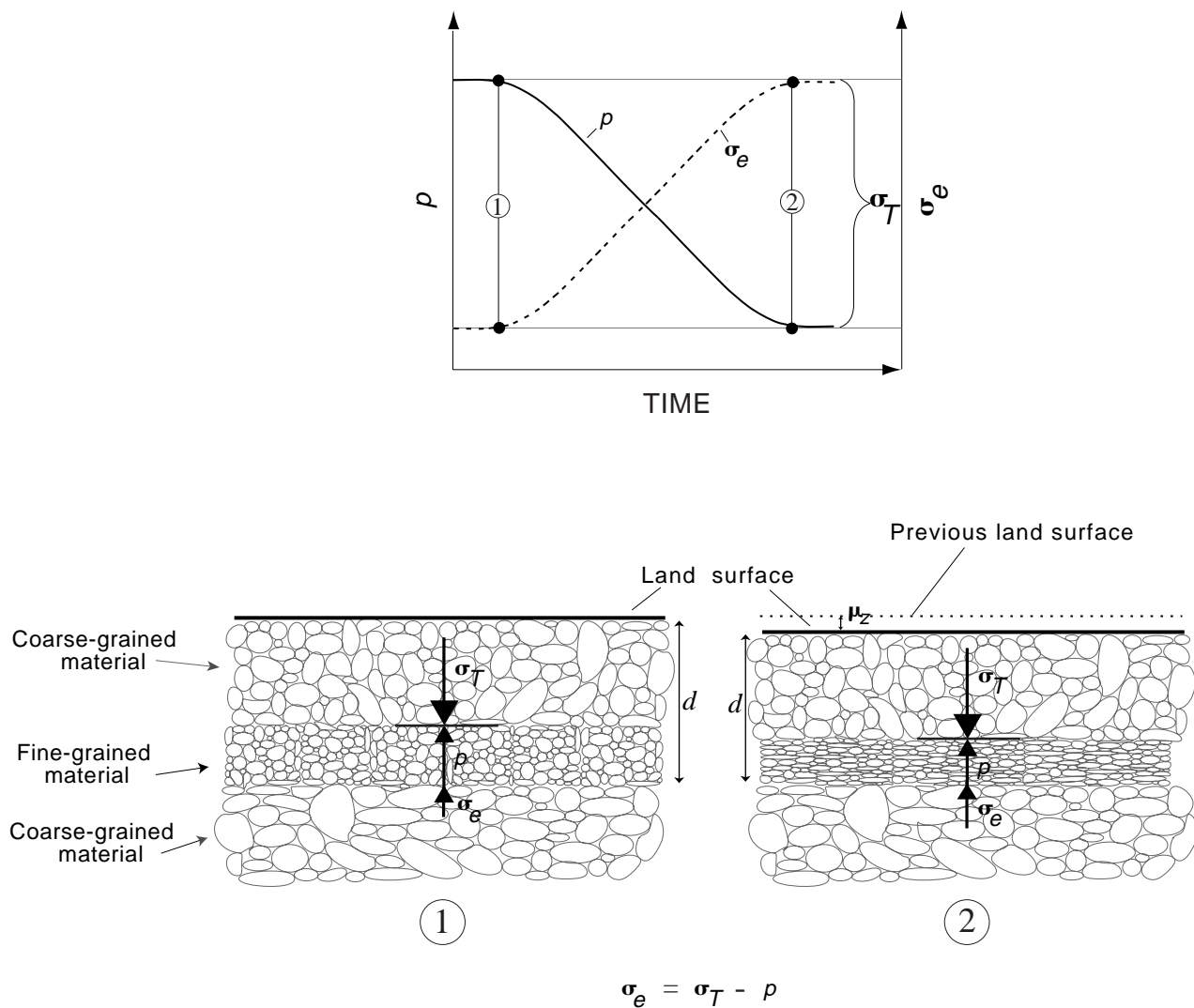
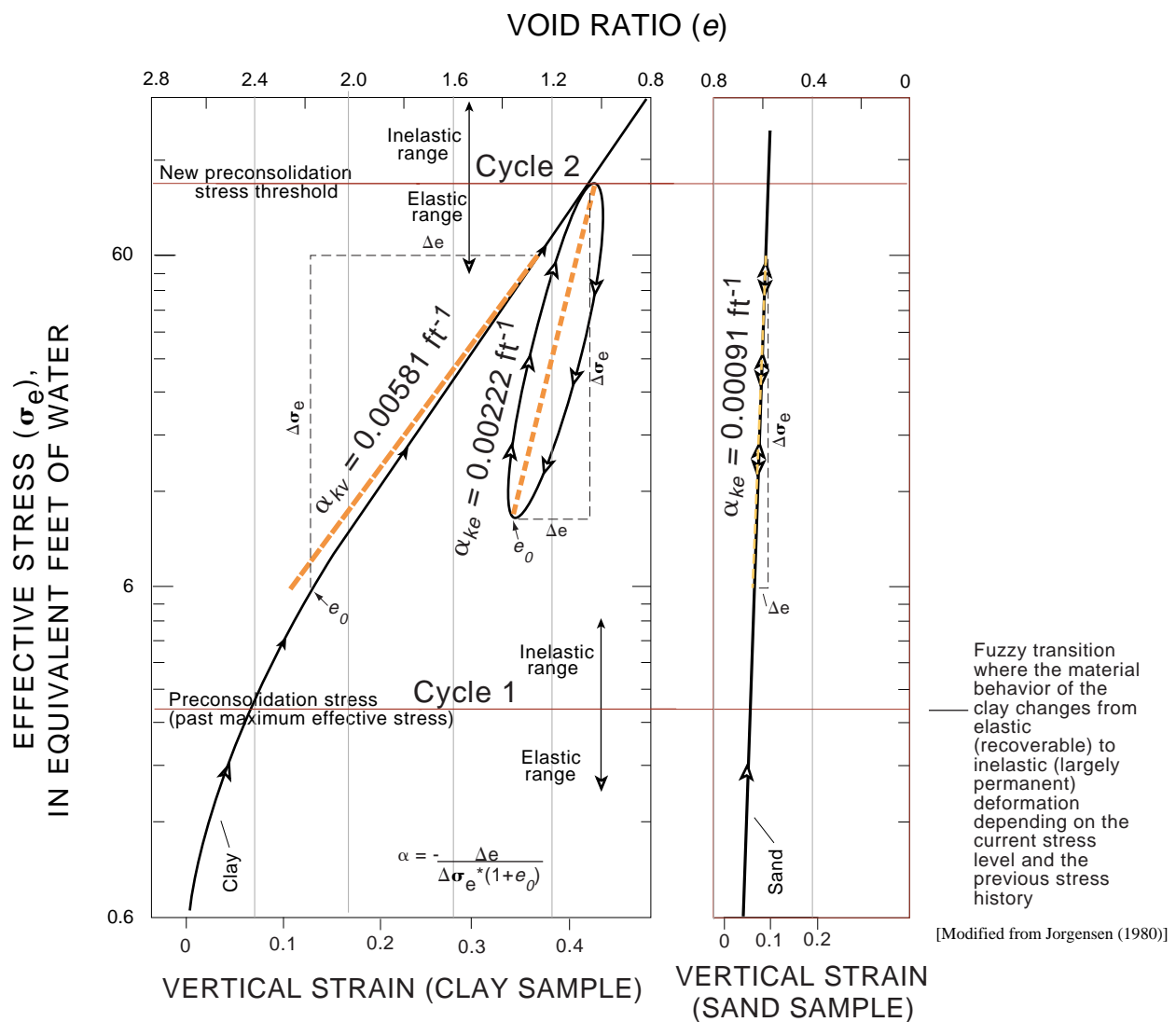


**Figure 15.** Principle of effective stress, as applied to land subsidence. Vertical displacement ( $\mu_z$ ) of land surface as a result of a decrease in pore-fluid pressure ( $p$ ) and resultant increase in effective stress ( $\sigma_e$ ) exerted on a horizontal plane located at depth ( $d$ ) below land surface in fine-grained material, under conditions of total stress ( $\sigma_T$ ) in a one-dimensional, fluid-saturated geologic medium.

the arrows on the stress/strain trajectory. During a drained laboratory consolidation test, drainage achieves a constant head ( $\Delta p=0$ ) on the sample. The change in effective stress is applied by changing the total stress ( $\Delta\sigma_e=\Delta\sigma_T$ ). For compressible, fine-grained clay-rich materials, the preconsolidation stress, which is evident by breaks in the slopes of the stress/strain trajectory, represents a critical stress threshold (Riley, 1969). For stresses beyond the preconsolidation stress, the susceptible fine-grained materials typically compress inelastically (compact). In the inelastic range, the materials deform proportionally more to incremental changes in the stress compared with deformation of materials in the elastic range. For coarse-grained sand-rich materials, there is negligible inelastic deformation

and the preconsolidation stress of these materials is not evident on stress/strain plots.

In the context of aquifer systems, as opposed to laboratory samples, preconsolidation stress often can be represented by the previous lowest ground-water level (hydraulic head) as measured in wells, but only after sufficient time is allowed for fluid pressures to equilibrate throughout the aquifer system (Riley, 1969). Practically, the equilibration of fluid pressure between the aquitards and the aquifers is a limiting criterion that often is not achieved (this is discussed in greater detail in a later section of this report “Theory of Hydrodynamic Consolidation”). However, for the purpose of discussion, under ideal conditions of pressure equilibration for a confined aquifer system where total



stress is constant, the previous lowest head may be taken as a first-order approximation of the preconsolidation stress. For aquifer systems where heads fluctuate in response to seasonal stresses such as pumping or ground-water recharge, the effective stresses also fluctuate (fig. 16), and the resultant aquitard-material deformation may alternate between elastic (recoverable) and inelastic (nonrecoverable) if the stresses cycle through the preconsolidation stress threshold. The hysteresis loop on figure 16 represents the trajectories of the elastic stress/strain behavior that might result from ground-water-level fluctuations that do not drop below the preconsolidation head.

An accurate estimate of the predevelopment, or native, preconsolidation stress is one of the most important requirements for a successful simulation of aquifer-system compaction (Hanson, 1989; Hanson and Benedict, 1994). Typically, alluvial ground-water basins are overconsolidated; native preconsolidation stresses generally are somewhat larger than the predevelopment effective stresses, and land subsidence occurs only after substantial drawdowns have increased effective stresses beyond the native preconsolidation stress. Holzer (1981) identified various natural mechanisms that can result in an overconsolidated condition in alluvial basins; these mechanisms include removal of overburden by erosion, prehistoric ground-water-level declines, desiccation, and diagenesis. Few investigations have examined the elastic responses of the aquifer systems to changes in effective stress under natural conditions (before irreversible subsidence owing to large-scale ground-water withdrawals). As a result, information on the critical head, which represents the native preconsolidation stress of the aquifer system, has been deduced post hoc from paired profiles of ground-water levels and land subsidence (Holzer, 1981; Anderson, 1988, 1989) measured at wells and at nearby bench marks, or inferred from simulation (Hanson and others, 1990; Hanson and Benedict, 1994).

### Elastic and Inelastic Compressibility (Specific Storage)

The compressibility of a material reflects its ability to undergo an inverse change in volume and a direct change in density under a change in stress. This relation between stress and strain is represented by the slope of the trajectories representing elastic and inelastic segments of the stress/strain diagram in figure 16. For the range of effective stresses typically induced

when pumping aquifer systems, the slope is a measure of the compressibility of the sample skeleton for the applied range of stress and is referred to as the skeletal component of compressibility.

For the purposes of this report, the skeletal specific storage of an aquifer system,  $S_{sk}^*$ , is expressed in terms of the skeletal compressibility,  $\alpha_{sk}^*$ , where the subscript  $k$  refers to the skeletal component of specific storage, or compressibility. Specific storage represents the volume of fluid taken into or released from a unit volume of aquifer-system material for a unit change in head. The water being exchanged is derived from two processes, expansion or compression of the material that results from a change in effective stress,  $\sigma_e$ , and expansion or compression of the fluid owing to a change in pore-fluid pressure. The skeletal component of specific storage addresses the first of these processes, which, for most unconsolidated alluvial aquifer systems, is the dominant component. Skeletal compressibilities of fine-grained aquitards and coarser-grained aquifers typically differ by several orders of magnitude; therefore, it is useful to define them separately. Elastic and inelastic skeletal specific storages of the aquitards,  $S'_{sk}$ , are

$$S'_{sk} = \begin{cases} S'_{ske} = \alpha'_{ke} \rho g, & \sigma_e < \sigma_{e(max)} \\ S'_{skv} = \alpha'_{kv} \rho g, & \sigma_e > \sigma_{e(max)} \end{cases} \quad (3)$$

and the skeletal specific storage of the aquifers,  $S_{sk}$ , is

$$S_{sk} = S_{ske} = \alpha_{ke} \rho g,$$

because inelastic skeletal compressibility in aquifers is negligible,  $\alpha_{kv}$  approaches 0.

The primes (') signify aquitard properties and the subscripts  $e$  and  $v$  refer to elastic and inelastic properties, respectively. For a change in effective stress, the aquitard deforms elastically when the effective stress remains less than the past maximum effective stress,  $\sigma_{e(max)}$ ; when the effective stress exceeds  $\sigma_{e(max)}$ , the aquitard deforms inelastically. For coarse-grained sediments typically found in aquifers, inelastic skeletal compressibility is negligible, and therefore, skeletal



specific storage of the aquifer,  $S_{sk}$ , is adequately represented by the fully recoverable, elastic component of skeletal specific storage,  $S_{ske}$ . In typical aquifer systems consisting of unconsolidated to semiconsolidated late Cenozoic sediments, the inelastic component of skeletal specific storage,  $S'_{skv}$ , generally is 30 to several hundred times larger than  $S'_{ske}$ , which is about 10 times larger than  $S_{ske}$  (Ireland and others, 1984; Hanson, 1989).

## Aquifer-System Storage Coefficients

The products of the elastic or inelastic skeletal specific storage values and the aggregate thickness of the aquitards,  $\Sigma b'$ , or aquifers,  $\Sigma b$ , are the skeletal storage coefficients of the aquitards ( $S'_k$ ) and the aquifers ( $S_k$ ), respectively,

$$S'_k = \begin{cases} S'_{ke} = S'_{ske}(\Sigma b'), & \sigma_e < \sigma_{e(max)} \\ S'_{kv} = S'_{skv}(\Sigma b'), & \sigma_e > \sigma_{e(max)} \end{cases} \quad (4)$$

$$S_k = S_{ke} = S_{ske}(\Sigma b),$$

for the elastic ( $S'_{ke}$  and  $S_{ke}$ ) and inelastic ( $S'_{kv}$ ) ranges of skeletal compressibility. A separate equation relates the fluid compressibility of water,  $\beta_f$ , to the component of aquifer-system storage attributed to the pore water,  $S_w$ :

$$S_w = S'_{sw}(\Sigma b') + S_{sw}(\Sigma b) = \beta_f \rho g [n'(\Sigma b') + n(\Sigma b)] \quad (5)$$

where  $n'$  and  $n$  are the porosities and  $S'_{sw}$  and  $S_{sw}$  are the specific storages of water of the aquitards and aquifers, respectively.

The aquifer-system storage coefficient,  $S^*$ , is defined as the sum of the skeletal storage coefficients of the aquitards and aquifers (equation 4), plus the storage attributed to water compressibility (equation 5),

$$S^* = S'_k + S_k + S_w. \quad (6)$$

For compacting aquifer systems,  $S'_{kv} \gg S_w$  and the inelastic storage coefficient of the aquifer system,  $S^*_v$ , is approximately equal to the inelastic aquitard skeletal storage coefficient,

$$S^*_v \approx S'_{kv}. \quad (7)$$

In confined aquifer systems subjected to large-scale overdraft, the volume of water derived from irreversible aquitard compaction typically can range from 10 to 30 percent of the total volume of water pumped (Riley, 1969). This represents a one-time mining of stored ground water and a small (typically less than 1 percent) permanent reduction in the storage capacity of the aquifer system (Riley, 1969; 1998).

Inherent in these concepts of specific storage (Jacob, 1940, 1950) are three potentially limiting assumptions—(1) all the skeletal strain associated with a change in hydraulic head is vertical; (2) the total stress on the skeleton remains constant with changes in head; and (3) the compressibility of the individual solid grains of the skeleton is negligible but that the compressibility is derived instead from a rearrangement of the skeletal structure. The third assumption generally is valid for poroelastic deformation of unconsolidated alluvial aquifers (Van der Kamp and Gale, 1983). The second assumption generally is valid for confined aquifer systems where there is no change in the elevation of hydraulic head associated with a change in total head. This assumption becomes invalid for a confined aquifer underlying a water-table (unconfined) aquifer when there are significant changes in the water-table elevation, and hence in the geostatic load.

The first assumption is perhaps the most limiting and the least well understood. This assumption attributes all the volume strain ( $\epsilon_{volume}$ ) to vertical strain ( $\epsilon_z$ ), such that there is no change in horizontal strain components ( $\epsilon_x$ ,  $\epsilon_y$ ) coinciding with the volume strain that results from a change in hydraulic head in the aquifer system, that is,  $\epsilon_{volume} = \epsilon_z$ ;  $\epsilon_x = \epsilon_y = 0$ . Poroelastic relations that incorporate a fully three-dimensional (volume) material stress/strain and coupled fluid flow have been developed (Biot, 1941; Verrij, 1969; Rice and Cleary, 1976); however, available field measurements of horizontal deformation have not yet demonstrated the need to include the more complex multidimensional poroelastic relations in the analysis of aquifer-system compaction. Although it is clear that some horizontal deformation coincides with hydraulic

head changes in aquifer systems (Wolf, 1970; Carpenter, 1993; Helm, 1994; Hsieh, 1996) and may play a role in the formation of earth fissures in compacting aquifer systems, its relative significance in the simulation of hydraulic head and (or) compaction has not yet been demonstrated adequately. The analyses presented here adhere to the simpler, conventional definition of specific storage and compressibility of aquifer systems typically used by hydrologists and are somewhat limited by the inherent assumptions.

## Theory of Hydrodynamic Consolidation

The theory of hydrodynamic consolidation (Terzaghi, 1925), an essential element of the aquitard-drainage model, describes the delay involved in draining aquitards when hydraulic heads are lowered in adjacent aquifers and the residual compaction that may continue long after aquifer heads are initially lowered. The drainage process is described well by a one-dimensional (vertical) diffusion equation for groundwater flow:

$$\partial^2 h / \partial z^2 = (S'_s / K'_v) \partial h / \partial t, \quad (8)$$

where  $S'_s$  is specific storage of the aquitard (approximately equal to  $S'_{skv}$  if effective stresses are greater than maximum past effective stress),  $K'_v$  is vertical hydraulic conductivity of the aquitard, and the ratio  $S'_s / K'_v$  is the inverse of the vertical hydraulic diffusivity of the aquitard. Depending on the thickness and vertical hydraulic diffusivity of an aquitard, the equilibration of pore-fluid pressure—and thus compaction—lags head declines in adjacent aquifers.

Drawing on the time-consolidation theory from the field of soil mechanics (Scott, 1963), Riley (1969) noted that a time constant,  $\tau$ , for compaction of a doubly draining aquitard following an instantaneous step load may be defined as

$$\tau = S'_s (b'/2)^2 / K'_v, \quad (9)$$

where  $b'$  is the aquitard thickness. The time constant is the time required for the aquitard to attain about 93 percent of the ultimate compaction following a step increase in applied load. The increase in load occurs as

an instantaneous step decrease in hydraulic head in the adjacent aquifers and constitutes the product of the volume of water that must flow from the aquitard to achieve consolidation and the impedance to the flow of that water. For a doubly draining aquitard subject to these conditions, the time constant is proportional to the square of the half-thickness of the aquitard. Riley (1969) showed how an approximate time constant for compaction of the aquifer system as a whole can be derived from time-series measurements of aquifer-head decline and aquifer-system compaction. He combined the time constant for the aquifer system with inelastic storage coefficient of the aquifer system (equation 7) (derived from stress/strain analysis) and the number and thickness of compacting aquitards to estimate an average value of  $K'_v$  for the aquitards.

Helm (1975, 1978) incorporated these concepts into a numerical aquitard-drainage model that closely simulated compaction recorded at 15 extensometer/piezometer sites in the Santa Clara and the San Joaquin Valleys. Extrapolating from Helm's model-derived values of  $S'_{skv}$  and  $K'_v$ , Ireland and others (1984) estimated aquifer-system time constants that ranged from 5 to 1,350 years and averaged 159 years (geometric mean). Riley (1998) noted that in parts of the San Joaquin Valley the large amounts of subsidence (about 30 ft) measured by the late 1960s may have been no more than 50 percent of the amount that ultimately would have occurred if fluid pressures in the thick aquitards equilibrated with 1960s water levels in the aquifers.

## PARAMETER RANGE ESTIMATES

Aquifer-system properties required for model input include vertical hydraulic conductivity, preconsolidation stress, and elastic and inelastic storage coefficients (specific storage). Estimates of vertical hydraulic conductivity for aquitards and aquifers were made on the basis of previously developed models, laboratory results, and measurements made near the Holly site. Predevelopment preconsolidation stress was approximated from time-series measurements of land subsidence and ground-water levels from paired bench marks and wells. Elastic and inelastic storage coefficients were estimated using a modified stress/strain analysis developed by Riley (1969); equivalent specific storages were then calculated using thicknesses of the aquifers and aquitards estimated from geophysical data collected at the Holly site.

## Vertical Hydraulic Conductivity

Values of aquifer vertical hydraulic conductivity were constrained using the frequency response of water levels to earth tides and atmospheric loading in piezometer HO-1 (Rummler, 1996) and in a well screened in the middle aquifer in the nearby Graham Ranch area (fig. 3) (Galloway, 1993). Values ranged from  $1.9 \times 10^{-2}$  to  $2.0 \times 10^{-2}$  ft/d. Values of vertical hydraulic conductivity for the aquitards were constrained using measurements for lacustrine clays given in Neuzil (1994), which range from  $1.8 \times 10^{-6}$  to  $1 \times 10^{-3}$  ft/d. Values from a well hydraulics test for the confining unit near the Holly site, which ranged from  $1.7 \times 10^{-2}$  to  $9.2 \times 10^{-2}$  ft/d (Weston, 1986), and a value of  $1.2 \times 10^{-2}$  ft/d determined from the simulation of flow across the confining unit (Durbin, 1978), were also considered for constraining the values of vertical hydraulic conductivity. Note that the vertical hydraulic conductivity values determined by Weston (1986) and simulated by Durbin (1978) are much higher than those measured by Neuzil (1994).

## Preconsolidation Stress

The predevelopment preconsolidation stress, or maximum effective stress prior to the development of ground-water resources, was estimated from time-series measurements of land subsidence and ground-water levels from paired bench marks and wells. Water-level information was obtained from the scarce historical measurements made in wells near the Holly site, and land-surface elevations at bench marks were obtained from Ikehara and Phillips (1994). Water-level data for several nearby wells monitored during different historical periods were combined to produce a composite hydrograph representative of the middle aquifer at the Holly site (fig. 17); the synthesis is detailed later in the “Boundary Conditions” section. Three bench marks were used in conjunction with the hydrograph—LS42, M1155, and P1155 located approximately 0.6 mi west, 0.5 mi east, and 1.6 mi west of the Holly site, respectively (fig. 3).

Measured or estimated changes in land-surface elevation for these bench marks and the HOLLY bench mark are available for various historical time intervals (table 1). The measurements and estimates for bench marks LS42 and P1155 were critical for estimating the range of preconsolidation stress. Between about 1929

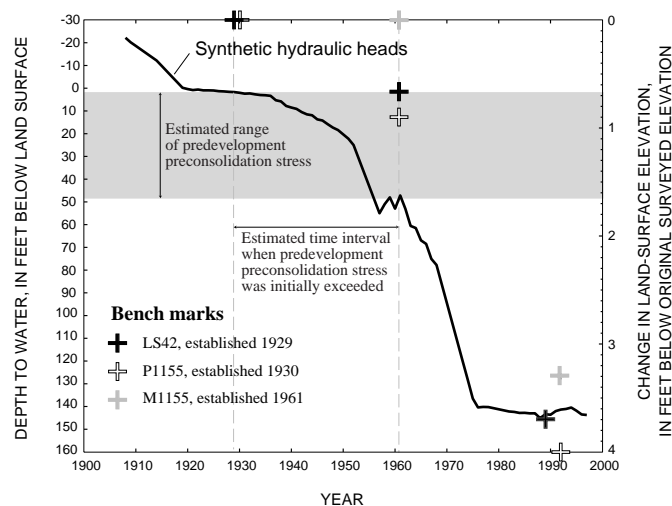


**Figure 17.** Change in land-surface elevation for various time intervals for selected bench marks (see table 1 for time intervals), and estimated water levels (1908–97) for the middle aquifer near the Holly site (8N/10W-1Q), Edwards Air Force Base, Antelope Valley, California. (See figure 3 for location of bench marks.)

**Table 1.** Measured or estimated land-surface-elevation changes for selected bench marks at Edwards Air Force Base, Antelope Valley, California

[Modified from Ikehara and Phillips, (1994). Location of bench marks are shown on figure 3]

Bench mark	Time interval	Land subsidence, in feet	Method
LS42	1929–61	0.7	Differential leveling
	1961–89	3.03	Differential leveling
	1929–89 (total)	3.7	
P1155	1930–61	.9	Estimated <sup>1</sup>
	1961–92	3.1	Differential leveling
	1930–92 (total)	4.0	Estimated <sup>1</sup>
M1155	1961–92	3.3	Differential leveling
	1992–98 <sup>2</sup>	.45	Differential GPS
	1992–98 <sup>3</sup>	.58	Differential GPS
HOLLY	1992–98 <sup>2</sup>	.38	Differential leveling
	1992–98 <sup>3</sup>	.51	Differential leveling

<sup>1</sup>See Ikehara and Phillips (1994) for description of estimation technique.

<sup>2</sup>August 1992–January 1998.

<sup>3</sup>August 1992–August 1998.

and 1961, the 0.7 to 0.9 ft of subsidence measured or estimated for these two bench marks (fig. 17; table 1) suggests that the predevelopment preconsolidation stress probably was initially exceeded during this time interval. This time interval corresponds to estimated

ground-water levels that range between land surface and about 50 ft below land surface (fig. 17).

### Elastic and Inelastic Storage Coefficients (Specific Storage)

Elastic and inelastic storage coefficients were estimated using a modified approach to an established graphical method (Riley, 1969). The Riley method is similar to the approach we used to determine the coefficients of compressibility from the stress/strain relations derived from laboratory consolidation tests. The method involves plotting applied stress (hydraulic head) on the  $y$ -axis and either vertical strain or displacement (compaction) on the  $x$ -axis. A change in water level (head) represents a change in applied stress, which is equivalent to the change in effective stress on a confined aquifer system with a constant total stress. Riley (1969) showed that for aquifer systems where pressure equilibration can occur rapidly between aquifers and aquitards, the inverse slopes measured from the predominant linear trends in the compaction-head trajectories represent measures of the skeletal storage coefficients. However, because of the effects of delayed pressure equilibration between the aquifers and the aquitards evident in the measured responses at the Holly site, the Riley method is not directly applicable to these responses.

A net compaction occurs during the winter despite a water-level recovery (fig. 18A). This likely is due to an imbalance between the elastic expansion of the aquifers and thin aquitards and the ongoing compaction of the thick, slowly draining aquitards. This mixed mechanical response causes “open” loops for the compaction-head trajectories for the range of seasonal fluctuations in ground-water levels (fig. 18B). This is in contrast to cyclical loading in the elastic range of deformation which causes “closed” hysteresis loops (fig. 16). The mixed response indicates that the stresses causing compaction of the thicker aquitards are not represented by the measured stresses. Because of the impedance of ground-water flow in the aquitards, changes in hydraulic head in the aquifers have not occurred throughout a significant part of the thicker aquitards. Thus, the seasonal relation between measured water levels and compaction at the Holly site is not only a function of the skeletal storage coefficients of the deforming aquifer system but also of the vertical hydraulic conductivity of the thick aquitards.

A modified approach to the Riley (1969) method involved attempting to isolate, on a seasonal basis, the elastic and inelastic components of the measured, mixed mechanical response of the aquifer system. In a simplistic view, the steplike variation in the measured compaction signal (fig. 18A) can be represented by a combination of two signals—one long-period, linear trend of compaction and one seasonally fluctuating component of compaction. The long-period, linear trend may represent the residual component of compaction occurring in the thicker, slowly draining aquitards. The seasonally fluctuating component may represent the cyclic, elastic deformation of the aquifers, the thinner aquitards, the fringes of the thicker aquitards, plus any additional compaction of thinner aquitards during the summer cycle of stress. This approach oversimplifies the time-dependent, residual compaction of the thicker aquitards that most likely occurs as decades of seasonal stresses in the aquifer propagate farther into the thick aquitards. However, this approach yielded some estimates for the elastic and inelastic components of skeletal storage coefficients used to constrain parameters for the more detailed modeling approach.

With respect to the periodic stresses related to seasonal ground-water discharge, four classes of response related to the vertical displacement of the aquifer system can be identified—elastic displacements in the winter, elastic displacements in the summer, inelastic displacements in the winter, and inelastic displacements in the summer. The time-series record for winter compaction represents a combination of the inelastic response of the thick, slowly draining, low-permeability aquitards and any elastic responses to water-level recovery in the aquifers, the thinner quickly equilibrating aquitards, and the fringes of thicker aquitards. The summer record predominately represents a composite of the inelastic response of the thick, slowly draining aquitards and any elastic responses to water-level decline in the aquifers, the thinner quickly equilibrating aquitards, and the fringes of thicker aquitards. Superimposed on each seasonal response are the daily, mostly elastic responses of the aquifers, the thin aquitards, and the fringes of thick aquitards owing to short-duration pumping (fig. 14B).

Winter water-level and compaction data used in the stress/strain analyses were selected on the basis of water-level-recovery rates. The winter data were bracketed between the autumn and spring data when water-level-recovery rates stabilized. The transition period

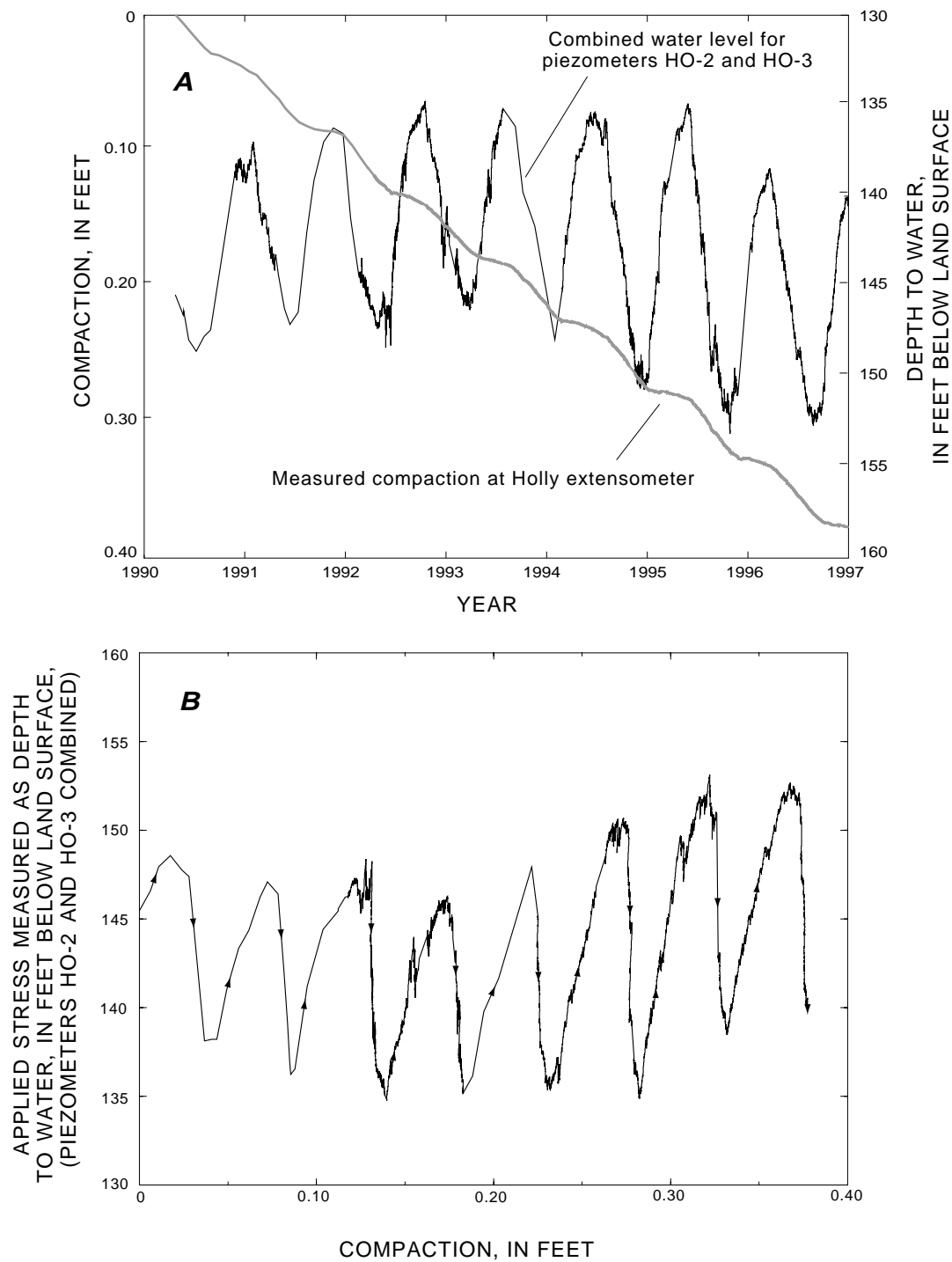


**Figure 18. A**, Combined water levels for piezometers HO-2 and HO-3 and cumulative vertical compaction at the Holly extensometer, and **B**, applied stress and compaction at the Holly site (8N/10W-1Q), Edwards Air Force Base, Antelope Valley, California, 1990-97.

between drawdown and recovery evident in the hydrograph for piezometers HO-2 and HO-3 record (fig. 18A) was not considered in these analyses. The lengths of the data sets averaged about 80 days. The raw compaction data (fig. 19A) were detrended (fig. 19B) to isolate the inelastic response from the elastic response (fig. 19A, B). The longer period, low-frequency component of the compaction signal representing the winter inelastic component was removed by subtracting a least-squares linear regression from selected winter data. The detrended record contains the elastic response to periods of higher frequency pumping. The same method was used on concurrent raw water-level data (fig. 19A) to remove the winter water-level-recovery trend (fig. 19B). The two detrended time series (fig. 19B) were then digitally filtered to remove high-frequency responses (fig. 19C) occurring at periods of less than 30 hours (or more than 0.8 cycles per day). This cutoff frequency minimizes the effects of diurnal and semidiurnal earth tides and barometric pressure-induced changes in the aquifer system that could potentially contaminate the water-level and compaction records. These filtered results were then plotted as displacement-stress trajectories (fig. 19D).

Summer water-level and compaction data used in the stress/strain analyses were selected on the basis of water-level-drawdown rates. The summer data were bracketed between spring and autumn when water-level-drawdown rates stabilize. The transition period between drawdown and recovery evident in the water-level record (fig. 18A) was not considered. Data-set lengths averaged about 125 days. The summer elastic response was isolated in the same manner that the winter elastic response was isolated (fig. 19E-G). The detrended and filtered summer season data sets were plotted as displacement-stress trajectories (fig. 19H).

The summer inelastic response in the compaction record is a composite of the effects of seasonal drawdown on the aquifers and aquitards and the ongoing long-term effects of any delayed pressure equilibration occurring in the thicker aquitards which generally are isolated from seasonal stresses. To isolate the summer inelastic response of the thin aquitards to seasonal drawdown for the aquifer system from the inelastic response of the thick aquitards, it was necessary to remove the delayed response attributed to the thicker

aquitards from the composite summer response (fig. 19I). The two responses were separated, in part, by removing the low-frequency trend determined from the winter season response attributed to compaction occurring in the thick, slowly equilibrating aquitards. Because the winter compaction measured in the aquifer system is masked, in part, by elastic expansion occurring in the aquifers, the thin, rapidly equilibrating aquitards, and the fringes of the thicker aquitards, the estimate for the inelastic response attributable to thick aquitards probably represents a slight underestimation of the actual response. By removing the underestimated winter inelastic response from the summer season response, the resulting residual summer inelastic response of thin aquitards attributable to seasonal drawdown is slightly overestimated. It was not necessary to repeat this process for the water levels because the measured water levels (fig. 19I), which are presumed to be representative of the hydraulic heads in the aquifers, were assumed to be equivalent to the stresses causing the compaction of the thin aquitards. Displacement-stress trajectories were plotted for the residual summer inelastic response (fig. 19J) using the concurrent raw water levels. Displacement-stress trajectories were not plotted for the winter inelastic response because the stresses causing the compaction of the thicker aquitards—pore-fluid pressures in the thick aquitards—were not measured during this study and are not known.

Estimates for elastic and inelastic skeletal storage coefficients were calculated on the basis of the displacement-stress relations for each of the three classes of aquifer-system displacement responses—summer elastic, winter elastic, and summer inelastic. Similar to Riley (1969), we calculated skeletal storage coefficients from the inverse slope of the predominant linear trend of the displacement-stress trajectories (fig. 19D, H, J). Each of the three classes of responses were analyzed for multiple seasons (table 2). The estimates of skeletal storage coefficients for the summer and winter elastic responses represent the elastic skeletal storage of the aquifer system (equation 4), and the estimates for the summer inelastic responses represent the inelastic storage of the aquifer system, which is approximately equivalent to the inelastic skeletal storage coefficient of the thin, rapidly

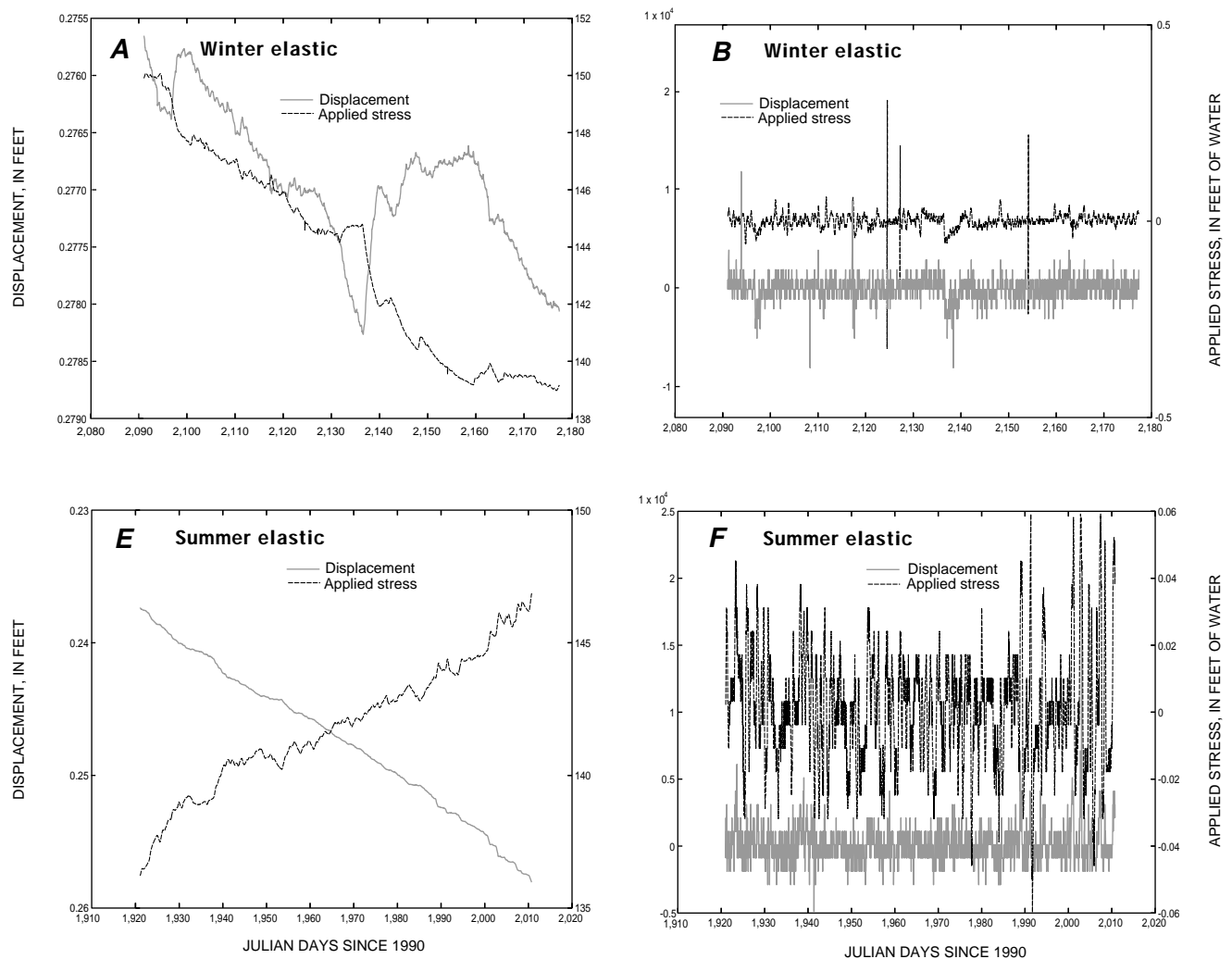


**Figure 19.** Sample time series used in stress/strain analyses of the Holly site (8N/10W-1Q), Edwards Air Force Base, Antelope Valley, California. **A**, Raw winter compaction (displacement) and water level (applied stress). **B**, Detrended winter compaction and water levels. **C**, Detrended and filtered winter compaction and water levels. **D**, Time series in “C” plotted as displacement-stress trajectories. **E**, Raw summer compaction and water levels. **F**, Detrended summer compaction and water levels. **G**, Detrended and filtered summer compaction and water levels. **H**, Time series in “G” plotted as displacement-stress trajectories. **I**, Summer only inelastic compaction and summer raw water levels. **J**, Time series in “I” plotted as displacement-stress trajectories.

equilibrating aquitards (equation 7). Estimates of the equivalent skeletal specific storages were computed using the estimated skeletal storage coefficients (table 2) and thicknesses in the depth interval measured by the extensometer—825 ft for the aquifer systems and 94 ft for the aggregate thickness of the thin aquitards.

The elastic skeletal storage coefficients estimated for the Holly site are comparable with values calculated by Poland and Ireland (1988) for ground-

water basins in the Santa Clara Valley, California, and by Hanson (1989) for ground-water basins in Arizona, but are somewhat smaller than the values reported by Heywood (1995a, b) for basins in New Mexico and Texas, and reported by Poland and others (1975) for basins in the San Joaquin Valley, California. Similarly, the estimated inelastic storage coefficients are comparable with values calculated by Hanson (1989) for Arizona but are somewhat smaller than those reported by

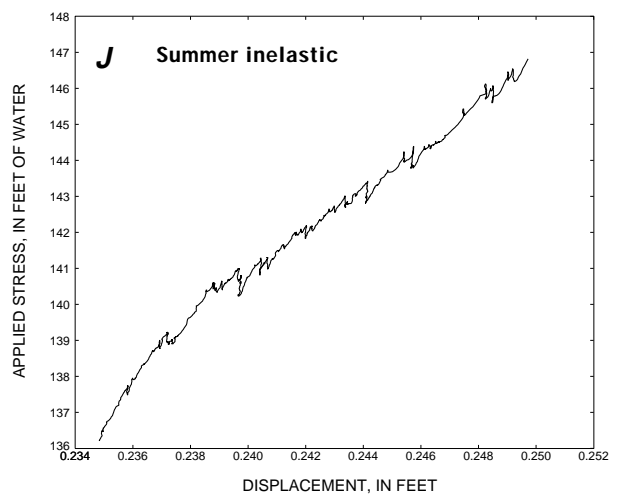
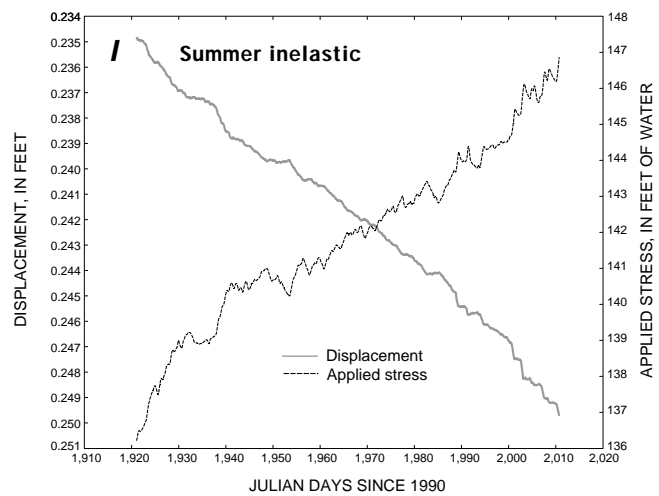
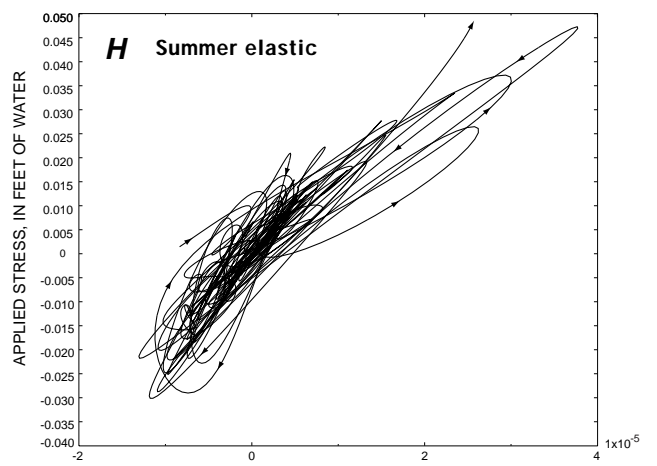
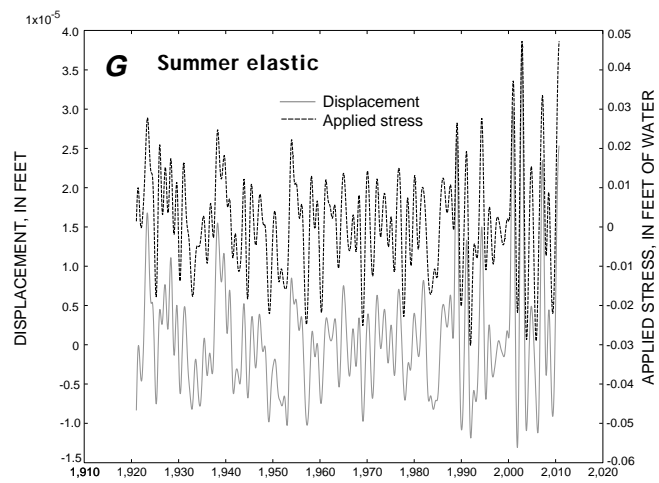
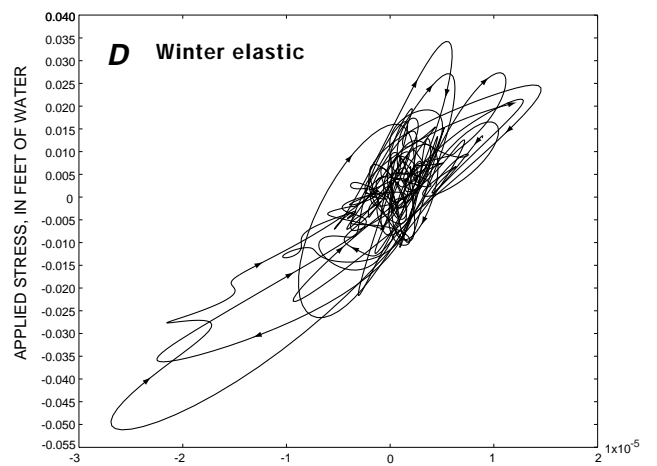
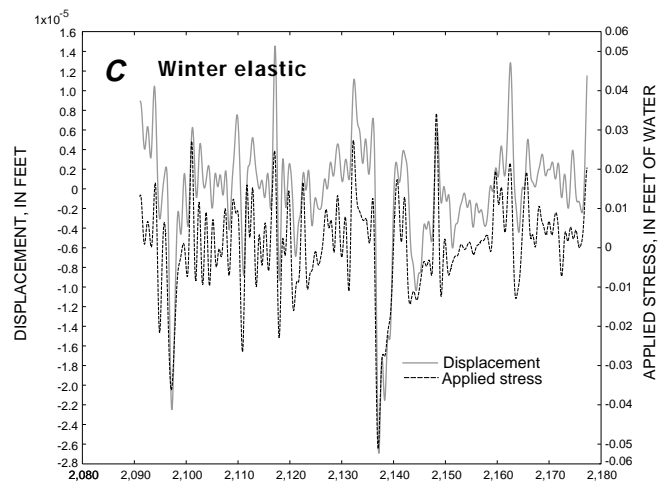


Figure 19. Continued.



**Table 2.** Summary of skeletal storage coefficients and equivalent skeletal specific storages estimated from the results of the stress/strain analyses of the Holly site (8N/10W-1Q), Edwards Air Force Base, Antelope Valley, California

[ft<sup>-1</sup>, per foot]

Type of response	Number of data sets	Skeletal storage coefficients		Skeletal specific storage (ft <sup>-1</sup> )
		Mean	Standard deviation	
Winter elastic .....	6	$7.4 \times 10^{-4}$	$1.5 \times 10^{-4}$	$9.0 \times 10^{-7}$
Summer elastic .....	4	$5.9 \times 10^{-4}$	$8.1 \times 10^{-5}$	$7.2 \times 10^{-7}$
Summer inelastic .....	4	$1.6 \times 10^{-3}$	$1.8 \times 10^{-4}$	$1.7 \times 10^{-5}$

Heywood (1995b) for New Mexico and by Riley (1969) for the San Joaquin Valley, California.

## HOLLY MODEL

A digital model was developed for the Holly site to simulate aquitard drainage, refine estimates of aquifer-system hydraulic parameters controlling compaction, and predict possible future compaction for three selected scenarios. A vertical one-dimensional, finite-difference model that simulates coupled aquifer-system compaction and ground-water flow was developed using MODFLOW-96 (McDonald and Harbaugh, 1988; Harbaugh and McDonald, 1996) and the IBS1 package (Leake and Prudic, 1991). The one-dimensional approach is discussed in the section “Assumptions and Limitations.” The model solves for hydraulic head and vertical displacement for specified aquifer-system properties as a function of depth and time. The Transient Specified-Flow and Specified-Head Boundaries (FHB1) package (Leake and Lilly, 1997) was used to specify constant-head boundaries using measured and estimated values of ground-water levels. The model parameters were adjusted within moderate ranges and available constraints to provide the best “history match” between measured and simulated compaction. In addition to IBS1 and FHB1, other MODFLOW-96 packages used in the Holly site model include Basic 5 (BAS5), Block-Centered Flow 5 (BCF5), and Strongly Implicit Procedure Solution 5 (SIP5) (McDonald and Harbaugh, 1988; Harbaugh and McDonald, 1996).

## Formulation of Numerical Model

A reasonable conceptual model is vital to the realistic simulation of any aquifer system. A conceptual hydrogeologic model of the Holly site, previously

developed by Londquist and others (1993), is well constrained stratigraphically by lithologic and geophysical logs (fig. 5), hydraulically by water levels measured at the nested piezometers (fig. 10), and mechanically by compaction measured at the borehole extensometer (fig. 14). For purposes of simulating the mechanical response (compression and expansion) of the aquifer system to water-level variations, a one-dimensional numerical formulation was developed using assumptions embedded in the aquitard-drainage model and was based on the conceptual model of the Holly site. Two periods were simulated for this study—the historical period (1908–97) and the recent period (1990–97). Although the historical model was developed primarily to constrain transient conditions in 1990 for use as initial conditions in the recent model, the dual time periods allow for comparisons of aquifer-system compaction owing to sustained ground-water-level drawdown through the period of ground-water development and seasonal ground-water-level cycling during the 1990s. Aspects of model formulation included designation of spatial and temporal discretization, boundary conditions, initial conditions, convergence and mass balance criteria, and limiting assumptions that arose from idealization of the aquifer system or from simplification of computations.

## Spatial and Temporal Discretization

The MODFLOW-96 numerical finite-difference model requires spatial and temporal discretization of the model domain. Spatial discretization is defined in terms of layers, rows, and columns that typically are associated with volumes, but in a one-dimensional (vertical) model are associated with thicknesses. Temporal discretization is defined by stress periods and time steps; these are time intervals used by MODFLOW-96 to calculate volumetric exchanges of water between adjacent cells within the model and into or out of the model.

Two one-dimensional aquitard-drainage models, one for the historical period (1908–97) and the other for the recent period (1990–97), are spatially discretized in MODFLOW-96 as a single layer with 1 row and 272 columns (fig. 20). This one-layer, columnwise arrangement effectively translates the aquifer systems, as represented in the conceptual model, from one-dimensional vertical to one-dimensional horizontal as represented in the numerical model. This adaptation of MODFLOW-96 and the IBS1 package for simulating one-dimensional vertical ground-water flow and compaction is presented by Leake and Prudic (1991) and was selected for this study for economy of the layer-wise formatting of MODFLOW-96 input and output.

The model domain was discretized on the basis of location and thickness of the fine-grained sediments determined from borehole resistivity logs and the

lithologic log of the Holly site (fig. 5). The fine-grained sediments were simulated as aquitards with both elastic and inelastic compressibility, and the coarse-grained sediments were simulated as aquifers with only elastic compressibility. For this report, sediments in the upper 840 ft (this excludes the lower aquifer) with resistivities of less than 15 ohm-m on the short-normal resistivity log were defined as fine-grained aquitards on the basis of similar criteria used for the Graham Ranch area (fig. 3) (Londquist and others, 1993). Sediments in the lower aquifer (840–1,091 ft below land surface) with resistivities of less than 10 ohm-m on the short-normal resistivity log (most often at 100 ft intervals) were defined as fine-grained aquitards. Coarse-grained aquitards are defined differently in the lower aquifer compared with more shallow aquitards to compensate for the resistivity shift (attributed to differences in water

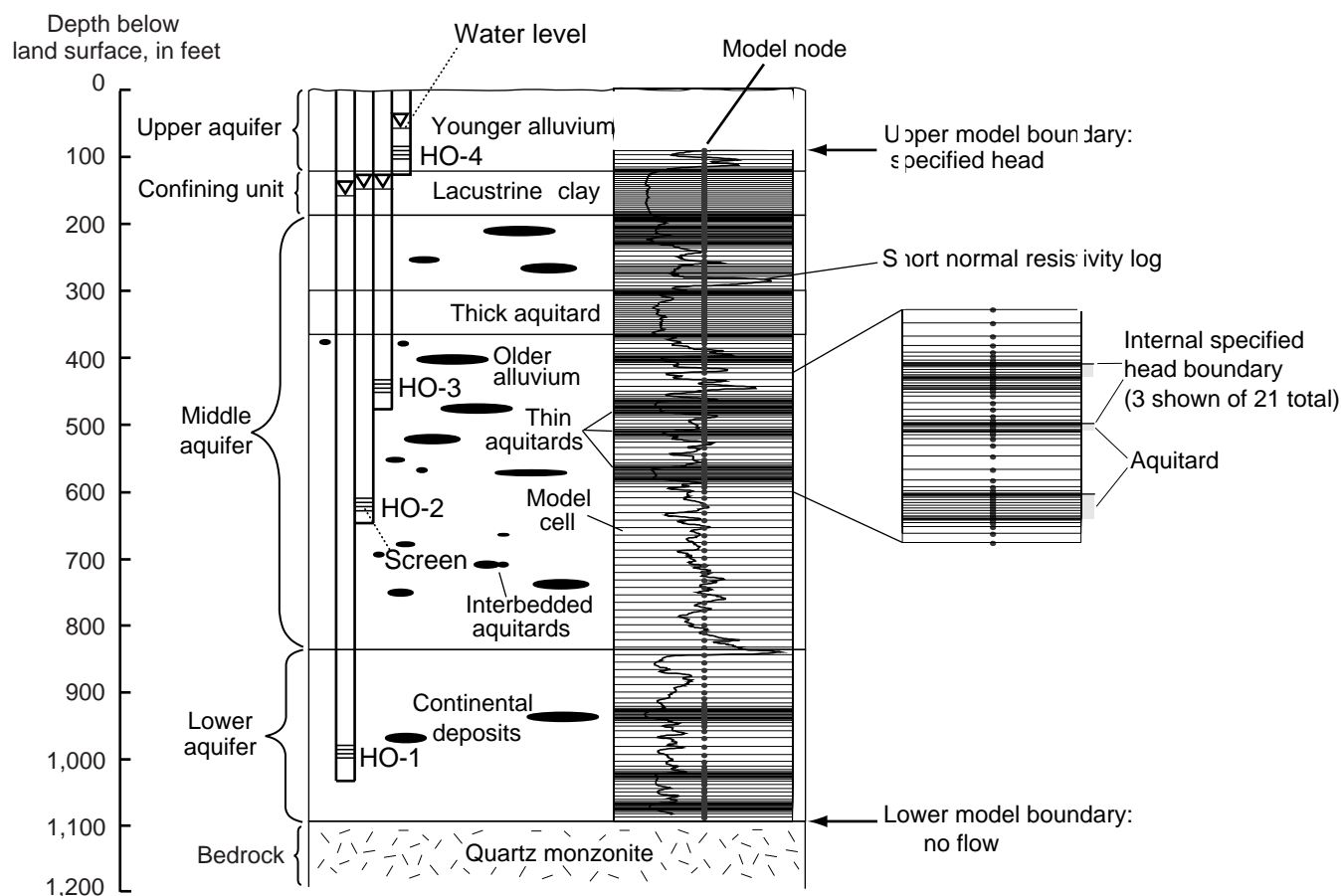


**Figure 20.** Relation of model domain to the conceptual model and short normal resistivity log of the Holly site (8N/10W-1Q), Edwards Air Force Base, Antelope Valley, California. See figure 5 for horizontal scale of resistivity log. The model domain represents a 1- × 1-ft vertical column; the horizontal dimension depicted is for illustration purposes only. (Modified from Londquist and others, 1993)

quality) evident on the resistivity logs (fig. 5). Then, using the guard resistivity log, more precise locations and thicknesses of fine-grained sediments were determined. Using these criteria, the aggregate thickness of the low-resistivity strata in the model domain (91 to 1,090 ft below land surface) is 256 ft, of which 223 ft is within the range measured by the extensometer (91 to 840 ft below land surface). The thickness of individual low-resistivity units interpreted as aquitards ranges from 1 to 66 ft.

Aquitards were modeled in one of two ways depending on the thickness of an individual aquitard—nonexplicitly for aquitards less than 5 ft in thickness and explicitly for aquitards 5 ft or greater in thickness. Assuming that thinner aquitards would equilibrate quickly, the thinnest fine-grained aquitard that was explicitly modeled for this study was 5 ft in thickness. “Explicitly modeled” means that at least four adjacent model nodes were assigned hydraulic parameters representative of 100 percent fine-grained sediment. Aquitards less than 5-ft thick shared a cell thickness with coarse-grained sediment representing aquifer material, and the node, or center of the cell, was assigned hydraulic parameters according to the appropriate proportion of aquitard to aquifer thicknesses for that cell. A total of 12 fine-grained aquitards ranging from 5- to 66-ft thick, with a total aggregate thickness of 217 ft, were explicitly modeled. Fine-grained aquitards that were not explicitly modeled account for the remaining 39 ft of the total aggregate thickness of modeled aquitards.

The finest level of discretization was applied to the aquitards and the boundaries between the aquitards and the aquifers. The thinnest cell representing 100 percent aquitard material represents 1 ft of aquitard material and the thickest cell generally represents 3 ft of material; however, two cells in the model represent 4 ft of aquitard material. Cells adjacent to the boundaries between the aquifers and the explicitly modeled aquitards were discretized by 1-ft thick cells in every instance except one, where one side of the boundary was a 2-ft thick cell.

A coarse discretization was applied to aquifers that contain only a small percentage of fine-grained compressible sediment or none at all. The largest cell, a maximum of 13 ft of sediment represented by a single node, was prescribed to aquifer sediment nonadjacent to aquitard boundaries.

The resulting grid is a 1- × 1-ft vertical column with variable-spaced layers (fig. 20). (The horizontal

dimension of the grid in figure 20 is for illustration purposes only). Variable spacing was required because more cells per length were needed to simulate the relatively large and highly nonlinear hydraulic gradient within the aquitards, and less cells per length were needed to simulate heads in the aquifers because there is essentially no gradient. The resulting discretization is relatively coarse in the aquifers (ranging from 1 to 13 ft and averaging nearly 5 ft) and relatively fine in the aquitards (ranging from 1 to 4 ft and averaging less than 2 ft). To avoid numerical instability that can occur with large thickness variations of adjacent cells in MODFLOW-96, the maximum variation in thickness of adjacent cells was 50 percent, except where adjacent cells represent thicknesses of 1 and 2 ft. This approach results in many model cells; however, the large number of cells used to represent the system did not significantly lengthen the computation time for the relatively simple one-dimensional simulations.

IBS1 simulates the ultimate compaction that will occur for a given head decline in the aquifer under the assumption that pressures equilibrate instantaneously between the aquitard and the aquifer rather than permitting slow drainage and resultant delayed, or residual, compaction of the aquitard. Using a horizontally translated grid of finely spaced nodes to explicitly model thicker aquitards compensates for this limitation in the IBS1 package. The small vertical thickness and the low diffusivity prescribed for several adjacent cells representing aquitards (greater than or equal to 5 ft thick) permits the slow propagation of head changes in the aquitard in response to head changes occurring in the adjacent aquifers during a model time step. This allows the simulation of residual pore pressures and residual compaction in the aquitards. For a particular aquitard, this approach can be limited by the duration of the model time step; if the time steps are too long, the simulated heads propagate too quickly through the aquitard because the hydraulic gradient is constant during a time step. The duration of model time steps was selected by experimentation (30 days for the historical model and 1 day for the recent model) which indicated that lengthening the time step caused more immediate compaction, and less residual compaction, in response to water-level declines and that shortening the time step did not significantly change the response.

The one-dimensional model is temporally discretized in MODFLOW-96 by stress periods and time steps; these time intervals are different for the historical and recent models. Stress periods for the historical

model were defined by available historical water-level data. Annual measurements of water levels in wells in Antelope Valley during the 1970s and 1980s represent the lowest measurement frequency since the early 1920s. As a result, 89 yearly stress periods (365.25 days) were chosen for the historical model. Monthly time steps (30.4375 days) were assigned to reduce mass-balance errors and poor piecewise approximations that could result because of large water-level changes that may occur during year-long time intervals. However, annual (stress period) results from MODFLOW-96 were used to history-match the sparse (approximately 30-year time intervals) land-surface-elevation change data collected or estimated near the Holly site (fig. 17).

For the recent model, prescription of stress periods and time steps was more flexible because of the frequent measurement of water levels at the Holly site. Stress periods of 22 days were chosen to ensure resolution of the seasonal compaction and water-level signals and to maximize the available water-level data for the Holly site at the time of model development. The 1990–97 model simulates 118 stress periods representing more than 7 years. Daily time steps were selected to minimize errors introduced by the assumption of instantaneous head equilibration between aquifers and aquitards for longer time steps as discussed by Helm (1975). For the recent model, daily (time step) results from MODFLOW-96 were used to history-match data collected daily at the Holly site.

## Boundary Conditions

Boundary conditions, or flow conditions, in the one-dimensional (vertical) model of the Holly site consist of specified (time-variant) heads for those parts of the coarse-grained aquifer that represent measured (or estimated) hydraulic head in the piezometers and a specified no-flow boundary at the base of the model (fig. 20). The upper, middle, and lower aquifers at the Holly site (fig. 7) are represented in the model by specifying heads in each aquifer. The upper model boundary is a time-variant, specified-head boundary that represents measured (or estimated) head in the upper aquifer at the Holly site. The boundary is 29 ft above the confining unit, about 91 ft below land surface. Aquitard drainage and aquifer-system compaction were not simulated for the upper aquifer because the entire model domain must remain saturated (the upper aquifer was represented in the model only to specify head above the confining unit). The effect of omitting compaction in the unconfined aquifer is discussed further in the section “Assumptions and Limitations.” Internal boundaries (within the model domain) consist of time-variant, specified heads that represent measured (or estimated) heads in the middle and lower aquifers at the Holly site. A no-flow boundary at the model base, 1,090 ft below land surface, represents impermeable quartz monzonite bedrock (basement complex).

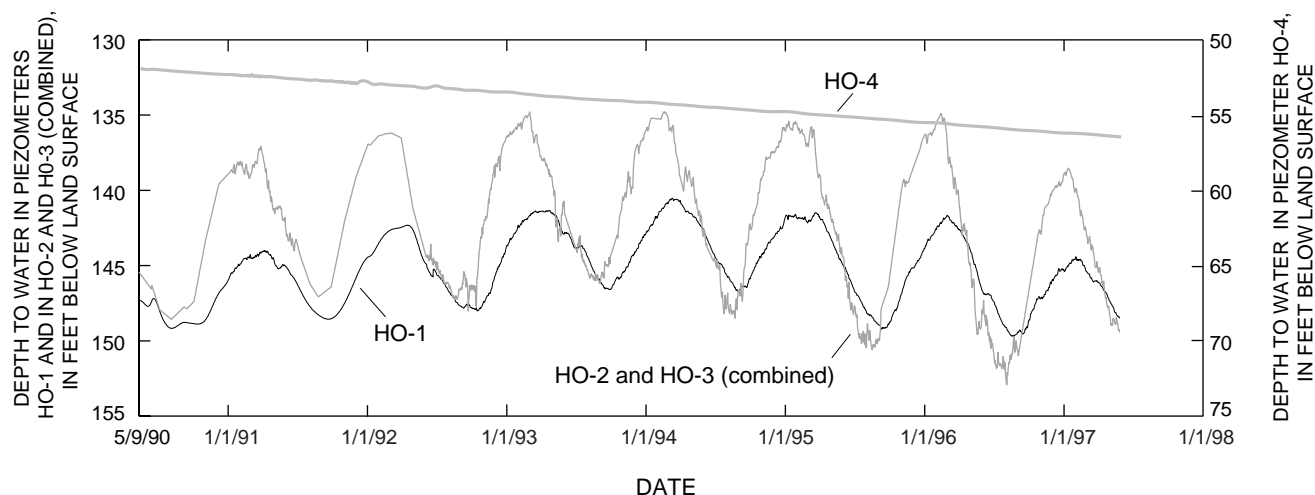


**Figure 21.** Measured or estimated depth to water for piezometers HO-1, HO-2 and HO-3 (combined), and HO-4 used in the 1990–97 model simulation of the Holly site (8N/10W-1Q), Edwards Air Force Base, Antelope Valley, California.

For the 1990–97 simulation, the water levels measured in the nested piezometers at the Holly site were used as input for the time-variant specified-head boundaries because these measurements provided a good definition of the hydraulic head of the aquifers throughout the simulated depth profile (figs. 7, 10, and 21). The shallowest piezometer (HO-4) monitors water levels in the upper aquifer (unconfined). The water level in this piezometer defines the upper boundary of the model (fig. 20). The intermediate piezometers (HO-2 and HO-3), which are screened in the middle aquifer, monitor water levels in the principal production zone. The water levels for the intermediate piezometers were combined for modeling purposes because the water levels for these piezometers track each other very closely, and only one or the other was instrumented at most times (figs. 10 and 21). Water-level data from the combined record for piezometers HO-2 and HO-3 were used for the internal time-variant specified-head boundaries within the middle aquifer. Measurements made in the deepest piezometer (HO-1) were used for the internal time-variant specified-head boundaries within the lower aquifer (figs. 20 and 21).

For the 1908–97 simulation, three composite hydrographs (representative of the three aquifers at the Holly site) were developed; the hydrographs were used for input as time-variant specified-head boundaries (fig. 22). Prior to the construction of the Holly site, ground-water-level information was limited for the

vicinity of the site; therefore, we estimated hydraulic head from available historical ground-water-level data. When data were sparse, we used interpolation techniques. The historical model begins in 1908—the time of the earliest recorded ground-water levels for wells near the Holly site (Johnson, 1911) and the time most representative of predevelopment conditions near the site.

A composite hydrograph of water levels for the upper aquifer at the Holly site was created using a simple linear interpolation for the period 1908 to 1990. The water level at the Holly site was estimated to be at land surface in 1908 and more than 50 ft below land surface in 1990. Water levels measured in piezometer HO-4 between 1990 and 1997 were used for the last 7 years of the hydrograph (fig. 22).

A composite hydrograph representative of the middle aquifer was developed on the basis of historical water levels from wells near the Holly site. Because most of the wells did not penetrate the lower aquifer during this period (1908–90), the composite hydrograph of the lower aquifer was based on the composite hydrograph of the middle aquifer and on recently (1990–97) measured water levels for both aquifers. Water levels in well 8N/10W-9M1 (fig. 3) for the period 1908–36 were compiled from Thompson (1929) and Meinzer and others (1945). Because measurements were made infrequently during much of this period, especially during the early years of record, we estimated changes in water levels using descriptions of the area by Johnson (1911) and Thompson (1929), who reported artesian conditions in the vicinity of the Holly site until sometime between about 1914 and 1919. For the period 1937–51, we used a simple linear interpolation to estimate water-level declines. For the period 1952–89, water levels for 8N/10W-28B1 (fig. 3) were used. The composite hydrograph represents water levels in the middle aquifer for every year from 1908 to 1989 (fig. 22).

Wells 8N/10W-9M1 and 8N/10W-28B1, which were used to construct the hydrograph, are located south of the Willow Springs Fault (fig. 2) where historical water levels were substantially lower than those measured north of the fault near the Holly site [more than 40 ft lower in 1952 (Dutcher and Worts, 1963), but nearly equivalent in 1990]. Because of the lower water levels in these wells, the composite hydrograph was adjusted for the middle aquifer. No water-level records prior to the 1950s were found for wells north of the Willow Springs Fault near the Holly site. Water-level

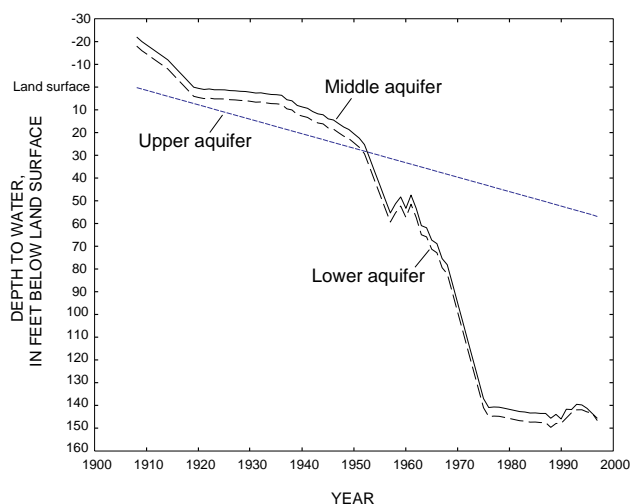


**Figure 22.** Water levels used for input in the historical model for the upper, middle, and lower aquifers at the Holly site (8N/10W-1Q), Edwards Air Force Base, Antelope Valley, California.

measurements were recorded in the 1950s for two wells north of the fault, but only well 8N/10W-2P1 (fig. 3) had more than one measurement recorded that decade. Same-year water levels in the composite hydrograph were compared with water levels for well 8N/10W-2P1; a ratio was used to adjust the composite hydrograph to water-level measurements of well 8N/10W-2P1. The result is a composite hydrograph representative of the middle aquifer at the Holly site prior to 1990. The combined water levels of the intermediate piezometers were used to complete the hydrograph of the middle aquifer to 1997 (fig. 22).

The composite hydrograph representative of the lower aquifer (fig. 22) was created by applying an offset of -4.0 ft to the composite hydrograph for the middle aquifer for 1908–89 and by using measured water levels for piezometer HO-1 for 1990–97. Water levels measured in the lower aquifer generally were lower than those in the middle aquifer, although not by a consistent amount (fig. 10). Water levels probably were higher in the lower aquifer than in the middle aquifer for at least part of the century, but because historical wells in the vicinity of the Holly site were not deep enough to penetrate the lower aquifer, no data are available to delineate the relational history between these two aquifers. The sensitivity of the model to the hydrograph of the lower aquifer was investigated by applying an equivalent offset in the opposite direction, +4.0 ft, so that heads in the lower aquifer were always higher than heads in the middle aquifer for 1908–89. The results of the simulations for the lower aquifer were nearly identical using the two composite hydrographs even though there was an 8-ft shift indicating the appreciable insensitivity of the model to the variation.

It was assumed that there was sufficient vertical connectivity between aquifers outside of the model column for heads in the aquifers to equilibrate rapidly. This assumption is supported by data from wells HO-2 and HO-3, which show essentially identical heads (fig. 10). This aquifer head distribution was implemented in the model by specifying constant (time-variant) heads in coarse-grained sediment between each aquitard. Consequently, 21 constant (time-variant) head boundaries were specified—one for each coarse-grained stratigraphic layer that was bounded above and below by aquitards.

## Initial Conditions

Transient conditions for ground-water flow and aquifer-system compaction that occurred at the Holly site prior to 1990 are largely unknown; therefore, a historical model was developed to better constrain the effects of transient conditions prior to 1990. The initial conditions for the historical model are representative of estimated steady-state conditions in 1908. The initial conditions for the more detailed and constrained recent model (1990–97) were derived from the historical model (1908–97).

Initial heads for each of the three aquifers are defined by the composite hydrographs (fig. 22). The initial head in the upper (unconfined) aquifer for 1908 was set equal to land surface; initial heads for the middle and lower (confined) aquifers were set to about 22 and 18 ft above land surface, respectively. For the confining unit, initial heads were assigned values that varied linearly from top to bottom, between land surface and 22 ft above land surface. All other aquitards were assigned the initial head of the aquifer in which it is contained.

A range of predevelopment preconsolidation stress values, in terms of hydraulic head, was estimated from the time series for paired bench marks and water levels (fig. 17) and iteratively refined with model output. The estimated range of predevelopment preconsolidation head was about 0 (at land surface) to 50 ft below land surface, which corresponds to the period 1929 to 1961, when land subsidence apparently began (fig. 17). The middle and lower aquifers were calibrated with preconsolidation heads of about 20 and 22 ft below land surface, respectively. Nodes representing the confining unit, 120 to 186 ft below land surface at the Holly site, were calibrated with values that varied linearly from top to bottom, between about 15 ft and 20 ft below land surface. All other aquitards interbedded in the confined aquifer system were assigned the preconsolidation head of the aquifer in which they are contained. Because compaction was not simulated for the upper aquifer, no fine-grained material was attributed to this unit and, thus, no preconsolidation-head values were needed.

## Convergence Criteria and Mass Balance Criteria

The strongly Implicit Procedure Solution 5 (SIP5), a solver option in MODFLOW-96, was used for the Holly models (historical and recent) to solve the governing equations for all nodes simultaneously and

iteratively until the solution converged or until the maximum number of iterations was exceeded. The convergence criterion used for the Holly model permitted a maximum difference of 0.001 ft in the solution from consecutive iterations.

Results of volumetric-flow computations made with BCF5 and IBS1 were used with MODFLOW-96 to calculate a mass balance for each stress period to provide an indication of the overall acceptability of the numerical approximation to the true solution. MODFLOW-96 uses a water-budget approach to compute mass balance independently of the equation solution process and, in this sense, may provide independent evidence of a valid solution (McDonald and Harbaugh, 1988). In the Holly models, two components of flow—flow to and from the specified-head nodes and flow into and out of storage—constitute the budget. IBS1 accounts for elastic and inelastic skeletal storage changes and augments the storage component of the budget computed by BCF5 (storage from expansion and compression of water) with these subcomponents. Cumulative water budgets and discrepancies between the volume of water moving into and out of the model, accounting for any changes in storage, were tallied at the end of each stress period. Discrepancies in the Holly models were less than 0.1 percent.

### Assumptions and Limitations

Assumptions and limitations in the model were derived from translating the complex and variable aquifer system into a digital computer model. Aquitard drainage was simplified to a one-dimensional diffusion process and further simplified for material deformation.

The Holly models simulate vertical Darcian flow within the aquitards, a widely applied and appropriate assumption for simulating the drainage of aquitards in large aquifer systems with permeability contrasts of several orders of magnitude between the aquifers and the aquitards (Neuman and Witherspoon, 1969; Hanson, 1989). Flows into, out of, and between cells representing aquifer material also are vertical and caused by head gradients between the aquifers and specified-head (variable) boundary conditions. The Holly models assume that lateral flow is negligible compared to changes in storage and related vertical flow.

IBS1 assumes that changes in effective stress are a function only of changes in head not of changes in geostatic load, that is, the change in total stress is zero. In a confined aquifer overlain by a confining unit and an unconfined aquifer, this assumption tends to result in an overestimation of the change in effective stress and associated deformation if the water table declines in the unconfined aquifer. Conversely, this assumption tends to result in an underestimation of the changes in effective stress and deformation if the water table recovers (Leake and Prudic, 1991). Compaction may be overestimated for the historical model because the water table declined about 56 ft (fig. 22) (conservatively, about 18 percent of the total geostatic load at the base of the upper aquifer) during the simulated period. For the 1990–97 simulation of the Holly site, this assumption may not be a significant source of error because the water table declined only about 4.5 ft (fig. 21) (conservatively, about 1.5 percent of the total geostatic load at the base of the upper aquifer) during the simulated period.

Compaction in the unconfined aquifer is not simulated in the Holly models because its seasonal contribution to total compaction is insignificant, as indicated in figure 21 by the small seasonal change in effective stress in the unconfined aquifer system compared with the confined aquifer system. The hydrograph for piezometer HO-4, screened in the upper aquifer, indicates that the water levels in the well are steadily declining. The associated rate of compaction also is steady. The water levels in piezometers HO-2 and HO-3 (screened in the middle aquifer) and HO-1 (screened in the lower aquifer) fluctuate seasonally, which indicates that compaction in the confined aquifer system has a seasonal component of compaction. Over long periods of time, the unconfined aquifer system probably plays a more important role in deformation at the Holly site.

The Holly models use the same constant (time-variant) heads for the entire middle aquifer. Piezometers HO-2 and HO-3 are screened below the thick aquitard (302–365 ft below land surface) in the middle aquifer; none of the piezometers at the Holly site are screened between the thick aquitard and the lacustrine clay confining unit (120–186 ft below land surface) (fig. 7). The assumption that the thick aquitard (302–365 ft below land surface) is laterally discontinuous permits the use of equivalent hydraulic heads above



and below this thick aquitard, but this may be an oversimplification.

The IBS1 package assumes that elastic deformation of the aquifer system is proportional to changes in effective stress and that inelastic compaction is proportional to increases in effective stress. Results of laboratory consolidation tests indicate that inelastic compaction of many of the fine-grained sediments is proportional to the increase in the logarithm of effective stress. Any error resulting from the linearization of this logarithmic relation will be less for deeper sediments because a given decline in head will result in a smaller percentage increase in effective stress in deeper sediments than in shallower sediments (Leake and Prudic, 1991). For the Holly models, particularly for the recent model (1990–97), increases in effective stress are a relatively small percentage of the initial state of stress; thus, any error introduced by this limitation probably is small. IBS1 assumes that the soil grains are incompressible, which is not a limiting assumption for the range of stresses considered in the Holly models.

IBS1 inherently assumes that changes in hydraulic head in aquitards equilibrate with changes in head in aquifers within a single model time step, which means that no residual pore pressure and no residual compaction is simulated—only ultimate compaction. For aquitards with delayed drainage, this assumption is invalid, and model simulations may result in an underestimation of storage changes and compaction for later time and an overestimation of those changes for early time (Leake and Prudic, 1991). Aquitards (at least 5-ft thick) simulated in the Holly models were vertically discretized into small-thickness cells to minimize the effects of this limitation in an attempt to explicitly model pressure diffusion in the aquitards (discussed earlier in the “Spatial and Temporal Discretization” section of this report).

For the simulations of the Holly models, specific storage and vertical hydraulic conductivity were assumed constant; however, in fact, they vary inversely with changes in effective stress. This assumption can result in an overestimation of compaction for later time because reductions in skeletal storage are directly related to decreases in compaction. Other than for a narrow elastic range, the more a material has compressed the smaller is its compressibility; thus, larger effective stresses will be required to compact at the equivalent rate. This relational response will be

affected partly by changes in the vertical hydraulic diffusivity owing to changes in vertical hydraulic conductivity and storage. Reductions in vertical hydraulic conductivity occur exponentially with increases in effective stress; hence, flow in aquitards will be overestimated for later times as these units compact into stiffer, less permeable assemblages. Because compaction is relatively small at the Holly site, especially during the period of record of the site, this limitation does not pose significant error in the recent (1990–97) model.

An additional limitation of the IBS1 package is that compaction calculations do not include cells used to specify head (Leake and Prudic, 1991). As a result, specified-head cells for aquifers that may contain a fraction of fine-grained compressible material may not adequately be simulated. To minimize the aggregate thickness of sediments excluded from the compaction calculations, heads were specified at the node of a cell or cells that represented the smallest thickness of sediments for each aquifer. The vertical hydraulic conductivity of the aquifer nodes was set high to ensure the rapid transmission of head changes throughout the vertical aquifer section. As a result of this method, 22 heads were specified and only 30 noncontiguous feet of aquifer material (4 percent of total) and 1 ft of aquitard material (0.4 percent of total) were not included in the calculations of sediment deformation.

## SIMULATIONS

Two periods, 1908–97 which represents the historical period and 1990–97 which represents the recent period, were modeled for the Holly site using two separate, but linked, models. The dual simulations provided a characterization of compaction at the Holly site related to nearly continuous ground-water-level decline throughout the period of ground-water development, combined with the effect of seasonal ground-water-level cycling from nearby pumping. The two periods were modeled in an iterative procedure to attain a single set of aquifer-system properties that provides a reasonable history match for the magnitude and the timing of aquifer-system compaction measured or estimated for each period. More emphasis was given to the recent model because it is better constrained by measured data.



The historical model was developed primarily to define the initial conditions at the Holly site in 1990. This model is being used to provide constraints for a regional three-dimensional ground-water flow model of EAFB that is being developed concurrently with this model.

## History Matching

The history-matching process constituted a trial-and-error adjustment of selected model parameters until the variance between simulated and measured or estimated aquifer-system compaction was minimal and until one set of parameters reasonably simulated compaction for both models. The curve showing historical

simulated compaction and measured or estimated land subsidence compares well to subsidence measured or estimated in 1961, but a comparison between measured and simulated subsidence for the late 1980s and early 1990s indicates that the simulated subsidence is underestimated (fig. 23). Simulated compaction (to a depth of 840 ft below land surface) for the recent model compares well with measured compaction at the Holly extensometer for the period 1990–97 (fig. 24A). The simulated displacement-stress trajectory also compares well in magnitude, timing, and phase with the measured displacement-stress trajectory (fig. 24B). Results of the simulated compaction of the recent model show a noticeable departure from measured compaction beginning mid-1996 (fig. 24A); less

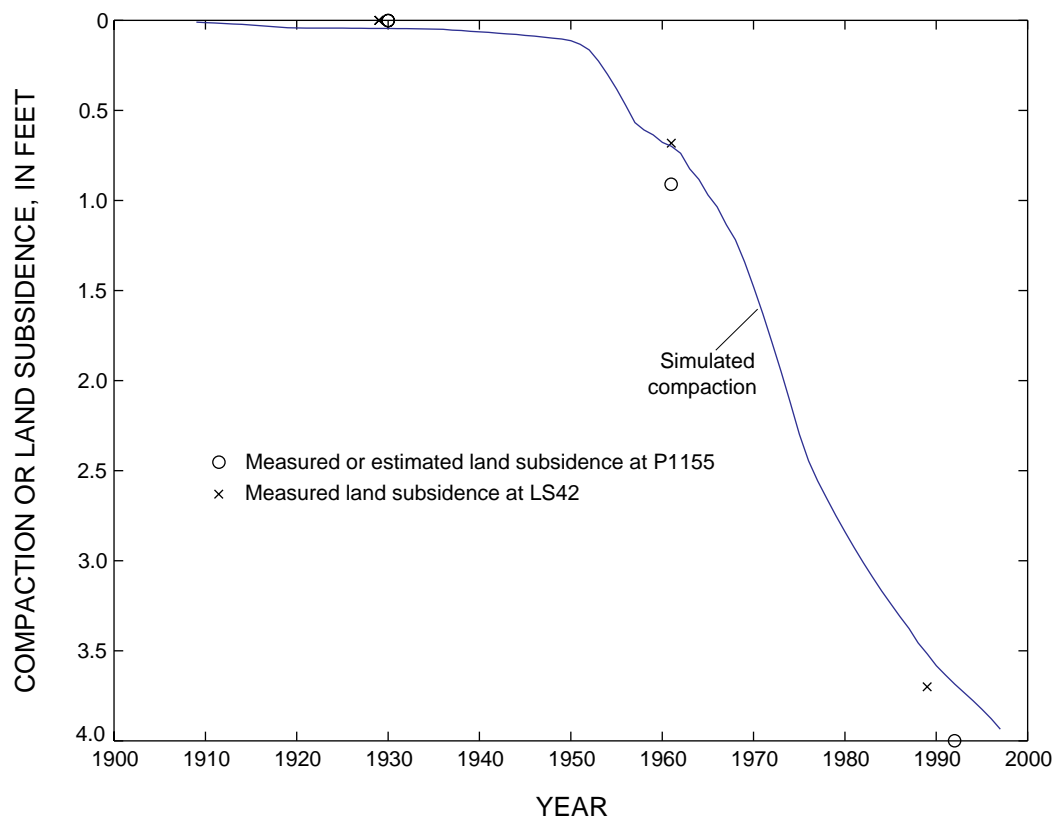


**Figure 23.** Simulated compaction and measured or estimated land subsidence at bench marks P1155 and LS42 near the Holly site (8N/10W-1Q), Edwards Air Force Base, Antelope Valley, California, 1908-97. (See figure 3 for location of bench marks.)

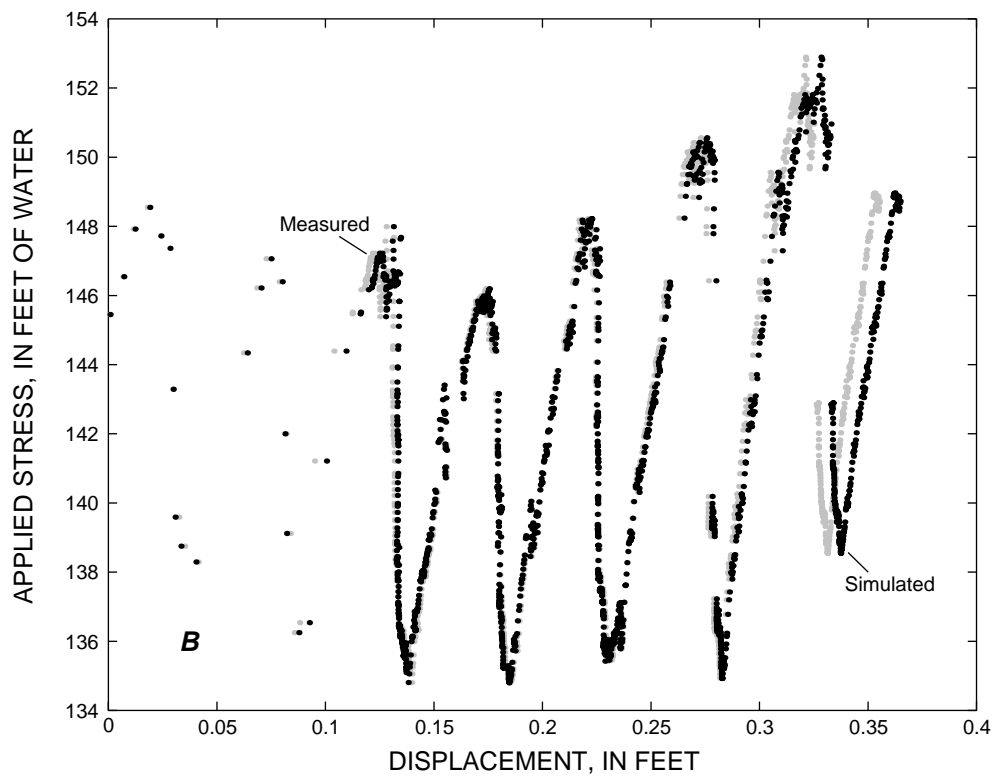
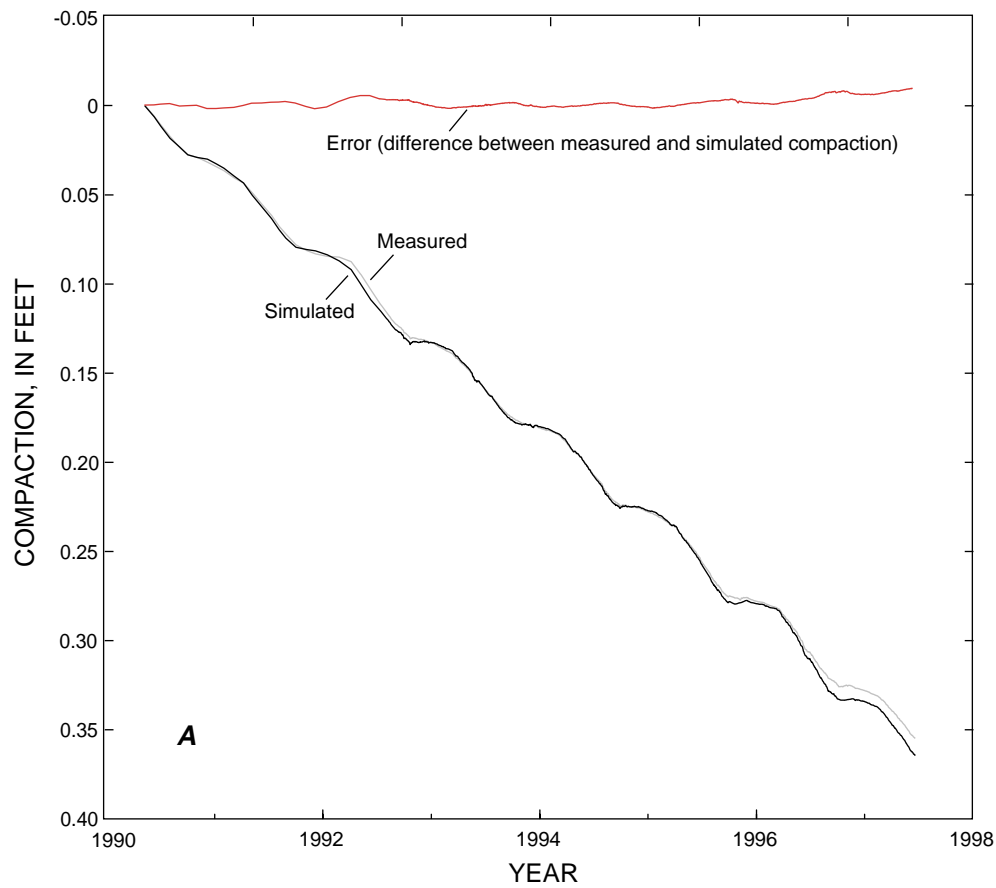


**Figure 24.** History matches for 1990–97 for (A) simulated and measured compaction and error and (B) simulated and measured displacement-stress trajectories for the Holly site (8N/10W-1Q), Edwards Air Force Base, Antelope Valley, California.

**Table 3.** Values of hydraulic parameters derived from the best history matches between simulated aquifer-system compaction and measured or estimated compaction at the Holly site (8N/10W-10), Edwards Air Force Base, Antelope Valley, California  
[ft, foot; ft/d, foot per day;  $\text{ft}^{-1}$ , per foot]

Hydraulic parameters	Value
Vertical hydraulic conductivity, aquifer .....	$3.0 \times 10^{-2}$ ft/d
Vertical hydraulic conductivity, aquitard (less than or equal to 18 ft thick) .....	$1.5 \times 10^{-5}$ ft/d
Vertical hydraulic conductivity, confining unit (120 to 186 ft below land surface) .....	$1.2 \times 10^{-5}$ ft/d
Vertical hydraulic conductivity, aquitard (302 to 365 ft below land surface)	$1.5 \times 10^{-5}$ ft/d
Skeletal elastic specific storage, aquifer system .....	$1.7 \times 10^{-6}$ $\text{ft}^{-1}$
Skeletal inelastic specific storage, aquitards (less than or equal to 18 ft thick) .....	$4.0 \times 10^{-5}$ $\text{ft}^{-1}$
Skeletal inelastic specific storage, aquitards (greater than 18 ft thick) .....	$3.5 \times 10^{-4}$ $\text{ft}^{-1}$
Specific storage, water .....	$4.2 \times 10^{-7}$ $\text{ft}^{-1}$

compaction occurred in the aquifer system than was simulated by the model. The comparisons of simulated and measured compaction for two time periods (figs. 23 and 24) indicate that the set of selected model parameters that provided the best “history match” (table 3) for both models reasonably matched the magnitude (storage) and timing (drainage) of measured compaction.

The two values of vertical hydraulic conductivity determined for the aquitards are in agreement with the values used for aquitards in aquitard-drainage models of other alluvial basins in California and Arizona (Helm, 1975; Hanson, 1989) and values computed by Riley (1969) and Neuzil (1994). The value for elastic specific storage is two times larger than the value estimated from the stress/strain analyses but is consistent with the values used in other models (Helm, 1975; Hanson, 1989). The value for elastic specific storage, however, is smaller (by a factor of 10) than that computed by Heywood (1995a) for the Hueco Basin in Texas. Two values of inelastic specific storage were determined for the two classes of aquitards—thick aquitards (greater than 18-ft in thickness) and thin aquitards (less than or equal to 18-ft in thickness). The values for the thick and the thin aquitards were about 21 and 2 times larger, respectively, than the values estimated from the stress/strain analyses. Note that the

stress/strain analyses did not account for slow drainage and results were not intended to be representative of thick aquitards. The value for the thicker aquitards, however, is more typical of the values computed by Poland and others (1975), Helm (1978), Hanson (1989), and Heywood (1995b); the value of inelastic specific storage for thinner aquitards is consistent with other values computed by Helm (1978) and Hanson (1989).

Time constants (equation 9), representing the time required for about 93 percent of the excess pore pressure to dissipate, were computed for the aquitards. For aquitards 5- to 18-ft thick, equivalent vertical hydraulic conductivity and inelastic skeletal specific storage values were used (table 3). For aquitards between 5- and 18-ft thick, time constants ranged from about 17 to 216 days. For the 63-ft thick aquitard (302 to 365 ft below land surface), the time constant was about 60 years. For the confining unit (120–186 ft below land surface), a strictly comparable time constant could not be calculated because this unit does not doubly drain, but replacing  $(b'/2)$  with  $b'$  in equation 9, which represents the length of the drainage path (Epstein, 1987), we calculated a time constant of 350 years.

The predevelopment preconsolidation stress (head) in the middle aquifer corresponded to an estimated 42 ft of ground-water-level decline before permanent compaction initiated (assuming hydraulic heads were about 22 ft above land surface in the middle aquifer in 1908). This preconsolidation stress threshold compares with values reported by Hanson (1989) for ground-water-level declines in alluvial basins in Arizona, which range from 50 to 150 ft, and by Holzer (1981) for other areas of subsidence, which range from 52 to 207 ft.

## Sensitivity Analysis

Sensitivity to changes in initial preconsolidation stress, elastic and inelastic storage, and vertical hydraulic conductivity was investigated for the Holly models. Sensitivity to initial preconsolidation stress was examined using the historical model; all other parameters were examined using the recent model.

The simulated magnitude of land subsidence is most sensitive to predevelopment preconsolidation

stress, which controls the threshold beyond which fine-grained material begins to compact. For a specified head decline spanning predevelopment preconsolidation stress, the total compaction varies inversely. Varying the predevelopment preconsolidation stress values determined from the best history match by plus or minus 10 ft resulted in simulated values of 3.5 and 4.3 ft of historical aquifer-system compaction, respectively, compared with 3.9 ft for the match value.

Results of the simulations of the recent model indicate that residual compaction is responsible for virtually all compaction measured at the Holly site. Therefore, we examined in detail the sensitivity of the recent model to the key parameters controlling the equilibration of residual pore pressures in the aquitards and residual compaction. These parameters are vertical hydraulic conductivity of the aquitards,  $K'_v$ , and the aquitard inelastic skeletal specific storage,  $S'_{skv}$  (fig. 25). Sensitivity was evaluated on the basis of the computed error,  $Sce$ , between measured and simulated compaction (displacement) for the depth interval of the aquifer system measured by the borehole extensometer. The error was computed as

$$Sce = \sqrt{[(\sum(\mu_{zo} - \mu_{zs})^2) / (n - 1)]}, \quad (10)$$

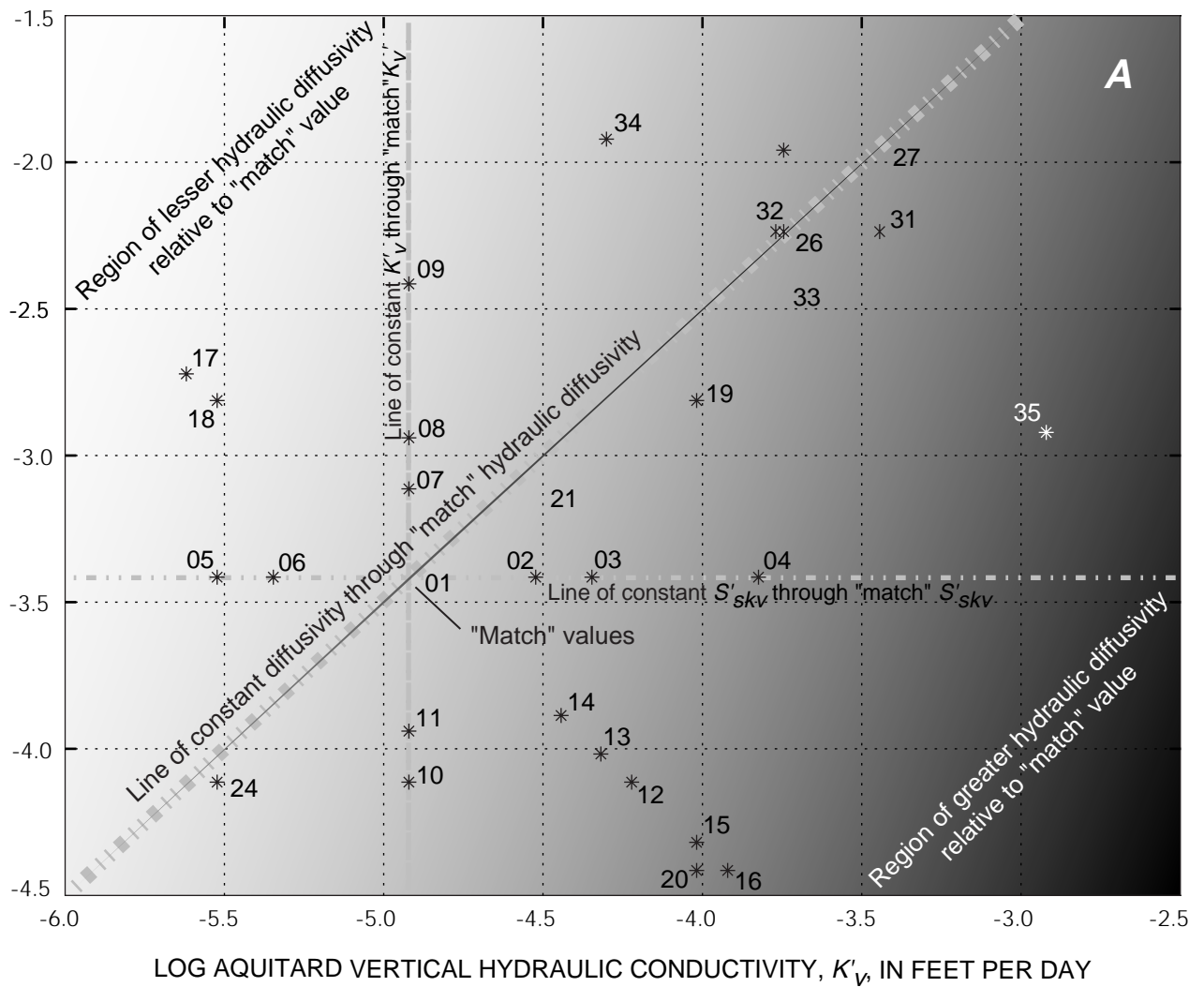
where  $\mu_{zo}$  and  $\mu_{zs}$  are measured and simulated displacement, respectively, and  $n$  equals 1,751, the number of daily displacement values compared, limited by availability of daily measured compaction values. A range of values from less than 1 to nearly 3 orders of magnitude from the history-matched values were tested. The tested range was limited by modeling errors caused largely by numerical instabilities for certain combinations of the parameters. Figure 25A shows the 35 pairs of  $K'_v$  and  $S'_{skv}$  values tested for the confining unit. The same parameters were adjusted proportionally for all aquitards, but only specific parameter values used for the confining unit are shown as representative values in figure 25. Within the range of tested values, several trends of variation were explored—variations in  $K'_v$  for a constant  $S'_{skv}$ , variations in  $S'_{skv}$  for a constant  $K'_v$ , and variations in both parameters for a constant value of the ratio, vertical hydraulic diffusivity. Several other combinations of the parameters also were tested.

The sensitivity analysis shows that the model is very sensitive to changes in  $K'_v$ ,  $S'_{skv}$ , and the vertical hydraulic diffusivity of the aquitards. Both the sensitivity of each parameter and its relative sensitivity among all three parameters varies significantly within the parameter space defined by the range of tested values. For values similar to the history-matched values, small changes in  $K'_v$  result in larger changes in the computed error than for similar changes in  $S'_{skv}$  (fig. 25B, C). For values less similar to the matched values, the model is slightly more sensitive to variations in  $S'_{skv}$  than  $K'_v$ . The largest errors resulted from variations in the direction of increasing  $K'_v$  and decreasing  $S'_{skv}$  for a constant hydraulic diffusivity equal to the history-matched value (fig. 25D). Variations in diffusivity were examined using selected combinations of  $K'_v$  and  $S'_{skv}$  positioned in the parameter space (fig. 25A) along a line perpendicular to the line of constant diffusivity and drawn through the history-matched values. The sensitivity of the model to changes in diffusivity reflects the combined sensitivities to the individual parameters,  $K'_v$  and  $S'_{skv}$  (fig. 25E).

Vertical hydraulic conductivity for the aquitards and elastic specific storage for the aquifer system were modified in the same manner. These modifications resulted in a slightly smaller standard error compared with the results of similar changes for vertical hydraulic conductivity and inelastic specific storage for the aquitards, with less deviation in standard error values among several simulations. The model is least sensitive to independent variations in aquifer-system elastic specific storage.

The results of the sensitivity analysis suggest that a good approach to history-matching would have been to begin with a larger-than-expected value for vertical hydraulic diffusivity of the aquitards, adjusting that value downward until the minimum error is achieved and then adjusting the value of  $S'_{skv}$  to minimize error.

The narrow range of expected  $S'_{skv}$ ,  $5 \times 10^{-6}$  to  $1 \times 10^{-4} \text{ ft}^{-1}$ , identified from measured field values for subsiding basins in Arizona, Texas, and California (Epstein, 1987; Hanson, 1989; Heywood, 1995a; Riley, 1998), and the increased sensitivity of the model to  $K'_v$  in the near range of the solution suggest that efforts to improve field measurements of  $K'_v$  [which can vary by a large range,  $2.8 \times 10^{-6}$  to  $2.8 \times 10^{-3} \text{ ft/d}$  (Neuzil, 1994)] could lead to better constrained simulations of



#### EXPLANATION

- ⊗ Parameter values from history match
- \* Parameter values used in sensitivity analysis
- 35 Model run number

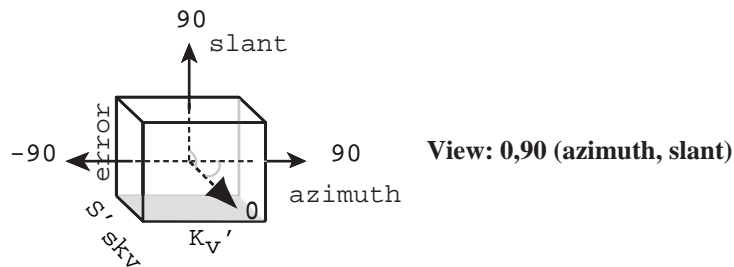
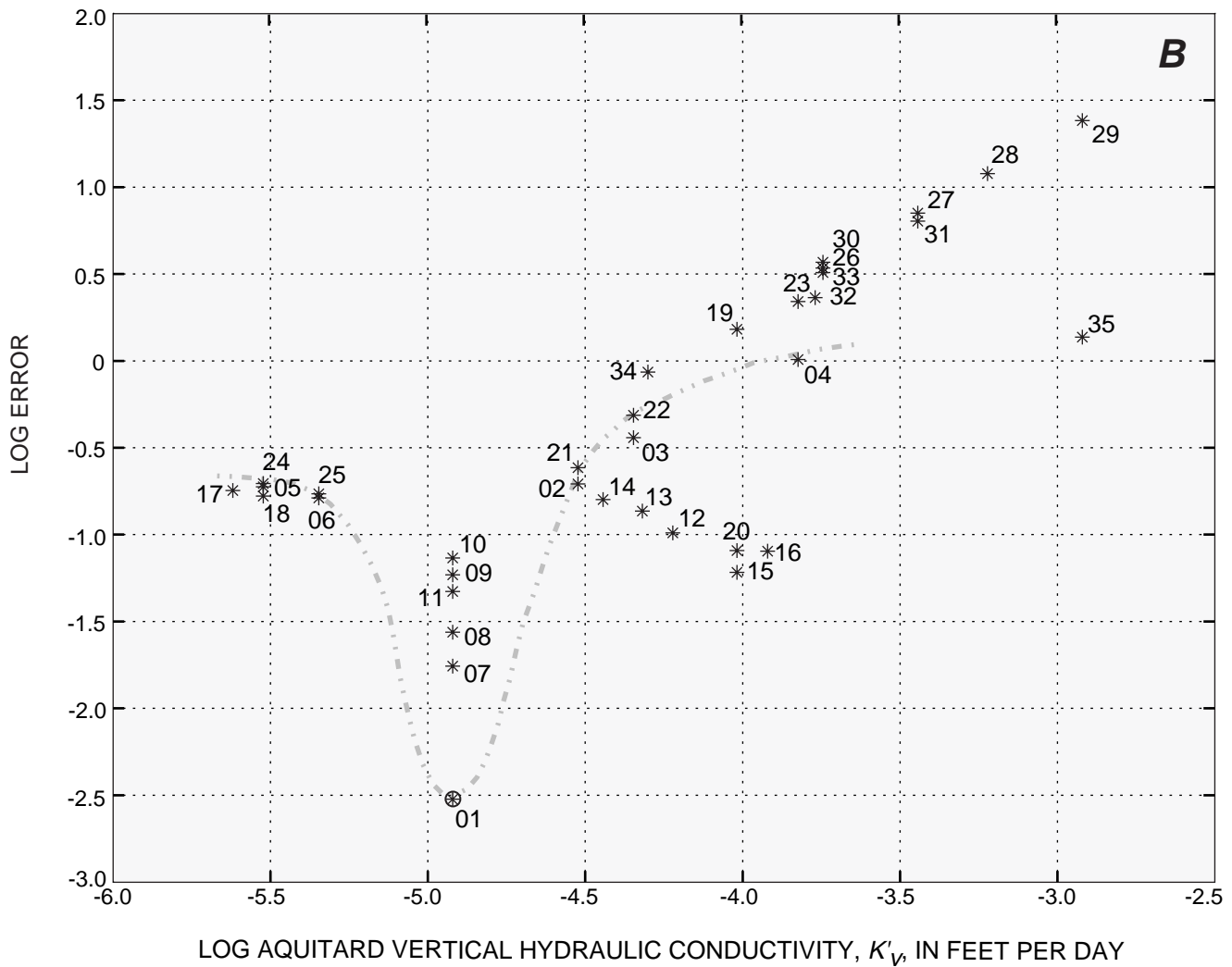


**Figure 25.** Distribution of error computed between measured and simulated compaction for 35 selected values of  $K'_v$  and  $S'_{skv}$  of the aquitards at the Holly site (8N/10W-1Q), Edwards Air Force Base, Antelope Valley, California. The parameter values shown are those simulated for the confining unit. The shaded plane in the cube represents the plane of view. **A**, Plan view of  $K'_v$ - $S'_{skv}$ -error space showing selected parameter values for the confining unit.



#### EXPLANATION

- Error surface in plane of "match" value of  $S'_{skv}$
- ⊗ Parameter values from history match
- \* Parameter values used in sensitivity analysis
- 35 Model run number

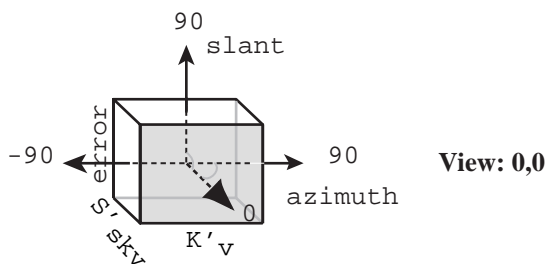
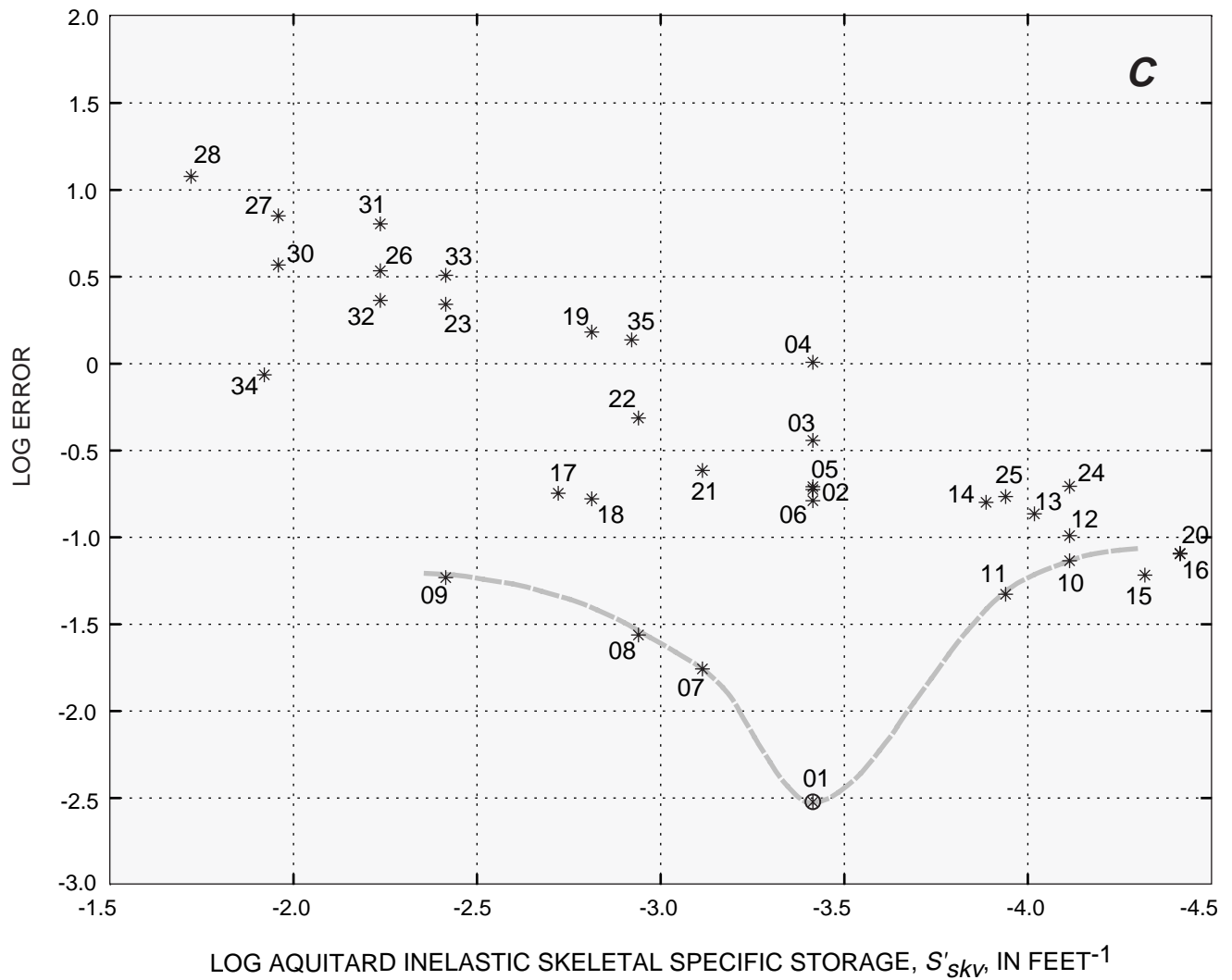


**Figure 25.** Continued. **B**, View of  $K'_v$ -error plane showing the trace of the error surface for a constant "match" value of  $S'_{skv}$  for variations in  $K'_v$



#### EXPLANATION

- Error surface in plane of "match" value of  $K'_v$
- ⊗ Parameter values from history match
- \* Parameter values used in sensitivity analysis
- 35 Model run number

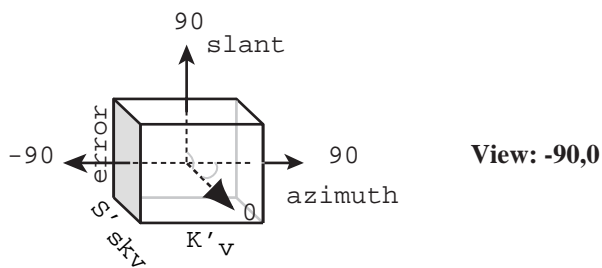
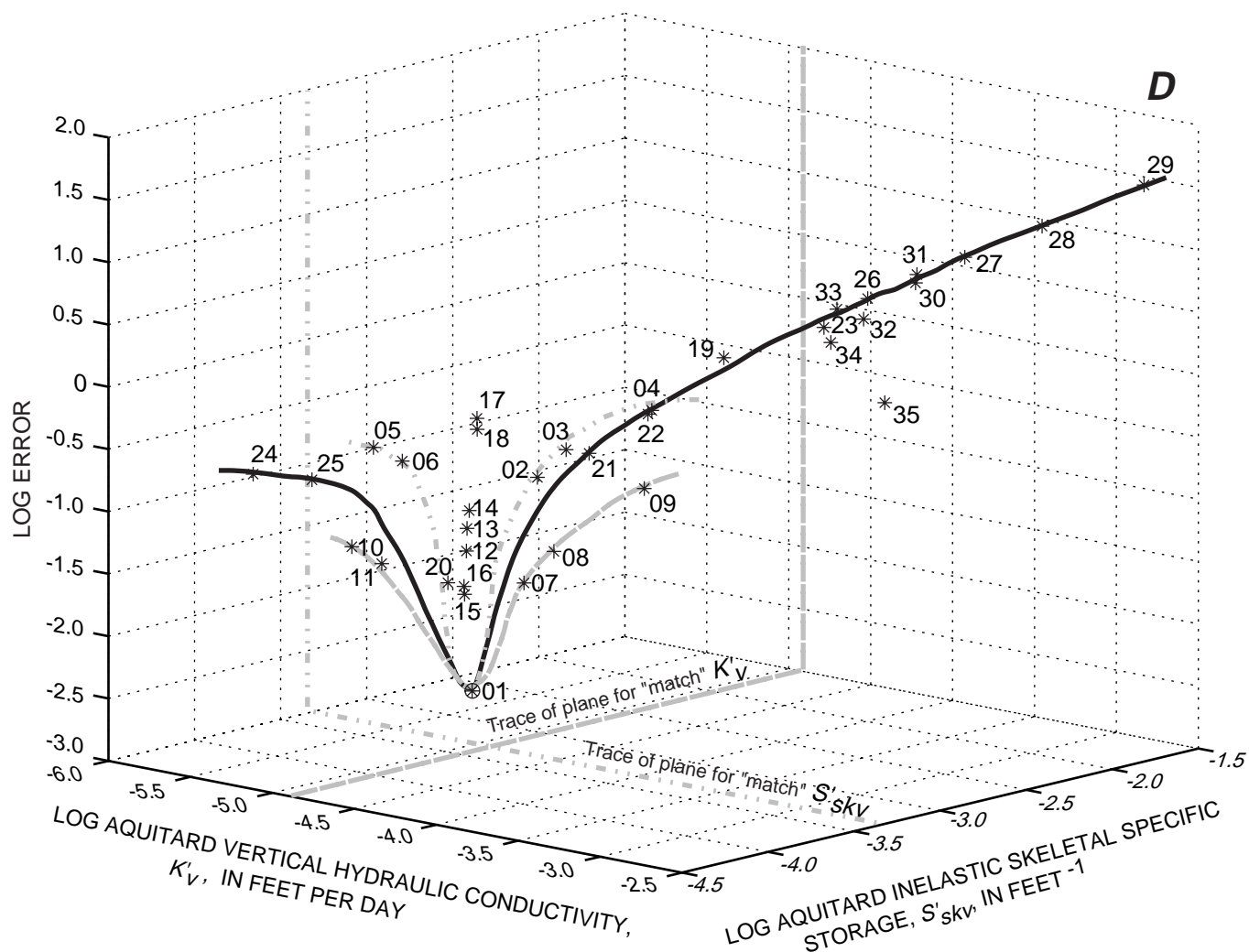


**Figure 25.** Continued. **C.** View of  $S'_{skv}$ -error plane showing the trace of the error surface for a constant "match" value of  $K'_v$  for variations in  $S'_{skv}$ .



#### EXPLANATION

- ..... Error surface in plane of "match" value of  $S'_{skv}$
- Error surface in plane of "match" value of  $K'_v$
- Error surface in plane of "match" value of aquitard vertical hydraulic diffusivity

- ⊗ Parameter values from history match
- \* Parameter values used in sensitivity analysis
- 35 Model run number

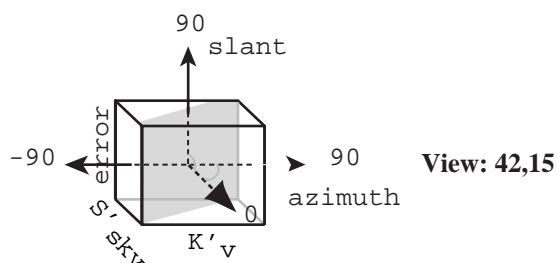
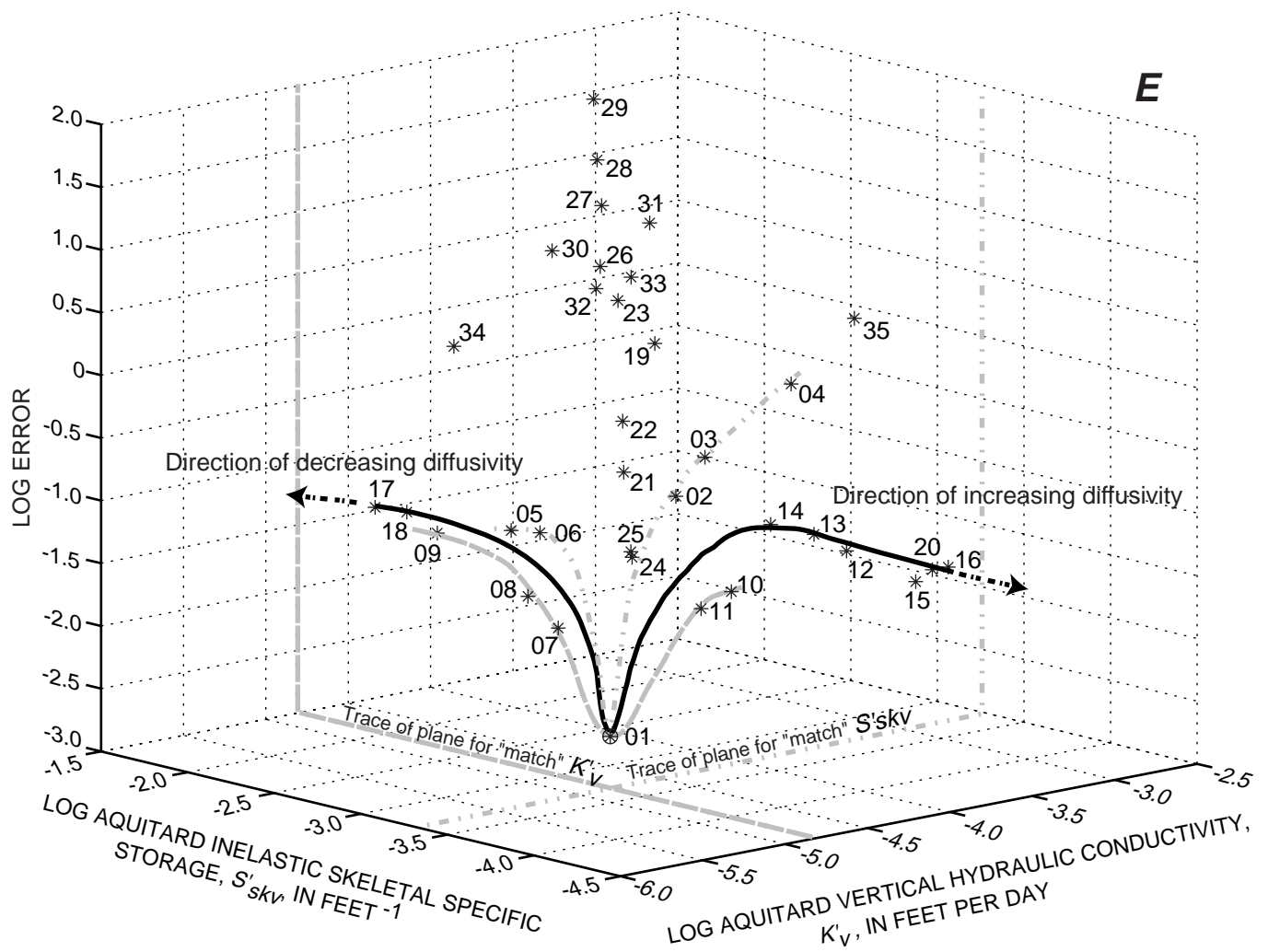


**Figure 25.** Continued. **D,** View showing the traces of the error surfaces for constant "match" values of vertical hydraulic diffusivity,  $S'_{skv}$  and  $K'_v$ . The view is in the plane of constant diffusivity-error space slanted 15 degrees.





#### EXPLANATION

..... Error surface in plane of "match" value of  $S'_{skv}$

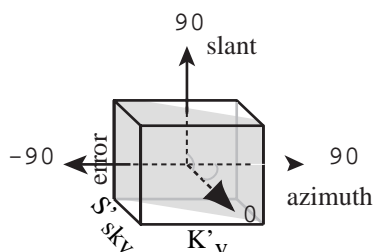
----- Error surface in plane of "match" value of  $K'_v$

———— Error surface through "match" value of aquitard vertical hydraulic diffusivity in plane perpendicular to plane of constant diffusivity

⊗ Parameter values from history match

\* Parameter values used in sensitivity analysis

35 Model run number



View: -48,15

**Figure 25.** Continued. *E*, View showing the traces of the error surfaces for a variable vertical hydraulic diffusivity and constant "match" values of  $S'_{skv}$  and  $K'_v$ . The view is in a plane (see orientation cube) perpendicular to the plane of constant diffusivity and slanted 15 degrees.

residual compaction and improved predictions of future land subsidence. On the other hand, because of the narrow range of expected  $S'_{kv}$  and the plausibility of obtaining reliable measurements of  $K'_v$ , the value of  $K'_v$  estimated from these modeling approaches could be comparable to, or better than, values measured in the field. These measurements and estimates are limited by the depth-integrated measurement inherent to conventional borehole extensometers, and therefore, average values of aquitard properties rather than specific values of individual aquitards should be expected.

## ANALYSES

### Simulated Compaction

The simulations for the two periods (1908–97 and 1990–97) provide information about how the aquifer-system components, aquifers and aquitards, contributed to overall compaction because of the continual lowering of water levels throughout the 1900s and because of seasonal water-level cycling in the 1990s.

Compaction simulated by the historical model totaled 3.93 ft for the period 1908–97; 3.75 ft (95 percent) of this total compaction occurred in the depth interval measurable by the extensometer. Of the total simulated compaction, the confining unit separating the upper and middle aquifers accounted for 31 percent of the total; the thick aquitard 302 to 365 ft below land surface accounted for 51 percent; aquitards 5- to 18-ft thick (aggregate aquitard thickness = 88 ft) accounted for 11 percent; and the rest of the system (aggregate aquitard thickness = 39 ft) accounted for about 7 percent (fig. 26A). Among the explicitly modeled aquitards, a linear relation exists between thickness and simulated ultimate compaction. In other words, all hydraulic parameters being equivalent in the model, a 10-ft-thick aquitard ultimately compacts twice as much as a 5-ft-thick aquitard (fig. 26B).

Total compaction simulated by the recent model was 0.36 ft; more than 99 percent of the compaction occurred in the same depth interval measurable by the extensometer. Of the total simulated compaction, the confining unit accounted for 42 percent, the thick aquitard

accounted for 57 percent, and the rest of the system accounted for about 1 percent (fig. 27A). In the simulation, aquitards less than or equal to 18-ft thick did not contribute significantly to compaction. For these quickly equilibrating thin aquitards, measured and simulated stresses for 1990–97 were, for the most part, less than the previous maximum stresses simulated by the historical model. These aquitards deformed mostly elastically during the 1990–97 period (fig. 27B).

Vertical distributions of hydraulic head in the aquitards can be used as a direct measure of residual compaction (Riley, 1998). A linear profile showing deviations in the simulated 1997 head distributions for two thick clay sequences—the confining unit and the thick aquitard 302 to 365 ft below land surface—indicate large residual pore pressures (fig. 28). The simulations indicate that more than 99 percent of the compaction measured by the extensometer (since its construction) is residual compaction occurring in these two thick clay sequences. Simulations of the historical model show that by 1976 aquitards less than or equal to 18-ft thick had significantly reduced compaction rates, and by 1988, heads in these aquitards were approaching an apparent equilibrium (fig. 26B).

### Future Compaction Scenarios

The vertical distributions of hydraulic head in the thicker aquitards at the end of the simulations (1997) indicate that excess fluid pressure remains in the thick aquitards (fig. 28), which represents the potential for significant residual compaction (at least 30 percent). To predict future compaction, scenarios representing three possible water-level responses at the Holly site to nearby pumping were simulated using history-matched model parameters.

For the first scenario, compaction was simulated in response to future water-level changes predicted on the basis of extrapolation of the Holly site hydrographs; the predicted water-level changes were considered to represent continued pumping rates and distributions at EAFB during the 1990s. This scenario was simulated for about 30 years (1997–2026); predicted water levels declined about 30 ft, to about 180 ft below land surface in the confined aquifer system. The second scenario simulated compaction in response to

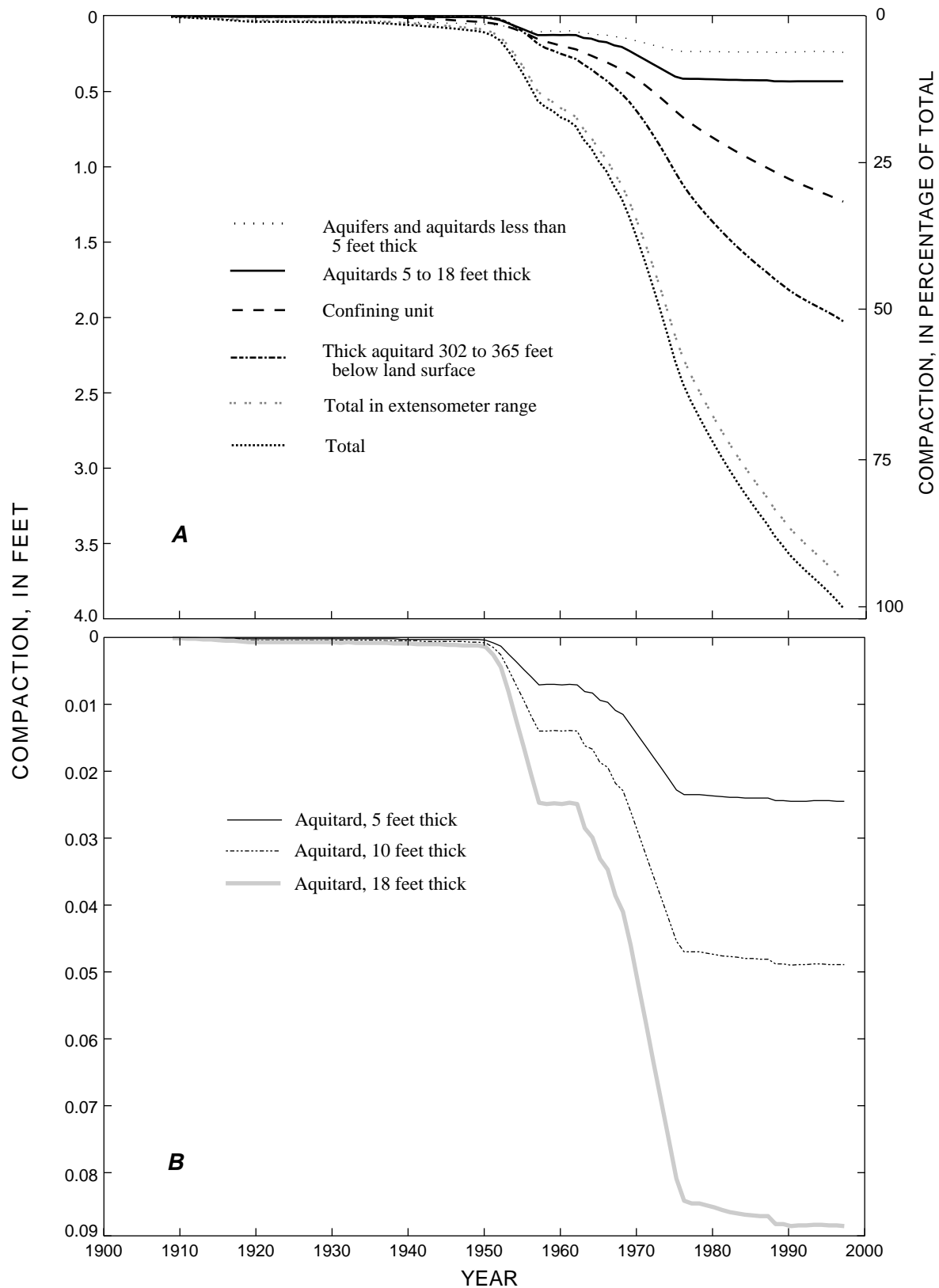


**Figure 26.** Simulated compaction by aquifer-system component, 1908–97, at the Holly site (8N/10W-1Q), Edwards Air Force Base, Antelope Valley, California. **A**, Proportion of component compaction to total compaction. **B**, Compaction for selected aquitards.

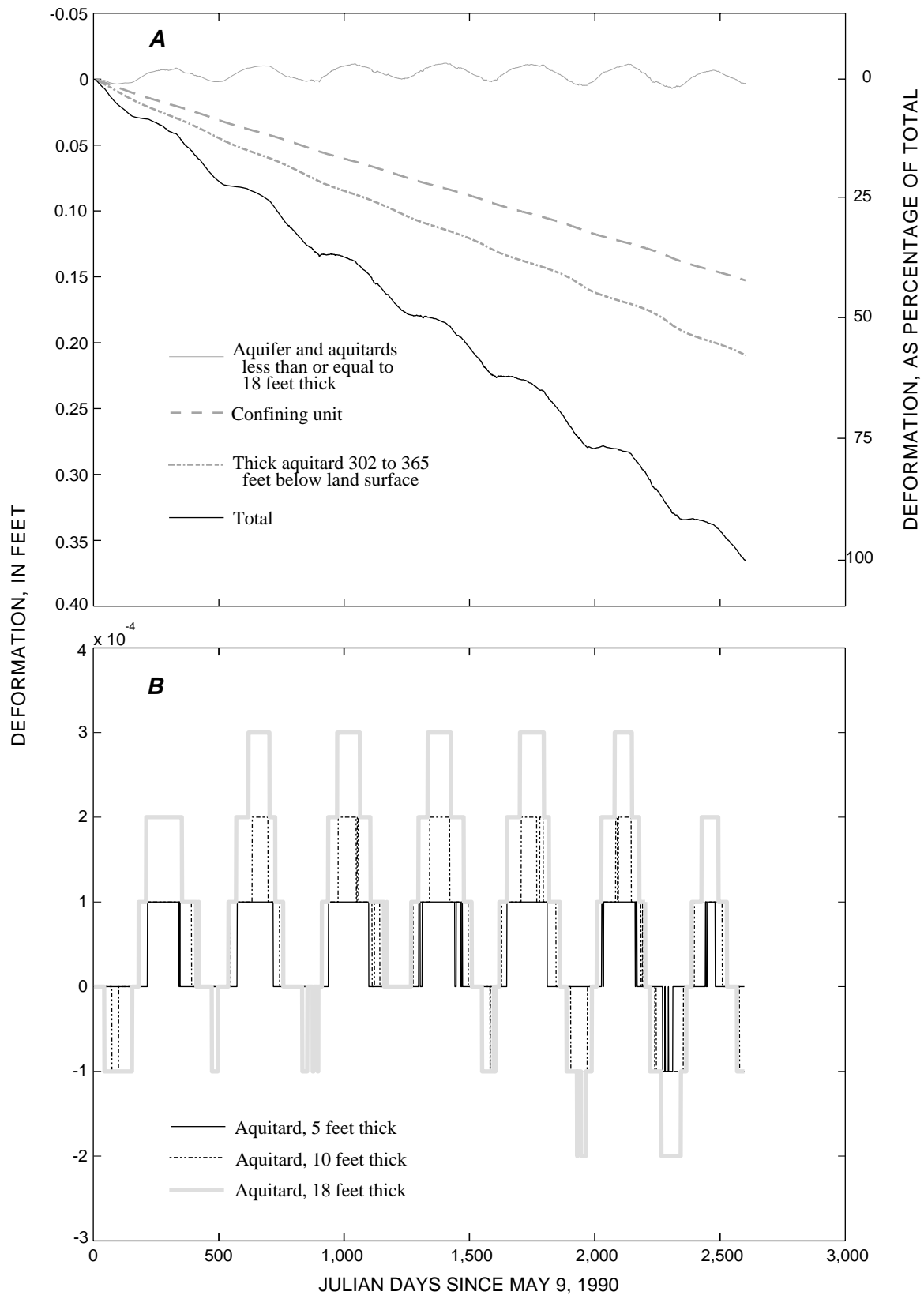


**Figure 27.** Simulated deformation by aquifer-system component, 1990–97, at the Holly site (8N/10W-1Q), Edwards Air Force Base, Antelope Valley, California. **A**, Proportion of component compaction to total compaction. **B**, Deformation for selected aquitards.

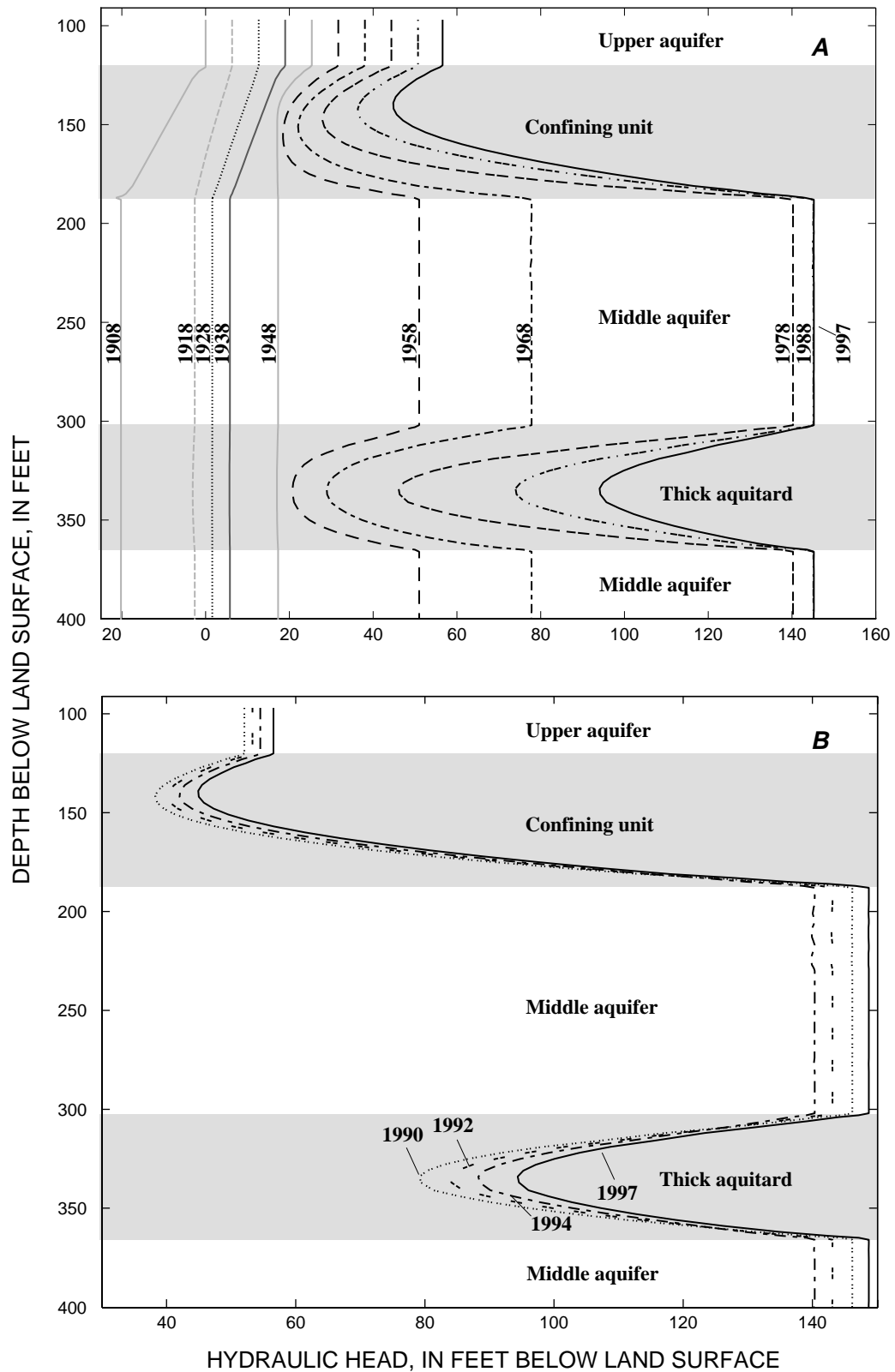


**Figure 28.** Hydraulic-head profiles of the Holly site (8N/10W-1Q), Edwards Air Force Base, Antelope Valley, California, for (A) 1908–97 and (B) 1990–97.

static water levels (1997 levels) for all the aquifers for about 100 years. The third scenario simulated compaction in response to water-level changes assuming a cessation of pumping at EAFB for about 100 years (1997–2096). This scenario assumed water-level recoveries for the confined aquifer system at the Holly site of about 30 ft, to about 115 ft below land surface. Comparisons of the results of the three scenarios indicate that in year 2026, 1.7 ft of compaction may occur if drawdown continues, 0.8 ft of compaction may occur if water levels remain at current (1997) levels, and 0.5 ft of compaction may occur if water levels recover.

In the first scenario, compaction at the Holly site was simulated using future water-level changes predicted on the basis of extrapolation of Holly site hydrographs. These future water-level changes may represent a scenario where pumping rates and distributions at EAFB during the 1990s would continue into the future. For the period 1997–2026, predicted drawdowns equaled 39 ft in the lower aquifer, 37 ft in the middle aquifer, and 10 ft in the upper aquifer. As a result of these predicted water-level changes, more than 1.7 ft of additional compaction occurred. Compaction in the confining unit constituted 36 percent of the total future compaction; the thick aquitard, 302 to 365 ft below land surface, constitutes 53 percent of the total compaction; other aquitards, 5- to 18-ft thick, constitute about 6 percent; and the rest of the system constitutes about 5 percent of the future compaction (fig. 29A). Figure 29B shows the migratory evolution of head distribution in the confining unit and the thick aquitard indicating continued progressive, albeit slow, dissipation of excess pore pressures. This simulation was stopped in the year 2026 to avoid causing water levels in the middle aquifer to decline below the bottom of the confining unit, thus converting at least parts of the middle aquifer to unconfined conditions, which invalidates many of the assumptions used in these analyses. However, if ground-water production were to cease in 2026, equilibration of heads in the thick units would cause significant additional compaction (fig. 29B).

In the second scenario, compaction at the Holly site was simulated for the next 99 years (through the year 2096), holding hydraulic heads in the aquifers constant at 1997 levels. An additional 1.3 ft of compaction occurred, all of which is attributed to the two

thickest aquitards. All compaction was residual compaction, about 54 percent derived from the thick aquitard, 302 to 365 ft below land surface, and the remaining 46 percent from the confining unit (fig. 30A). For this scenario, both thick aquitards approach hydraulic equilibrium by the year 2096 (fig. 30B).

In the third scenario, aquifer-system compaction at the Holly site was simulated using estimated water-levels that may occur if no pumping occurs after 1997 at any wells on EAFB. This scenario also was simulated for 99 years (through the year 2096). For the period 1997–2096, estimated recoveries equaled 32 ft in the lower aquifer and 29 ft in the middle aquifer, and estimated drawdown in the upper aquifer equaled 23 ft. As a result of the estimated water-level changes, about 0.8 ft of additional net compaction occurs (fig. 31A). By the end of the simulation, all units except the confining unit showed elastic net rebound (more rebound than compaction), albeit a small amount. In reality, the fringes of thick aquitards begin to rebound immediately, while interior parts of the aquitard continue to compact. In the third scenario, the thinner aquitards (less than or equal to 18 ft thick) and the aquifer material began to rebound immediately, the thick aquitard started to rebound (net) in year 2033, and the confining unit continued to compact throughout the simulation. Although the two thick aquitards have the same hydraulic parameters, except for a slightly different vertical hydraulic conductivity (table 3), the confining unit continued to compact because it drains mostly downward into the underlying aquifer while the thick aquitard drains both downward and upward into adjacent aquifers, dissipating pressure at about twice the rate as the confining unit.

The head distribution in the confining unit was not in equilibrium by 2096 while the other thick aquitard had nearly attained equilibrium; pore pressures near the center of the unit were equivalent to those in the surrounding aquifer (fig. 31B). As recovery proceeded, the thick aquitard underwent some small elastic expansion (fig. 31B) at its upper and lower boundaries as it took water back into storage at the outer margins (fig. 31B).

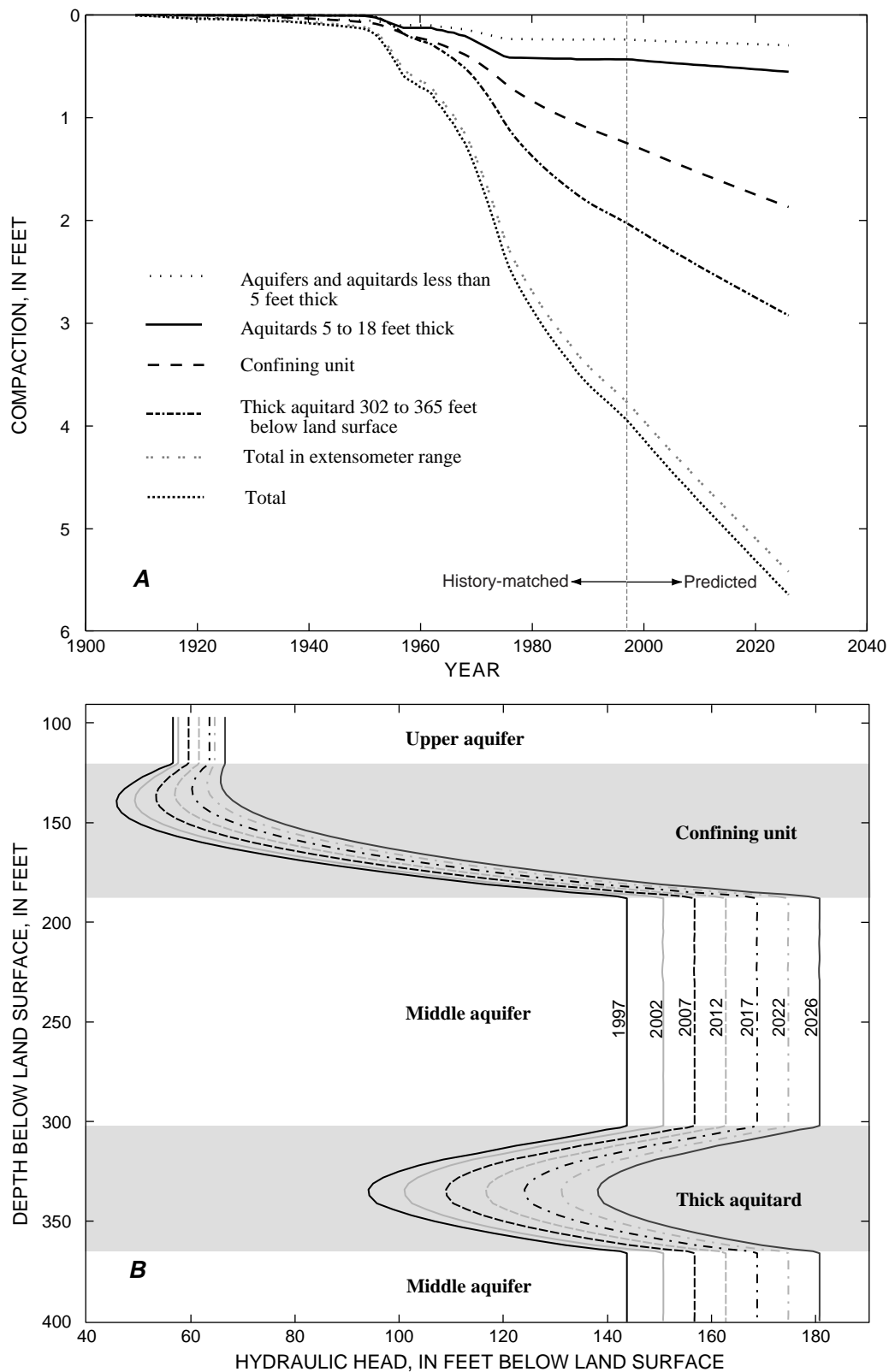


**Figure 29.** Future scenario—1996 pumping rates for 1997 to 2026 at the Holly site (8N/10W-1Q), Edwards Air Force Base, Antelope Valley, California. **A**, Simulated compaction by aquifer-system component, 1908–2026. **B**, Predicted head profile, 1997–2026.

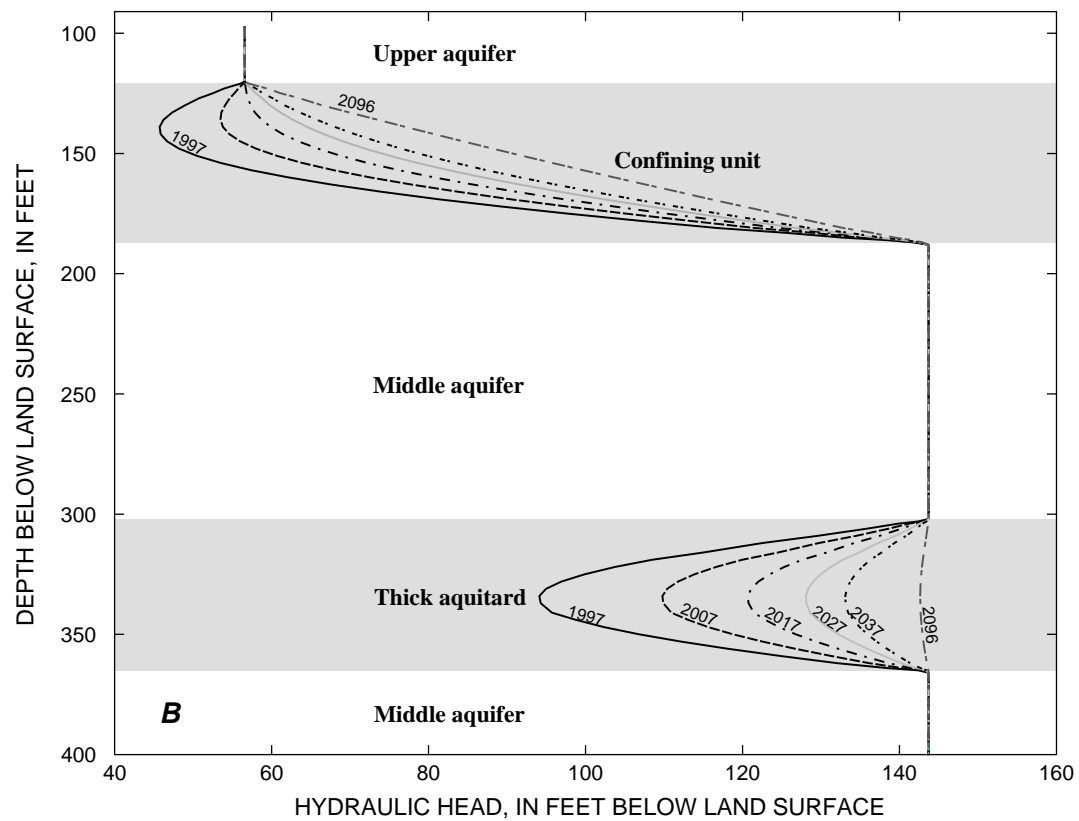
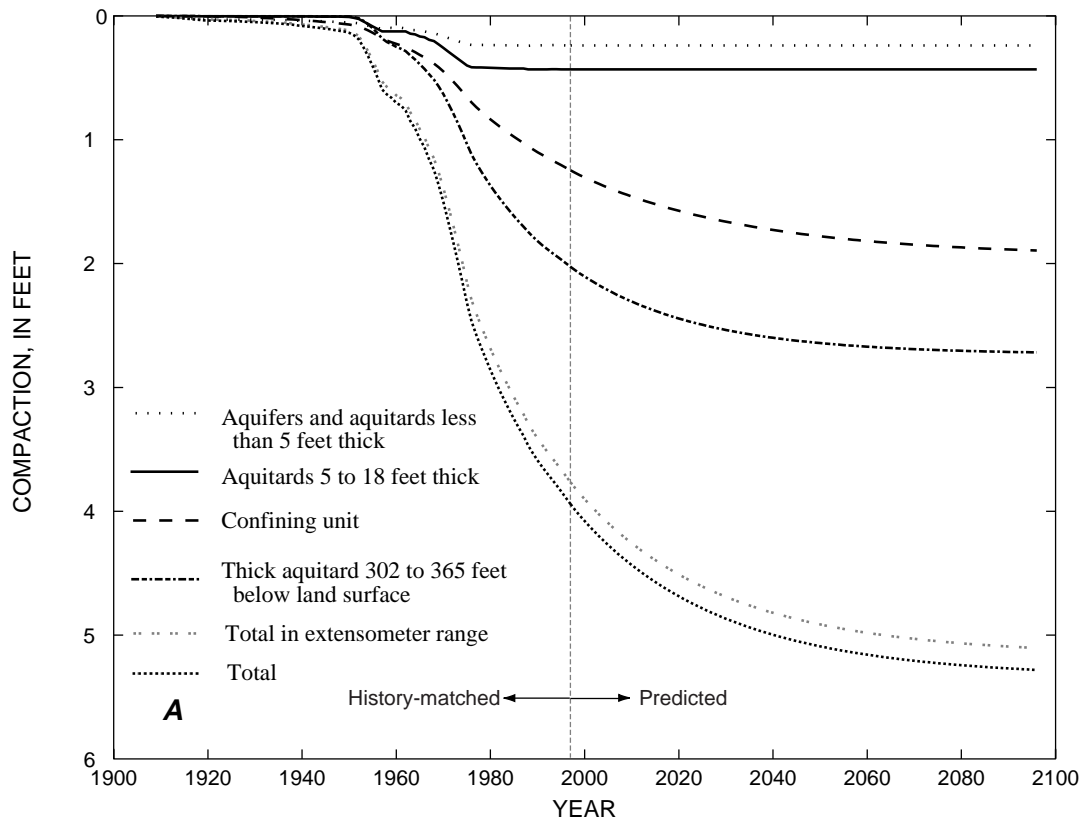


**Figure 30.** Future scenario—1997 aquifer water levels held constant through year 2096 at the Holly site (8N/10W-1Q), Edwards Air Force Base, Antelope Valley, California. **A**, Simulated compaction by aquifer-system component, 1908–2096. **B**, Predicted head profile, 1997–2096.



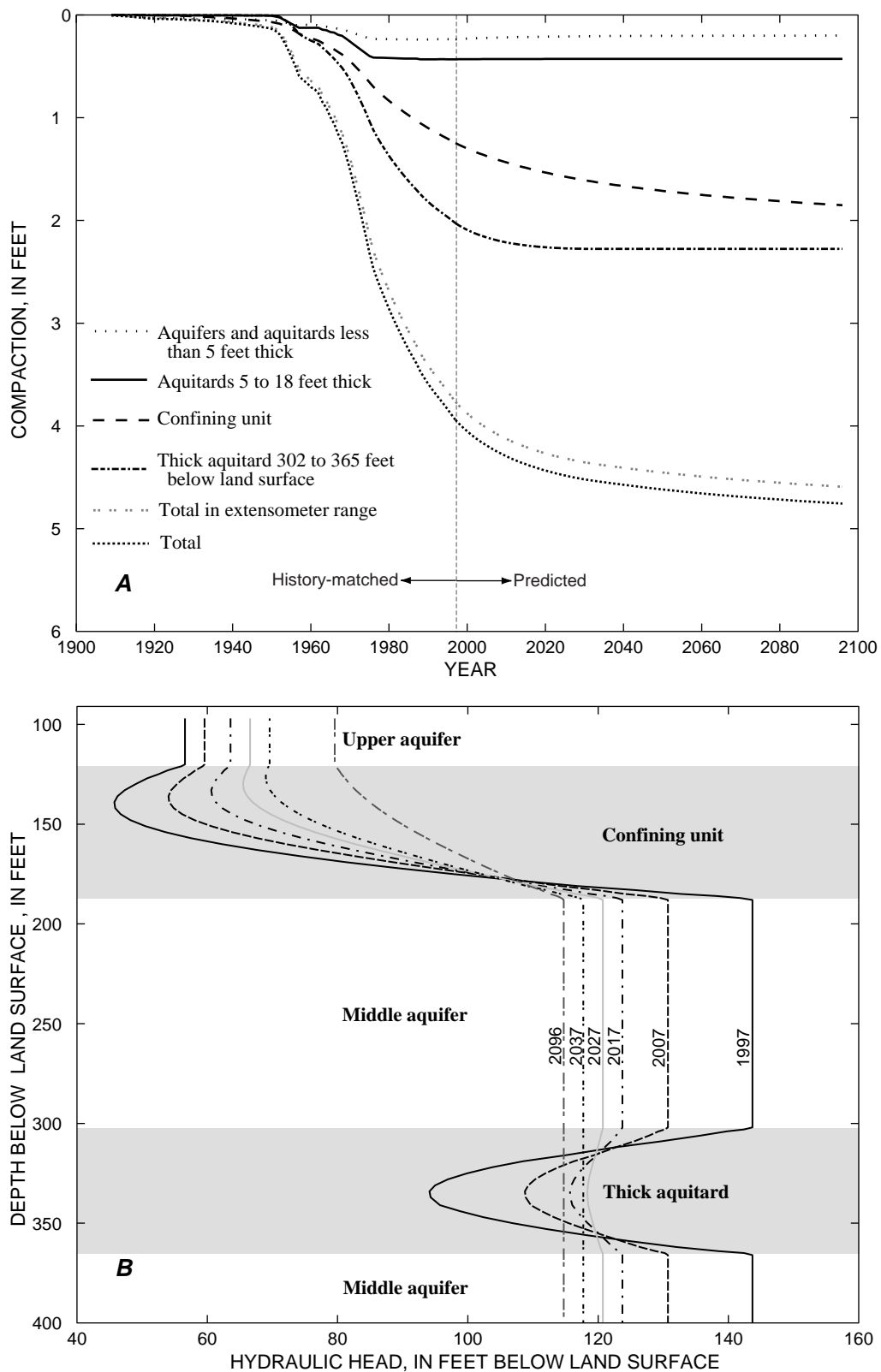


**Figure 31.** Future scenario—no pumping for 1997 to 2096 at the Holly site (8N/10W-1Q), Edwards Air Force Base, Antelope Valley, California. **A**, Simulated compaction by aquifer-system component, 1908–2096. **B**, Predicted head profile, 1997–2096.

## SUMMARY

Land subsidence resulting from ground-water-level declines has long been recognized as a problem in Antelope Valley, California, and in other alluvial basins in the arid and semiarid southwestern United States. Historical and continued depletion of ground-water resources in Antelope Valley has resulted in land subsidence that will persist into the future. Two separate, but linked, models were developed to simulate aquifer-system compaction and land subsidence and to explore future compaction and subsidence at the Holly site. The models were calibrated by history-matching simulated aquifer-system compaction to measured and estimated historical aquifer-system compaction for two periods—historical (1908-97) and recent (1990-97). The calibration resulted in refined estimates of the hydraulic parameters controlling compaction. The calibrated models were used to predict aquifer-system compaction and subsidence for three future scenarios.

A single set of aquifer-system property values was used to model two periods. The history match for the historical model (1908-97) was based on the few land-subsidence measurements from areas near the Holly site. The history match for the recent (1990-97) model was better constrained by the more than 7-year time series of aquifer-system compaction and water-level measurements for the Holly site, and therefore, more consideration was given to these results. Because the single set of simulation parameters provides a good history match for both time scales, a greater confidence in the hydraulic parameters for the aquifer system resulted.

Simulation results indicate that almost all compaction occurring at the Holly site is in the two thick aquitards—one aquitard is a regionally extensive confining unit consisting of lacustrine clay that separates the unconfined and confined aquifer systems at the Holly site, and the second aquitard is a more-localized thick aquitard within the middle aquifer. In the simulations, pore pressures in the thick aquitards did not equilibrate to rapid historical water-level declines in the confined aquifer system, and therefore, pore pressures in the thick aquitards lag the pore pressures in the adjacent aquifers. These residual pore pressures result in delayed drainage from the thick aquitards, which, in turn, results in residual compaction. Results of model simulation of the Holly site indicate that residual pore pressures remained in these two thick aquitards in

1997, which indicates that ultimate compaction and land subsidence have yet to occur. Results of the scenarios of future possible water-level changes examined using the Holly site models indicate that if water levels decline or recover about 30 ft from current levels, an additional 1.7 or 0.8 ft of compaction, respectively, may occur, with most of the future compaction occurring in the two thick aquitards. It also may be inferred by the areal extent of the lacustrine confining unit that other parts of the Lancaster subbasin have also not yet realized all the compaction that ultimately may occur as a result of historical ground-water-level declines of more than 150 ft, declines that slowed significantly more than 20 years ago.

The results of the models, in terms of residual compaction, emphasize the importance of long-term management of ground-water resources because, although water levels during the past 20 years have remained relatively stable compared with historical water levels, aquifer-system compaction continues owing to past stresses on the aquifer system. Management of ground water can help mitigate potential aquifer-system compaction and resultant land subsidence.

## REFERENCES CITED

- Anderson, S.R., 1988, Potential for aquifer compaction, land subsidence, and earth fissures in Tucson Basin, Pima County, Arizona: U.S. Geological Survey Hydrologic Investigations Atlas HA-713, scale 1:2,500,000, 3 sheets.
- , 1989, Potential for aquifer compaction, land subsidence, and earth fissures in Avra Valley, Pima and Pinal Counties, Arizona: U.S. Geological Survey Hydrologic Investigations Atlas HA-718, 1:2,500,000, 3 sheets.
- Benda, W.K., Erd, R.C., and Smith, W.C., 1960, Core logs from five test holes near Kramer, California: U.S. Geological Survey Bulletin 1045-F, p. 319-393.
- Biot, M.A., 1941, General theory of three-dimensional consolidation: *Journal of Applied Physics*, v. 12, p. 155-165.
- Blodgett, J.C., and Williams, J.S., 1992, Land subsidence and problems affecting land use at Edwards Air Force Base and vicinity, California, 1990: U.S. Geological Survey Water-Resources Investigations Report 92-4035, 25 p.
- Bloyd, R.M., Jr., 1967, Water resources of the Antelope Valley-East Kern Water Agency area, California: U.S. Geological Survey Open-File Report, 73 p.

- California Department of Finance, 1992, California annual population and housing data April 1, 1980, to April, 1990, for cities, counties, and the state: California Department of Finance Report E-8090, p. 59–88.
- California Department of Water Resources, 1947, Report to the Assembly of the State Legislature on water supply of Antelope Valley in Los Angeles and Kern Counties pursuant to House Resolution Number 101 of February 16, 1946: California Department of Water Resources, 21 p.
- Carlson, C.S., Leighton, D.A., Phillips, S.P., and Metzger, L.F., 1998, Regional water table (1996) and water-table changes in the Antelope Valley ground-water basin, California: U.S. Geological Survey Water-Resources Investigations 98-4022, 2 sheets.
- Carlson, C.S., and Phillips, S.P., 1998, Water-level changes (1975-98) in the Antelope Valley, California: U.S. Geological Survey Open-File Report 98-561, 2 sheets.
- Carpenter, M.C., 1993, Earth-fissure movements associated with fluctuations in ground-water levels near the Picacho Mountains, south-central Arizona, 1980-84: U.S. Geological Survey Professional Paper 497-H, 49 p.
- Dibblee, T.W., Jr., 1960 [1961], Geology of the Rogers Lake and Kramer quadrangles, California: U.S. Geological Survey Bulletin 1089-B, p. 73–139.
- 1963, Geology of the Willow Springs and Rosamond quadrangles, California: U.S. Geological Survey Bulletin 1089-C, p. 141–253.
- 1967, Areal geology of the western Mojave Desert, California: U.S. Geological Survey Professional Paper 522, 153 p.
- Dinehart, R.L., and McPherson, K.R., 1998, Topography, surface features, and flooding of Rogers Lake Playa, California: U.S. Geological Water-Resources Investigations Report 98-4093, 30 p.
- Durbin, T.J., 1978, Calibration of a mathematical model of the Antelope Valley ground-water basin, California: U.S. Geological Survey Water-Supply Paper 2046, 51 p.
- Dutcher, L.C., and Worts, G.F., Jr., 1963, Geology, hydrology, and water supply of Edwards Air Force Base, Kern County, California: U.S. Geological Survey Open-File Report, 225 p.
- Epstein, V.J., 1987, Hydrologic and geologic factors affecting land subsidence near Eloy, Arizona: U.S. Geological Survey Water-Resources Investigations Report 87-4143, 28 p.
- Freeman, L.A., 1996, Time-series ground-water-level and aquifer-system compaction data, Edwards Air Force Base, Antelope Valley, California, January 1991 through September 1993: U.S. Geological Survey Open-File Report 96-186, 32 p.
- Galloway, D.L., 1993, Coseismic volume strain associated with the Landers earthquake: An analysis of aquifer fluid-pressure responses, Antelope Valley, California (abs): EOS, Transactions of the American Geophysical Union, Spring Meeting Supplement, v. 74. no. 16, p. 317.
- Galloway, D.L., Hudnut, K.W., Ingebritsen, S.E., Phillips, S.P., Peltzer, G., Rogez, F., and Rosen, P.A., 1998a, Detection of aquifer-system compaction and land subsidence using interferometric synthetic aperture radar, Antelope Valley, Mojave Desert, California: Water Resources Research, v. 34, no. 10, p. 2573–2585.
- Galloway, D.L., Phillips, S.P., and Ikehara, M.E., 1998b, Land subsidence and its relation to past and future water supplies in Antelope Valley, California, *in* Borchers, J., ed., Land Subsidence—Case Studies and Current Research: Proceedings of the Dr. Joseph F. Poland Symposium on Land Subsidence, Association of Engineering Geologists Special Publication 8, p. 529–539.
- Green, J.H., 1964, Compaction of the aquifer system and land subsidence in the Santa Clara Valley, California: U.S. Geological Survey Water-Supply Paper 1779-T, 11 p.
- Hanson, R.T., 1989, Aquifer-System Compaction, Tucson Basin and Avra Valley, Arizona: U.S. Geological Survey Water-Resources Investigations Report 88-4172, 69 p.
- Hanson, R.T., Anderson, S.R., and Pool, D.R., 1990, Simulation of ground-water flow and potential land subsidence, Avra Valley, Arizona: U.S. Geological Survey Water-Resources Investigations Report 90-4178, 41 p.
- Hanson, R.T., and Benedict, J.F., 1994, Simulation of ground-water flow and potential land subsidence, upper Santa Cruz Basin, Arizona: U.S. Geological Survey Water-Resources Investigations Report 93-4196, 47 p.
- Harbaugh, A.W., and McDonald, M.G., 1996, User's Documentation for MODFLOW-96, an update to the U.S. Geological Survey modular finite-difference ground-water flow model: U.S. Geological Survey Open-File Report 96-485, 56 p.
- Helm, D.C., 1975, One-dimensional simulation of aquifer system compaction near Pixel, California—1. Constant parameters: Water Resources Research, v. 11, no. 3, p. 465–478.
- 1978, Field verification of a one-dimensional mathematical model for transient compaction and expansion of a confined aquifer system, Verification of Mathematical and Physical Models in Hydraulic Engineering, *in* Proceedings 26th Hydraulic Division Specialty Conference: American Society of Civil Engineers, p. 189–196.
- 1994, Horizontal aquifer movement in a Theis-Thiem confined system: Water Resources Research, v. 30, p. 953–964.

- Hewett, D.F., 1954, General geology of the Mojave Desert region California, in Jahns, R.H., ed., *Geology of Southern California*: California Department of Mines and Geology, Bulletin 170, chapter 2, p. 5–20.
- Heywood, C.E., 1995a, Investigation of aquifer-system compaction in the Hueco basin, El Paso, Texas, USA, in *Proceedings of the Fifth International Symposium on Land Subsidence*: International Association of Hydrological Sciences Publication 234, p. 35–45.
- 1995b, Piezometric-extensometric estimations of specific storage in the Albuquerque Basin, New Mexico, in Prince, K.R., and Leake, S.A., U.S. Geological Survey Subsidence Interest Group conference, Las Vegas, Nevada, February 14–16, 1995: *Proceedings of the Technical Meeting*: U.S. Geological Survey Open-File Report 97-47, p. 21–26.
- Holzer, T.L., 1981, Preconsolidation stress of aquifer systems in areas of induced land subsidence: *American Geophysical Union, Water Resources Research*, v. 17, no. 3, p. 693–704.
- 1984, Ground failure induced by ground-water withdrawal from unconsolidated sediment: *Geological Society of America, Reviews in Engineering Geology*, 6, p. 67–105.
- 1998, The history of the aquitard-drainage model, in Borchers, J., ed., *Land Subsidence—Case Studies and Current Research*, *Proceedings of the Dr. Joseph F. Poland Symposium*: Association of Engineering Geologists Special Publication 8, p. 7–12.
- Hsieh, P.A., 1996, Deformation-induced changes in hydraulic head during ground-water withdrawal: *Groundwater*, v. 34, p. 1082–1089.
- Ikehara, M.E., and Phillips, S.P., 1994, Determination of land subsidence related to ground-water-level declines using global positioning system and leveling surveys in Antelope Valley, Los Angeles and Kern Counties, California: U.S. Geological Survey Water-Resources Investigations Report 94-4184, 101 p.
- Ireland R. L., Poland, J.F., and Riley, F.S., 1984, Land subsidence in the San Joaquin Valley, California, as of 1980: U.S. Geological Survey Professional Paper 437-I, 93 p.
- Jacob, C.E., 1940, On the flow of water in an elastic artesian aquifer: *EOS, American Geophysical Union Transactions*, v. 21, p. 574–586.
- 1950, Flow in groundwater, in Rouse, H., ed.: *Engineering Hydraulics*, Wiley, New York, p. 321–386.
- Johnson, H.R., 1911, Water resources of Antelope Valley, California: U.S. Geological Survey Water-Supply Paper 278, 92 p.
- Jorgensen, D.G., 1980, Relationships between basic soils-engineering equations and basic ground-water flow equations: U.S. Geological Survey Water-Supply Paper 2064, 40 p.
- Leake, S.A., 1990, Interbed storage changes and compaction in models of ground-water flow: *Water Resources Research* 26, p. 1939–1950.
- Leake, S.A., and Prudic, D.E., 1991, Documentation of a computer program to simulate aquifer-system compaction using the modular finite-difference ground-water flow model: U.S. Geological Survey Techniques of Water-Resources Investigations, book 6, chap. A2, 68 p.
- Leake, S.A., and Lilly, M.R., 1997, Documentation of a computer program (fhhb1) for assignment of transient specified-flow and specified-head boundaries in applications of the modular finite-difference ground-water flow model (MODFLOW): U.S. Geological Survey Open-File Report 97-571, 50 p.
- Londquist, C.J., Rewis, D.L., Galloway, D.L., and McCaffrey, W.F., 1993, Hydrogeology and land subsidence, Edwards Air Force Base, Antelope Valley, California, January 1989-December 1991: U.S. Geological Survey Water-Resources Investigations Report 93-4114, 74 p.
- Los Angeles County Department of Regional Planning, 1994, Addendum to the report on Antelope Valley Population Projections for the Year 2020.
- Mabey, D.R., 1960, Gravity survey of the western Mojave Desert, California: U.S. Geological Survey Professional Paper 316-D, p. 51–73.
- Mankey, E.T., 1963, Tabulation of Elevation Differences for Earth Movement Study in Antelope Valley from 1928 to 1960: County of Los Angeles, Department of County Engineer, Survey Division, J.N. 0301.02, variously paged, and Survey Division File Map No. 65-56.
- McDonald, M.G., and Harbaugh, A.W., 1988, A modular three-dimensional finite-difference ground-water flow model: U.S. Geological Survey Techniques of Water-Resources Investigations, book 6, chap. A1, 548 p.
- Meinzer, O.E., 1928, Compressibility and elasticity of artesian aquifers: *Economic Geology*, v. 23, no. 3, p. 263–291.
- Meinzer, O.E., and Hard, H.A., 1925, The artesian-water supply of the Dakota sandstone in north Dakota with special reference to the Edgeley Quadrangle: U.S. Geological Survey Water-Supply Paper 520-E, p. 73–95.
- Meinzer, O.E., Wenzel, L.K., and others, 1945, Water levels and artesian pressure in observation wells in the United States in 1943: Part 6. Southwestern States and Territory of Hawaii: U.S. Geological Survey Water-Supply Paper 991, p. 109.

- Miller, R.E., 1961, Compaction of an aquifer system computed from consolidation tests and decline in artesian head, *Short Papers in the Geologic and Hydrologic Sciences: U.S. Geological Survey Professional Paper 424-B*, p. B54-B58.
- Motts, W.S., and Carpenter, David, 1970, Geology and hydrology of Rogers Playa and Rosamond Playa, California, *in* Motts, W.S., ed., *Geology and hydrology of selected playas in western United States*: Amherst, University of Massachusetts, Final Scientific Report Contract No. AFL 19(628)-2486, Air Force Cambridge Laboratories, p. 23–65.
- Neuman, S.P., and Witherspoon, P.A., 1969, Theory of flow in a confined two-aquifer system: *American Geophysical Union, Water Resources Research*, v. 5, no. 4, p. 803–816.
- Neuzil, C.E., 1994, How permeable are clays and shales?: *Water Resources Research*, v. 30, no. 2, p. 145–150.
- Poland, J.F., 1960, Land subsidence in the San Joaquin Valley and its effect on estimates of ground-water resources, *International Association of Scientific Hydrology Commission of Subterranean Waters: IASH Publication 52*, p. 324–335.
- Poland, J.F., and Green, J.H., 1962, Subsidence in the Santa Clara Valley, California—a progress report: *U.S. Geological Survey Water-Supply Paper 1619-C*, 16 p.
- Poland, J.F., and Ireland, R.L., 1988, Land subsidence in the Santa Clara Valley, California, as of 1982: *U.S. Geological Survey Professional Paper 497-F*, 61 p.
- Poland, J.F., Lofgren, B.E., Ireland, R.L., and Pugh, R.G., 1975, Land Subsidence in the San Joaquin Valley, California, as of 1972: *U.S. Geological Survey Professional Paper 437-H*, 78 p.
- Rantz, S.E., 1969, Mean annual precipitation in the California region: *U.S. Geological Survey Open-File Report*, 2 sheets, scale 1:1,000,000.
- Rewis, D.L., 1993, Drilling, construction, and subsurface data for piezometers on Edwards Air Force Base, Antelope Valley, California, 1991-92: *U.S. Geological Survey Open-File Report 93-148*, 35 p.
- , 1995, Ground-water-level monitoring, basin boundaries, and potentiometric surfaces of the aquifer system at Edwards Air Force Base, California, 1992: *U.S. Geological Survey Water-Resources Investigations Report 95-4131*, 61 p.
- Rice, J.R., and Cleary, M.P., 1976, Some basic stress diffusion solutions for fluid-saturated elastic porous media with compressible constituents: *Reviews of Geophysics and Space Physics*, v. 14, p. 227–241.
- Riley, F.S., 1969, Analysis of borehole extensometer data from central California, *in* Tison, L.J., *Land Subsidence: International Association of Hydrological Sciences Publication 89*, v. 2, p. 423–431.
- , 1984, Developments in Borehole Extensometry, *in* Johnson, A.I., Carbognin, L., and Ubertini, L., eds., *Land Subsidence: International Association of Hydrological Sciences Publication 151*, p. 169–186.
- , 1998, Mechanics of aquifer systems—The scientific legacy of Joseph F. Poland, *in* Borchers, J., ed., *Land Subsidence—Case Studies and Current Research: Proceedings of the Dr. Joseph F. Poland Symposium on Land Subsidence*, Association of Engineering Geologists Special Publication 8, p. 13–27.
- Roeloffs, E.A., Danskin, W.R., Farrar, C.D., Galloway, D.L., Hamlin, S.N., Quilty, E.G., Quinn, H.M., Schaefer, D.H., Sorey, M.L., and Woodcock, D.E., 1995, Hydrologic effects associated with the June 28, 1992, Landers, California, earthquake sequence: *U.S. Geological Survey Open-File Report 95-42*, 68 p.
- Rummler, Michelle, 1996, Aquifer hydraulic properties determined from the frequency response of water levels in wells to earth tides and atmospheric loading: Sacramento, California, California State University, Sacramento, unpublished senior thesis, 46 p.
- Scott, R.F., 1963, *Principles of soil mechanics*: Palo Alto, Addison-Wesley, 550 p.
- Snyder, J.H., 1955, *Ground water in California—The experience of Antelope Valley*: Berkeley, California, University of California, Division of Agriculture Science, Giannini Foundation Ground-Water Studies No. 2, 171 p.
- Templin, W.E., Phillips, S.P., Cherry, D.E., DeBortoli, M.L., and others, 1995, *Land Use and Water Use in the Antelope Valley, California*: U.S. Geological Survey Water-Resources Investigations Report 94-4208, 97 p.
- Terzaghi, Karl, 1925, *Principles of soil mechanics: IV; settlement and consolidation of clay*: *Erdbaumechanik*, 95, 3, 874–878.
- , 1943, *Theoretical soil mechanics*: New York, Wiley, 510 p.
- Thayer, W.N., 1946, *Geologic features of Antelope Valley, California*: Los Angeles County Flood Control District Report, 20 p.
- Thompson, D.G., 1929, *The Mojave Desert region, California, a geographic, geologic, and hydrographic reconnaissance*: U.S. Geological Survey Water-Supply Paper 578, 759 p.
- Tolman, C.F., and Poland, J.F., 1940, Ground-water, salt-water infiltration, and ground-surface recession in Santa Clara Valley, Santa Clara County, California: *American Geophysical Union Transactions*, pt. 1, p. 23–24.
- Van der Kamp, G., and Gale, J.E., 1983, Theory of earth tide and barometric effects in porous formations with compressible grains: *Water Resources Research*, v. 19, p. 538–544.

- Verruij, A., 1969, Elastic storage of aquifers, *in* DeWiest, R.J.M., ed.: Flow through porous media, Academic Press, p. 331–376.
- Waring, G.A., 1915, Springs of California: U.S. Geological Survey Water-Supply Paper 338, 402 p.
- Weeks, E.P., 1979, Barometric fluctuations in wells tapping deep unconfined aquifers: Water Resources Research, v. 15, p. 1167–1176.
- Weir, J.E., Jr., Crippen, J.R., and Dutcher, L.C., 1965, A progress report and proposed test-well drilling program for the water-resources investigation of the Antelope Valley-East/Kern Water Agency Area, California: U.S. Geological Survey Open-File Report, 120 p.
- Weston, Roy F., Inc., 1986, Water supply availability and distribution system evaluation, Edwards Air Force Base, California: Prepared for Edwards Air Force Base, Air Force Systems Command, Andrews Air Force Base, Washington, DC.
- Wolff, R.G., 1970, Relationship between horizontal strain near a well and reverse water level fluctuation: Water Resources Research, v. 6, p. 1721–1728.